BOND PROPERTIES OF CFCC PRESTRESSING STRANDS IN PRETENSIONED CONCRETE BEAMS

by

Nolan G. Domenico

A Thesis
Submitted to the University of Manitoba
In Partial Fulfillment of the
Requirements for the Degree of

Master of Science in Civil Engineering

Department of Civil and Geological Engineering
University of Manitoba
Winnipeg, Manitoba

National Library
of Canada

Acquisitions and
Bibliographic Services Branch

395 Wellington Street
Ottawa, Ontario
K1A 0N4

Bibliothèque nationale
du Canada

Direction des acquisitions et
des services bibliographiques

395, rue Wellington
Ottawa (Ontario)
K1A 0N4

Your file Votre référence

Our file Notre référence

ISBN 0-612-13082-7

Canada

Name _____

Dissertation Abstracts International is arranged by broad, general subject categories. Please select the one subject which most nearly describes the content of your dissertation. Enter the corresponding four-digit code in the spaces provided.

CIVIL ENGINEERING — SUBJECT TERM

0543 — SUBJECT CODE

U·M·I

Subject Categories

THE HUMANITIES AND SOCIAL SCIENCES

COMMUNICATIONS AND THE ARTS
Architecture 0729
Art History 0377
Cinema 0900
Dance 0378
Fine Arts 0357
Information Science 0723
Journalism 0391
Library Science 0399
Mass Communications 0708
Music 0413
Speech Communication 0459
Theater 0465

EDUCATION
General 0515
Administration 0514
Adult and Continuing 0516
Agricultural 0517
Art 0273
Bilingual and Multicultural 0282
Business 0688
Community College 0275
Curriculum and Instruction 0727
Early Childhood 0518
Elementary 0524
Finance 0277
Guidance and Counseling 0519
Health 0680
Higher 0745
History of 0520
Home Economics 0278
Industrial 0521
Language and Literature 0279
Mathematics 0280
Music 0522
Philosophy of 0998
Physical 0523
Psychology 0525
Reading 0535
Religious 0527
Sciences 0714
Secondary 0533
Social Sciences 0534
Sociology of 0340
Special 0529
Teacher Training 0530
Technology 0710
Tests and Measurements 0288
Vocational 0747

LANGUAGE, LITERATURE AND LINGUISTICS
Language
- General 0679
- Ancient 0289
- Linguistics 0290
- Modern 0291

Literature
- General 0401
- Classical 0294
- Comparative 0295
- Medieval 0297
- Modern 0298
- African 0316
- American 0591
- Asian 0305
- Canadian (English) 0352
- Canadian (French) 0355
- English 0593
- Germanic 0311
- Latin American 0312
- Middle Eastern 0315
- Romance 0313
- Slavic and East European 0314

PHILOSOPHY, RELIGION AND THEOLOGY
Philosophy 0422
Religion
- General 0318
- Biblical Studies 0321
- Clergy 0319
- History of 0320
- Philosophy of 0322

Theology 0469

SOCIAL SCIENCES
American Studies 0323
Anthropology
- Archaeology 0324
- Cultural 0326
- Physical 0327

Business Administration
- General 0310
- Accounting 0272
- Banking 0770
- Management 0454
- Marketing 0338

Canadian Studies 0385
Economics
- General 0501
- Agricultural 0503
- Commerce-Business 0505
- Finance 0508
- History 0509
- Labor 0510
- Theory 0511

Folklore 0358
Geography 0366
Gerontology 0351
History
- General 0578
- Ancient 0579
- Medieval 0581
- Modern 0582
- Black 0328
- African 0331
- Asia, Australia and Oceania 0332
- Canadian 0334
- European 0335
- Latin American 0336
- Middle Eastern 0333
- United States 0337

History of Science 0585
Law 0398
Political Science
- General 0615
- International Law and Relations 0616
- Public Administration 0617

Recreation 0814
Social Work 0452
Sociology
- General 0626
- Criminology and Penology 0627
- Demography 0938
- Ethnic and Racial Studies 0631
- Individual and Family Studies 0628
- Industrial and Labor Relations 0629
- Public and Social Welfare 0630
- Social Structure and Development 0700
- Theory and Methods 0344

Transportation 0709
Urban and Regional Planning 0999
Women's Studies 0453

THE SCIENCES AND ENGINEERING

BIOLOGICAL SCIENCES
Agriculture
- General 0473
- Agronomy 0285
- Animal Culture and Nutrition 0475
- Animal Pathology 0476
- Food Science and Technology 0359
- Forestry and Wildlife 0478
- Plant Culture 0479
- Plant Pathology 0480
- Plant Physiology 0817
- Range Management 0777
- Wood Technology 0746

Biology
- General 0306
- Anatomy 0287
- Biostatistics 0308
- Botany 0309
- Cell 0379
- Ecology 0329
- Entomology 0353
- Genetics 0369
- Limnology 0793
- Microbiology 0410
- Molecular 0307
- Neuroscience 0317
- Oceanography 0416
- Physiology 0433
- Radiation 0821
- Veterinary Science 0778
- Zoology 0472

Biophysics
- General 0786
- Medical 0760

EARTH SCIENCES
Biogeochemistry 0425
Geochemistry 0996
Geodesy 0370
Geology 0372
Geophysics 0373
Hydrology 0388
Mineralogy 0411
Paleobotany 0345
Paleoecology 0426
Paleontology 0418
Paleozoology 0985
Palynology 0427
Physical Geography 0368
Physical Oceanography 0415

HEALTH AND ENVIRONMENTAL SCIENCES
Environmental Sciences 0768
Health Sciences
- General 0566
- Audiology 0300
- Chemotherapy 0992
- Dentistry 0567
- Education 0350
- Hospital Management 0769
- Human Development 0758
- Immunology 0982
- Medicine and Surgery 0564
- Mental Health 0347
- Nursing 0569
- Nutrition 0570
- Obstetrics and Gynecology 0380
- Occupational Health and Therapy 0354
- Ophthalmology 0381
- Pathology 0571
- Pharmacology 0419
- Pharmacy 0572
- Physical Therapy 0382
- Public Health 0573
- Radiology 0574
- Recreation 0575
- Speech Pathology 0460
- Toxicology 0383

Home Economics 0386

PHYSICAL SCIENCES
Pure Sciences
Chemistry
- General 0485
- Agricultural 0749
- Analytical 0486
- Biochemistry 0487
- Inorganic 0488
- Nuclear 0738
- Organic 0490
- Pharmaceutical 0491
- Physical 0494
- Polymer 0495
- Radiation 0754

Mathematics 0405
Physics
- General 0605
- Acoustics 0986
- Astronomy and Astrophysics 0606
- Atmospheric Science 0608
- Atomic 0748
- Electronics and Electricity 0607
- Elementary Particles and High Energy 0798
- Fluid and Plasma 0759
- Molecular 0609
- Nuclear 0610
- Optics 0752
- Radiation 0756
- Solid State 0611

Statistics 0463

Applied Sciences
Applied Mechanics 0346
Computer Science 0984
Engineering
- General 0537
- Aerospace 0538
- Agricultural 0539
- Automotive 0540
- Biomedical 0541
- Chemical 0542
- Civil 0543
- Electronics and Electrical 0544
- Heat and Thermodynamics 0348
- Hydraulic 0545
- Industrial 0546
- Marine 0547
- Materials Science 0794
- Mechanical 0548
- Metallurgy 0743
- Mining 0551
- Nuclear 0552
- Packaging 0549
- Petroleum 0765
- Sanitary and Municipal 0554
- System Science 0790

Geotechnology 0428
Operations Research 0796
Plastics Technology 0795
Textile Technology 0994

PSYCHOLOGY
General 0621
Behavioral 0384
Clinical 0622
Developmental 0620
Experimental 0623
Industrial 0624
Personality 0625
Physiological 0989
Psychobiology 0349
Psychometrics 0632
Social 0451

Nom _____

Dissertation Abstracts International est organisé en catégories de sujets. Veuillez s.v.p. choisir le sujet qui décrit le mieux votre thèse et inscrivez le code numérique approprié dans l'espace réservé ci-dessous.

_____ ☐☐☐ U·M·I

SUJET — CODE DE SUJET

Catégories par sujets

HUMANITÉS ET SCIENCES SOCIALES

COMMUNICATIONS ET LES ARTS
Architecture 0729
Beaux-arts 0357
Bibliothéconomie 0399
Cinéma 0900
Communication verbale 0459
Communications 0708
Danse 0378
Histoire de l'art 0377
Journalisme 0391
Musique 0413
Sciences de l'information 0723
Théâtre 0465

ÉDUCATION
Généralités 515
Administration 0514
Art 0273
Collèges communautaires 0275
Commerce 0688
Économie domestique 0278
Éducation permanente 0516
Éducation préscolaire 0518
Éducation sanitaire 0680
Enseignement agricole 0517
Enseignement bilingue et multiculturel 0282
Enseignement industriel 0521
Enseignement primaire. 0524
Enseignement professionnel 0747
Enseignement religieux 0527
Enseignement secondaire 0533
Enseignement spécial 0529
Enseignement supérieur 0745
Évaluation 0288
Finances 0277
Formation des enseignants 0530
Histoire de l'éducation 0520
Langues et littérature 0279
Lecture 0535
Mathématiques 0280
Musique 0522
Orientation et consultation 0519
Philosophie de l'éducation 0998
Physique 0523
Programmes d'études et enseignement 0727
Psychologie 0525
Sciences 0714
Sciences sociales 0534
Sociologie de l'éducation 0340
Technologie 0710

LANGUE, LITTÉRATURE ET LINGUISTIQUE
Langues
- Généralités 0679
- Anciennes 0289
- Linguistique 0290
- Modernes 0291

Littérature
- Généralités 0401
- Anciennes 0294
- Comparée 0295
- Médiévale 0297
- Moderne 0298
- Africaine 0316
- Américaine 0591
- Anglaise 0593
- Asiatique 0305
- Canadienne (Anglaise) 0352
- Canadienne (Française) 0355
- Germanique 0311
- Latino-américaine 0312
- Moyen-orientale 0315
- Romane 0313
- Slave et est-européenne 0314

PHILOSOPHIE, RELIGION ET THÉOLOGIE
Philosophie 0422
Religion
- Généralités 0318
- Clergé 0319
- Études bibliques 0321
- Histoire des religions 0320
- Philosophie de la religion 0322

Théologie 0469

SCIENCES SOCIALES
Anthropologie
- Archéologie 0324
- Culturelle 0326
- Physique 0327

Droit 0398
Économie
- Généralités 0501
- Commerce-Affaires 0505
- Économie agricole 0503
- Économie du travail 0510
- Finances 0508
- Histoire 0509
- Théorie 0511

Études américaines 0323
Études canadiennes 0385
Études féministes 0453
Folklore 0358
Géographie 0366
Gérontologie 0351
Gestion des affaires
- Généralités 0310
- Administration 0454
- Banques 0770
- Comptabilité 0272
- Marketing 0338

Histoire
- Histoire générale 0578
- Ancienne 0579
- Médiévale 0581
- Moderne 0582
- Histoire des noirs 0328
- Africaine 0331
- Canadienne 0334
- États-Unis 0337
- Européenne 0335
- Moyen-orientale 0333
- Latino-américaine 0336
- Asie, Australie et Océanie 0332

Histoire des sciences 0585
Loisirs 0814
Planification urbaine et régionale 0999
Science politique
- Généralités 0615
- Administration publique 0617
- Droit et relations internationales 0616

Sociologie
- Généralités 0626
- Aide et bien-être social 0630
- Criminologie et établissements pénitentiaires 0627
- Démographie 0938
- Études de l' individu et de la famille 0628
- Études des relations interethniques et des relations raciales 0631
- Structure et développement social 0700
- Théorie et méthodes. 0344
- Travail et relations industrielles 0629

Transports 0709
Travail social 0452

SCIENCES ET INGÉNIERIE

SCIENCES BIOLOGIQUES
Agriculture
- Généralités 0473
- Agronomie. 0285
- Alimentation et technologie alimentaire 0359
- Culture 0479
- Élevage et alimentation 0475
- Exploitation des pâturages 0777
- Pathologie animale 0476
- Pathologie végétale 0480
- Physiologie végétale 0817
- Sylviculture et faune 0478
- Technologie du bois 0746

Biologie
- Généralités 0306
- Anatomie 0287
- Biologie (Statistiques) 0308
- Biologie moléculaire 0307
- Botanique 0309
- Cellule 0379
- Écologie 0329
- Entomologie 0353
- Génétique 0369
- Limnologie 0793
- Microbiologie 0410
- Neurologie 0317
- Océanographie 0416
- Physiologie 0433
- Radiation 0821
- Science vétérinaire 0778
- Zoologie 0472

Biophysique
- Généralités 0786
- Medicale 0760

SCIENCES DE LA TERRE
Biogéochimie 0425
Géochimie 0996
Géodésie 0370
Géographie physique 0368
Géologie 0372
Géophysique 0373
Hydrologie 0388
Minéralogie 0411
Océanographie physique 0415
Paléobotanique 0345
Paléoécologie 0426
Paléontologie 0418
Paléozoologie 0985
Palynologie 0427

SCIENCES DE LA SANTÉ ET DE L'ENVIRONNEMENT
Économie domestique 0386
Sciences de l'environnement 0768
Sciences de la santé
- Généralités 0566
- Administration des hôpitaux 0769
- Alimentation et nutrition 0570
- Audiologie 0300
- Chimiothérapie 0992
- Dentisterie 0567
- Développement humain 0758
- Enseignement 0350
- Immunologie 0982
- Loisirs 0575
- Médecine du travail et thérapie 0354
- Médecine et chirurgie 0564
- Obstétrique et gynécologie 0380
- Ophtalmologie 0381
- Orthophonie 0460
- Pathologie 0571
- Pharmacie 0572
- Pharmacologie 0419
- Physiothérapie 0382
- Radiologie 0574
- Santé mentale 0347
- Santé publique 0573
- Soins infirmiers 0569
- Toxicologie 0383

SCIENCES PHYSIQUES
Sciences Pures
Chimie
- Généralités 0485
- Biochimie 487
- Chimie agricole 0749
- Chimie analytique 0486
- Chimie minérale 0488
- Chimie nucléaire 0738
- Chimie organique 0490
- Chimie pharmaceutique 0491
- Physique 0494
- PolymÈres 0495
- Radiation 0754

Mathématiques 0405
Physique
- Généralités 0605
- Acoustique 0986
- Astronomie et astrophysique 0606
- Électronique et électricité 0607
- Fluides et plasma 0759
- Météorologie 0608
- Optique 0752
- Particules (Physique nucléaire) 0798
- Physique atomique 0748
- Physique de l'état solide 0611
- Physique moléculaire 0609
- Physique nucléaire 0610
- Radiation 0756

Statistiques 0463

Sciences Appliqués Et Technologie
Informatique 0984
Ingénierie
- Généralités 0537
- Agricole 0539
- Automobile 0540
- Biomédicale 0541
- Chaleur et thermodynamique 0348
- Conditionnement (Emballage) 0549
- Génie aérospatial 0538
- Génie chimique 0542
- Génie civil 0543
- Génie électronique et électrique 0544
- Génie industriel 0546
- Génie mécanique 0548
- Génie nucléaire 0552
- Ingénierie des systèmes 0790
- Mécanique navale 0547
- Métallurgie 0743
- Science des matériaux 0794
- Technique du pétrole 0765
- Technique minière 0551
- Techniques sanitaires et municipales 0554
- Technologie hydraulique 0545

Mécanique appliquée 0346
Géotechnologie 0428
Matières plastiques (Technologie) 0795
Recherche opérationnelle 0796
Textiles et tissus (Technologie) 0794

PSYCHOLOGIE
Généralités 0621
Personnalité 0625
Psychobiologie 0349
Psychologie clinique 0622
Psychologie du comportement 0384
Psychologie du développement 0620
Psychologie expérimentale 0623
Psychologie industrielle 0624
Psychologie physiologique 0989
Psychologie sociale 0451
Psychométrie 0632

BOND PROPERTIES OF CFCC PRESTRESSING STRANDS

IN PRETENSIONED CONCRETE BEAMS

BY

NOLAN G. DOMENICO

A Thesis submitted to the Faculty of Graduate Studies of the University of Manitoba in partial fulfillment of the requirements of the degree of

MASTER OF SCIENCE

ABSTRACT

An experimental program was conducted at the University of Manitoba to examine the bond characteristics of carbon fibre reinforced plastic prestressing strands (CFCC) in pretensioned concrete beams. The bond characteristics are examined through measurements of the transfer and development lengths as well as their corresponding bond stresses for 15.2 mm diameter and 12.5 mm diameter seven-wire CFCC strands. Ten prestressed concrete beams pretensioned by CFCC strands were constructed and tested using different shear span values. This thesis proposes equations to predict the transfer and flexural bond lengths for CFCC. The proposed equations are in excellent correlation with the measured values. This information is important for the design of concrete structures prestressed by CFCC and provides data for the development of design considerations and codes for concrete beams pretensioned by CFCC tendons.

ACKNOWLEDGMENTS

This research program was carried out under the direct supervision of Dr. S. H. Rizkalla, Department of Civil and Geological Engineering, University of Manitoba. The author would like to express his sincere gratitude to Dr. Rizkalla for his guidance, encouragement, and advice throughout this investigation.

The author also wishes to thank the Tokyo Rope Manufacturing Company Limited for providing the materials used in this program.

The author also wishes to express his appreciation for the technical assistance of Mr. Ed Lemke, Mr. Rob Graham, P. Eng, Mr. Scott Sparrow, and Mr. Kim Majury of the Structural Engineering Construction and Research and Development Facility.

Thanks are also extended to Mr. Amr Abdelrahman, Mr. Erwin Klassen, Mr. Zaki Mahmoud, Mr. Craig Michaluk, and Miss Susan Grieef for their assistance during fabrication and testing of the specimens.

Finally, the author wishes to express his heartfelt thanks to his parents Joe Domenico and Judy Jackson and his girlfriend Sheri whose encouragement and support made completion of this thesis possible.

TABLE OF CONTENTS

ABSTRACT i
ACKNOWLEDGMENTS ii
TABLE OF CONTENTS iii
LIST OF TABLES vi
LIST OF FIGURES vii
LIST OF SYMBOLS x

CHAPTER 1 INTRODUCTION
1.1. General 1
1.2. Objectives 2
1.3. Scope 3

CHAPTER 2 LITERATURE REVIEW
2.1. Introduction 4
2.2. Fibre Reinforced Plastics 4
2.2.1 Glass 6
2.2.2 Aramid 7
2.2.3 Carbon 7
2.2.3.1 Carbon Fibre Composite Cable (CFCC) 8
2.3. Bond Testing 9
2.3.1. Pull-Out Testing 9
2.3.1.1. Steel Reinforcements 10
2.3.1.2. FRP Reinforcements 12
2.3.2. Beam Testing 15
2.3.2.1. Reinforced Concrete 15
2.3.2.1.1. Steel Reinforcements 16
2.3.2.1.2. FRP Reinforcements 16
2.3.2.2. Prestressed Concrete 19
2.3.2.2.1. Steel Reinforcements 19
2.3.2.2.2. FRP Reinforcements 20
2.3.3. Transfer Prisms 23
2.3.3.1. FRP Reinforcements 23
2.4. Temperature Effects 24
2.5. Code Requirements 25
2.5.1. CSA Code 25
2.5.2. ACI Code 27
2.5.3. CEB-FIP Code 28
2.6. Conclusion 30

CHAPTER 3 THE EXPERIMENTAL PROGRAM
3.1. General 35
3.2. Purpose 36
3.3. Materials 37
3.3.1. CFCC Prestressing Strands 37
3.3.2. Concrete 39
3.4. Test Specimens 40
3.5. Jacking and Casting Set-up 40
3.6. Testing Setup 41
3.7. Instrumentation 43

CHAPTER 4 EXPERIMENTAL RESULTS
4.1. General 60
4.2. Prestress Losses 60
4.3. Transfer Length 61
4.4. Flexural Bond Length 64
4.5. Flexural Behaviour 65
4.5.1. Beam A1 66
4.5.2. Beam A2 67
4.5.3. Beam A3 68
4.5.4. Beam C4 70
4.5.5. Beam D5 71
4.5.6. Beam B6 71
4.5.7. Beam B7 72
4.5.8. Beam B8 73
4.5.9. Beam C9 75
4.5.10. Beam D10 75

CHAPTER 5 ANALYSIS AND DISCUSSION
5.1. Introduction 119
5.2. Transfer Length 119
5.3. Flexural Bond Length 122
5.4. Development Length 124
5.5. Bond Stresses 125
5.5.1. Transfer Bond Stresses 126
5.5.2. Flexural Bond Stresses 128
5.6. Parametric Study 129
5.6.1. Effect of Strand Diameter 130
5.6.2. Effect of Prestress Level 130
5.6.3. Effect of Concrete Cover 131
5.7. Ultimate Strength of CFCC 132

CHAPTER 6 SUMMARY AND CONCLUSION

6.1. Summary 148
6.1.1. Experimental Program 148
6.1.2. Bond Lengths 149
6.1.3. Flexural Behaviour 151
6.1.4. Bond Stresses 151
6.2. Conclusions 152
6.3. Design Recommendations 153
6.4. Suggestions For Future Research 154

REFERENCES 155

LIST OF TABLES

3.1	Beam Specifications	45
3.2	Characteristics of CFCC Strands as Reported by the Manufacturer	46
3.3	Concrete Mix Design	47
4.1	Prestressing Losses For All Beams	77
4.2	Measured Transfer Lengths For All Beams	78
4.3	Test Results For Series A and B	79
4.4	Test Results For All Beams	80
4.5	Concrete Properties For All Beams	80
5.1	Experimental Bond Lengths	133
5.2	CFCC Tensile Strengths	133

LIST OF FIGURES

2.1	FRP Stress-strain Relationships	31
2.2	Variation of Strand Stress Within the Development Length	32
2.3	Details of Pull-Out Specimen and Test	32
2.4	Cousins, et. al. Test Layout	33
2.5	Typical Flexural Bond Test Layout	34
3.1a	Cross-Sections of Beam Types A and B	48
3.1b	CFCC Prestressing Strands	49
3.2	Plan of Prestressing and Casting Setup For Two Beam Specimens	50
3.3	Elevation of First Test Setup	51
3.4	Front View Schematic of Test Setup	52
3.5	Side View Schematic of Test Setup	53
3.6	Locations of Strain Gauges	54
3.7	Locations of Demec Points	55
3.8a	Prestressing and Casting Setup	56
3.8b	Close-up of Jacking End	56
3.9	Reinforcement at End of Beam	57
3.10a	Test Setup	57
3.10b	Loading Spreader Beam	58
3.10c	Test Setup - Left End Lateral Support	58
3.10d	Test Setup - Right End Lateral Support	59
3.10e	End View of Test Setup	59
4.1	Beam Cross-Sections	81
4.2	Creep and Relaxation Losses For Beam A1	82
4.3	Creep and Relaxation Losses For Beam A2	82
4.4	Creep and Relaxation Losses For Beam A3	83
4.5	Creep and Relaxation Losses For Beam C4	83
4.6	Creep and Relaxation Losses For Beam D5	84
4.7	Creep and Relaxation Losses For Beam B6	84
4.8	Creep and Relaxation Losses For Beam B7	85
4.9	Creep and Relaxation Losses For Beam B8	85
4.10	Creep and Relaxation Losses For Beam C9	86
4.11	Creep and Relaxation Losses For Beam D10	86
4.12	Cable Strain Before and After Release For Beam A1	87
4.13	Cable Strain Before and After Release For Beam A2	87
4.14	Cable Strain Before and After Release For Beam A3	88
4.15	Cable Strain Before and After Release For Beam C4	88
4.16	Cable Strain Before and After Release For Beam D5	89
4.17	Cable Strain Before and After Release For Beam B6	89
4.18	Cable Strain Before and After Release For Beam B7	90
4.19	Cable Strain Before and After Release For Beam B8	90
4.20	Cable Strain Before and After Release For Beam C9	91

4.21	Cable Strain Before and After Release For Beam D10	91
4.22	Cable Strain in Transfer Zone For Beam A3	92
4.23	Cable Strain in Transfer Zone For Beam C4	92
4.24	Cable Strain in Transfer Zone For Beam D5	93
4.25	Cable Strain in Transfer Zone For Beam B6	93
4.26	Cable Strain in Transfer Zone For Beam B7	94
4.27	Cable Strain in Transfer Zone For Beam B8	94
4.28	Cable Strain in Transfer Zone For Beam C9	95
4.29	Cable Strain in Transfer Zone For Beam D10	95
4.30	Concrete Strain After Transfer For Beam A3	96
4.31	Concrete Strain After Transfer For Beam C4	96
4.32	Concrete Strain After Transfer For Beam D5	97
4.33	Concrete Strain After Transfer For Beam B6	97
4.34	Concrete Strain After Transfer For Beam B7	98
4.35	Concrete Strain After Transfer For Beam B8	98
4.36	Concrete Strain After Transfer For Beam C9	99
4.37	Concrete Strain After Transfer For Beam D10	99
4.38	Series A Test Results	100
4.39	Series B Test Results	100
4.40	Moment-Deflection Relationship For Beam A1	101
4.41	Moment-Deflection Relationship For Beam A2	101
4.42	Moment-Deflection Relationship For Beam A3	102
4.43	Moment-Deflection Relationship For Beam C4	102
4.44	Moment-Deflection Relationship For Beam D5	103
4.45	Moment-Deflection Relationship For Beam B6	103
4.46	Moment-Deflection Relationship For Beam B7	104
4.47	Moment-Deflection Relationship For Beam B8	104
4.48	Moment-Deflection Relationship For Beam C9	105
4.49	Moment-Deflection Relationship For Beam D10	105
4.50	Strain in Extreme Compression Fibre at Midspan For Beam A1	106
4.51	Strain in Extreme Compression Fibre at Midspan For Beam A2	106
4.52	Strain in Extreme Compression Fibre at Midspan For Beam A3	107
4.53	Strain in Extreme Compression Fibre at Midspan For Beam C4	107
4.54	Strain in Extreme Compression Fibre at Midspan For Beam D5	108
4.55	Strain in Extreme Compression Fibre at Midspan For Beam B6	108
4.56	Strain in Extreme Compression Fibre at Midspan For Beam B7	109
4.57	Strain in Extreme Compression Fibre at Midspan For Beam B8	109
4.58	Strain in Extreme Compression Fibre at Midspan For Beam C9	110
4.59	Strain in Extreme Compression Fibre at Midspan For Beam D10	110
4.60	Failure of Beam A3	111
4.61	Failure of Beam A3 - Close-up	111
4.62	Failure of Beam C4	112
4.63	Failure of Beam C4 - Close-up	112
4.64	Failure of Beam D5	113

4.65	Failure of Beam D5 - Close-up	113
4.66	Failure of Beam B6	114
4.67	Failure of Beam B6 - Close-up	114
4.68	Failure of Beam B7	115
4.69	Failure of Beam B7 - Close-up	115
4.70	Failure of Beam B8	116
4.71	Failure of Beam B8 - Close-up	116
4.72	Failure of Beam C9	117
4.73	Failure of Beam C9 - Close-up	117
4.74	Failure of Beam D10	118
4.75	Failure of Beam D10 - Close-up	118
5.1	Measured Transfer Lengths For CFCC	134
5.2	Transfer Length Comparison Against Effective Prestress Level	134
5.3	Transfer Length Comparison Against Strand Diameter	135
5.4	Transfer Length Comparison Against Concrete Compressive Strength	135
5.5	Failure of Series A Beams (15.2 mm strand)	136
5.6	Failure of Series B Beams (12.5 mm strand)	136
5.7	Measured Flexural Bond Lengths	137
5.8	Flexural Bond Length Comparison Against Strand Diameter	138
5.9	Flexural Bond Length Comparison Against Concrete Compressive Strength	138
5.10	Development Length Correlation	139
5.11	Development Length Comparison Against Effective Prestress Level	140
5.12	Development Length Comparison Against Strand Diameter	140
5.13	Transfer Length Average Bond Stresses	141
5.14	Transfer Length Bond Stress Index	141
5.15	Transfer Bond Strength Correlation	142
5.16	Flexural Bond Strength Correlation	142
5.17	Effect of Strand Diameter on Transfer and Flexural Bond Lengths	143
5.18	Effect of Strand Diameter on Transfer and Flexural Bond Strengths	143
5.19	Effect of Strand Diameter on Transfer and Flexural Bond Indexes	144
5.20	Effect of Strand Prestress Level on Transfer Length	144
5.21	Effect of Strand Prestress Level on Transfer Bond Strength	145
5.22	Effect of Strand Prestress Level on Transfer Bond Index	145
5.23	Effect of Concrete Cover on Transfer Length	146
5.24	Effect of Concrete Cover on Transfer Bond Strength	146
5.25	Effect of Concrete Cover on Transfer Bond Index	147

LIST OF SYMBOLS

A_b	cross-sectional area of reinforcing bar
A_p	cross-sectional area of prestressing reinforcement
A_s	nominal cross-sectional area of steel reinforcement
c	concrete cover
C_p	circumference of prestressing reinforcement
C_T	regression coefficient for transfer length equation
d_b	nominal diameter of reinforcement
f'_c	concrete compressive strength
f'_{ci}	concrete compressive strength at time of prestress transfer
f_{pe}	effective prestressing stress in reinforcement
f_{ps}	stress in strand at critical section
f_{pu}	ultimate strength of prestressing reinforcement
f_r	modulus of rupture of concrete
f_s	stress in steel bar
f_{se}	effective prestressing stress in steel reinforcement
f_y	yield strength of reinforcement
L	embedment length
L_d	development length
L_{fb}	flexural bond length
L_T	transfer length
P_o	nominal perimeter of bar
U	bond stress
U_{fb}	average bond stress in flexural bond zone
U'_{fb}	average bond stress index in flexural bond zone
U_T	average bond stress in transfer zone
U'_T	average bond stress index in transfer zone

CHAPTER 1

INTRODUCTION

1.1. General

Construction materials such as steel and timber are in effect homogeneous whereas reinforced concrete depends on the interaction of many components for its behaviour and ultimate strength. The main interaction of this composite material depends mainly on the bond between the reinforcement and the surrounding concrete. The behaviour is dependant on transfer of stress between one material to the other. In pretensioned prestressed concrete the stress transfer is accomplished by virtue of the bond between the concrete and the reinforcement. The bond strength is affected by many factors such as variations in the loading of a member, changes in temperature , creep in concrete, and corrosion of the reinforcement. Many studies, both analytical and experimental, have been done to examine the effect of these factors and others on the bond characteristics.

In reinforced concrete structures, corrosion of reinforcement has been identified to be one of the most severe problems causing deterioration. This has been addressed quite often and many solutions have been presented. Some of these solutions are the use of coatings for the reinforcement such as epoxy coatings or other plastic coatings, cathodic protection, or the use of advanced composite materials in place of steel. In recent years structures using coatings or cathodic protection have been deteriorating leading one to believe that these solutions are not as effective as originally claimed. Therefore more

engineers are turning to the use of advanced composite materials, or more specifically fibre reinforced plastics (FRP), to replace steel reinforcement. The materials are relatively new technology therefore much research efforts are needed in order for designers to gain confidence in this technological breakthrough.

1.2. Objectives

The purpose of this research program is to investigate the bond characteristics of carbon fibre reinforced plastic prestressing strands in pretensioned concrete beams. The bond characteristics will be examined through determination of the transfer and development lengths for 15.2 mm diameter and 12.5 mm diameter seven-wire CFCC strands. This research program has the following specific objectives:

A. Determine the transfer and development length of concrete beams pretensioned by 12.5 mm diameter CFCC strands.

B. Determine the transfer and development length of concrete beams pretensioned by 15.2 mm diameter CFCC strands.

C. Determine the effect of the initial prestress level on the transfer length and bond strength development of CFCC strands used for pretensioned concrete beams.

D. Determine the influence of the concrete cover on the transfer length and bond stress development in beams prestressed with CFCC strands.

1.3. Scope

The scope of this study consists of an experimental investigation and an analytical study. The experimental investigation involves fabrication and testing to failure of ten pretensioned concrete beams prestressed by CFCC strands. The analytical study involves rationalizing the experimental results of the transfer and development lengths, to include the material and geometric characteristics of the concrete and CFCC strands.

CHAPTER 2

LITERATURE REVIEW

2.1. Introduction

Many studies, both experimental and analytical, have been reported describing the bond properties of steel reinforcement used for concrete structures. This chapter will review the general characteristics of the new advanced composite reinforcements recently introduced to replace steel to overcome the corrosion problem. The chapter will also review the work being conducted to determine the bond characteristics in general and as related to FRP reinforcements.

2.2. Fibre Reinforced Plastics

Fibre reinforced plastic (FRP) materials are a promising new development which may revolutionize the concrete construction industry. These materials offer an alternative to steel as reinforcement for concrete structures. There are many advantages and disadvantages for FRP reinforcements in comparison to steel. These will be outlined in this section as well as some examples of FRP products and material properties.

FRP reinforcements are composite materials consisting of synthetic or organic high strength fibres which are impregnated in a resin material. They can be manufactured in the form of bars, grids, rods, or cables of almost any shape and size for reinforcement and

prestressing of concrete structural members. The fibre portion of this material can be made from carbon, aramid, or glass fibres with each having different material characteristics. Thus fibres can be selected according to the most advantageous characteristics for any particular application.

In general, the advantages of FRP reinforcement in comparison to steel reinforcement are as follows:

A. High ratio of strength to mass density (10 to 15 times greater than steel)

B. Carbon and Aramid fibre reinforcements have excellent fatigue characteristics (as much as three times higher than steel) However, the fatigue strength of glass FRP reinforcement may be significantly below steel's

C. Excellent corrosion resistance and electromagnetic neutrality

D. Low axial coefficient of thermal expansion, especially for carbon fibre reinforced composite materials.

The disadvantages of FRP reinforcement include:

A. High cost (5 to 50 times more than steel)

B. Low modulus of elasticity (for Aramid and glass FRP)

C. Low ultimate failure strain

D. High ratio of axial to lateral strength causing concern for anchorages when using FRP reinforcement for prestressing

E. Long term strength can be lower than the short-term strength for FRP reinforcement due to creep rupture phenomenon

F. Susceptibility of FRP to damage by ultra-violet radiation

G. Aramid fibres can deteriorate due to water absorption

H. High transverse thermal expansion coefficient in comparison to concrete

The tensile characteristics of reinforcement made from Carbon Fibre Reinforced Plastic (CFRP), Aramid Fibre Reinforced Plastic (AFRP), and Glass Fibre Reinforced Plastic (GFRP), are compared to steel in Figure 2.1.

2.2.1 Glass

Two types of glass fibres are commonly used in the construction industry, namely E-glass and S-glass. E-glass type is the most widely used GFRP due to its lower cost as compared to S-glass type, however S-glass has a higher tensile strength. Fresh drawn glass fibres exhibit a tensile strength in the order of 3450 MPa, but surface flaws produced by abrasion tend to reduce the strength to 1700 MPa. This strength is further degraded under fatigue loading due to the growth of flaws and also degrades in the presence of water. Commercially GFRP prestressing tendons and rods are available under the brand names of Isorod by Pultall Inc. (Canada), IMCO by IMCO Reinforced Plastics Inc. (USA), Jitec by Cousin Frere (France), Kodiak by IGI International Grating (USA), Plalloy by Asahi Glass Matrex (Japan), Polystal by Bayer AG and Strag Bau-AG (Germany), and C-bar by Marshell Ind. (USA).

2.2.2 Aramid

Aramid (abbreviation for aromatic polyamide) based FRP products have a tensile strength in the range of 2650 to 3400 MPa and an elastic modulus of from 73 to 165 GPa. AFRP prestressing tendons are produced in different shapes such as spiral wound, braided, and rectangular rods. It has been reported that there is no fatigue limit for Aramid fibres, however creep-rupture phenomenon has been observed. Aramid fibres are also quite sensitive to ultra-violet radiation. Commercially, AFRP prestressing tendons and rods are available under the brand names of Technora by Teijin (Japan), Fibra by Mitsui (Japan), Arapree by AKZO and Hollandsche Beton Groep (Holland), Phillystran by United Ropeworks (USA), and Parafil Ropes by ICI Linear Composites (UK).

2.2.3 Carbon

Carbon fibres can be produced from two materials, namely textile (PAN-based) and PITCH-based material. The most common textile material is poly-acrylonitrile (PAN). PITCH-based material is a by product of petroleum refining or coal coking. Carbon fibres have exceptionally high tensile strength to weight ratios with strength ranging from 1970 to 3200 MPa and tensile modulus ranging from 270 to 517 GPa. These fibres also have a low coefficient of linear expansion on the order of 0.2×10^{-6} m/m/C, and high fatigue strength. However, disadvantages are their low impact resistance, high electrical conductivity, and high cost. Commercially available CFRP prestressing tendons are

available under the brand names of Carbon Fibre Composite Cable (CFCC) by Tokyo Rope (Japan), Leadline by Mitsubishi Kasai (Japan), Jitec by Cousin Frere (France), and Bri-Ten by British Ropes (UK).

2.2.3.1 Carbon Fibre Composite Cable (CFCC)

Carbon Fibre Composite Cables (CFCC) made in Japan by Tokyo Rope Manufacturing Co. use PAN (polyacrylonite) type carbon fibres supplied by Toho Rayon. Individual wires are manufactured by a roving prepreg process where the epoxy resin is heat cured. The prepreg is twisted to create a fibre core and then wrapped by synthetic yarns. The purpose of the yarn is to protect the fibres from ultra-violet radiation and mechanical abrasion, and also improves the bond properties of the wire to concrete. Cables are then made from one, seven, nineteen, or thirty-seven wires and are twisted to allow better stress distribution through the cross-section.

Tokyo Rope currently produces cables with diameters from 3 to 40 mm in any length up to 600 metres. For 12.5 and 15.2 mm diameter CFCC cables the ultimate tensile strengths are 2100 and 2150 MPa respectively. Both sizes have a tensile elastic modulus of 137 GPa and an ultimate tensile failure strain of 1.5 to 1.6%. The thermal coefficient of expansion is approximately 0.6×10^{-6} /C which is about 1/20 that of steel. The relaxation is about 3.5% after 30 years at 80% of the ultimate load, this is about 50% less than that of steel. Also pull-out tests show that CFCC has a bond strength to concrete of 6.67 MPa, which is more than twice that of steel (ref. 51).

2.3. Bond Testing

In pretensioned prestressed concrete the prestressing force is transferred to the concrete by bond at the end region of a member. The distance along the member in which the effective prestressing force is developed is called the transfer length. The additional length required to develop the strand strength from the effective prestressing stage to ultimate is called the flexural bond length. The sum of these two lengths is called the development length. These lengths are best illustrated by Cousins, Johnston, and Zia (1990) which may be seen in Figure 2.2 . Different tests have been standardized to examine these aspects of concrete reinforcement. Tests include pull-out tests, flexural bond tests, and transfer length tests.

2.3.1. Pull-Out Testing

The pull-out test is used to determine the overall development length of concrete reinforcement. This is a relatively simple test which uses relatively small specimens. Specimens for this test consist of a length of reinforcement with one end encased in a concrete block over some length. The test is performed by holding the concrete block fixed and pulling on the free end of the reinforcement until failure occurs by either bond slip or material failure. Details of pull-out specimens and testing arrangement are shown in Figure 2.3 reproduced from Mathey and Watstein (1961).

2.3.1.1. Steel Reinforcements

ASTM standard A775/A775M which deals with epoxy coated steel reinforcing bars refers to the report FHWA-RD-74-18 for pull-out testing which states that the pull-out specimens shall be a concrete prism 10 by 10 by 12 inches (250x250x300 mm) with a No. 6 (No. 20) reinforcing bar embedded along the longitudinal axis of the specimen. It also states that 2x2-W1.2 welded wire fabric shall be used in the concrete in the form of an 8 inch diameter cage extending the length of the concrete prism concentric with the reinforcing bar. The critical bond stress shall be determined as the smaller of the following: the stress corresponding to a free end slip of 0.002 in. (0.05 mm), or the stress corresponding to a loaded end slip of 0.01 in. (0.25 mm). FHWA-RD-74-18 also states that the bond stress be computed from the following formula:

$$U = \frac{f_s A_s}{P_o L} \tag{2.1}$$

where,

U = bond stress

f_s = stress in the reinforcing bar

A_s = nominal cross-sectional area of the bar

P_o = nominal perimeter of the bar

L = length of embedment of the bar

Tests done by Mathey and Watstein (1961) on high-yield-strength deformed bars as well as by others utilized these specimens and testing procedures.

ASTM standard A882/A882M deals with epoxy coated prestressing steel strand and states using pull-out testing on strands up 0.6 inches in diameter. The test includes concrete prisms 6 by 6 inches (150x150 mm) of varying length without the use of any welded wire fabric reinforcement. It also states that the specimens should be tested when the concrete reaches a range of compressive strength of 4000 and 5000 psi (30 and 35 MPa) and that the critical bond stress occurs when a free-end slip of 0.001 inches (0.025 mm). The standard also has some minimum force requirements at 0.001 inch slip for different strand diameters and embedment lengths.

Some pull-out tests done by others use similar specimens and procedures but with some variations. Martin (1982) used pull-out testing on deformed bars using cube specimens of 250x250x250 mm with a certain length of the bars debonded to yield a bond length equal to five times bar diameter. Jiang, Andonian, and Shah (1982) developed a new type of specimen which consisted of a reinforcing bar split longitudinally into two halves and embedded in the opposite sides of the prism cross-section rather than concentric with the prism. The two rod halves were pulled from both ends by a testing machine. Demec points were placed along the length of the rods and on the adjacent concrete in order to measure all localized slip and strain. This was done in order to determine the bond stress distribution along the embedment length rather than just an average bond stress. Most of their experimental results agreed reasonably well with their theoretical results.

Testing conducted by Bennet and Snounou (1982) in Great Britain used another type of specimen using varying stresses in a fatigue-like fashion. Their specimens used

plain steel bars debonded over a certain length to give a short bond length of only 25 mm. The purpose of the short bond length was to determine the frictional properties of the bars under varying stress.

An innovative test designed by Cousins, Badeaux, and Moustafa (1992) was developed to simulate the bond behaviour more realistically for a pretensioned strand. The method included prestressing a strand and casting a concrete prism around a certain length of the strand. After curing of the concrete they used a hydraulic actuator to force the concrete block off the strand. The test layout is shown in Figure 2.4 . As the force in the actuator is increased, the stress in the strand on one side of the block will increase and the stress in the other side of the strand will decrease. This will produce swelling of the prestressing strand on the opposite side of the concrete block from the actuator and effectively reproduce the actual bonding mechanism within the transfer length commonly known as the Hoyer effect. The results of their tests yielded higher yet more realistic bond strengths than those of direct pull-out tests.

2.3.1.2. FRP Reinforcements

Shima, Suga, and Honma (1993) performed pull-out bond tests on braided Aramid fibre bars, carbon fibre seven-wire strands and a conventional seven wire steel strand. The Aramid bars were of 12, 14, and 16 mm diameter, the carbon strands were 12.5 mm in diameter, and the steel strands were 15.2 mm in diameter. The specimens were 30x30 cm in cross-section with lengths of 80 times the bar diameter for the fibre reinforcing

materials and 100 times the strand diameter for the steel strands. The three concrete compressive strengths were 40, 55, and 84 MPa. It was concluded that the bond stress of a carbon fibre strand and of a steel strand is proportional to 1/2 to 2/3 power of concrete compressive strength. For a braided Aramid fibre bar the effect of variations in concrete compressive strength was quite small. It was also concluded that the local slip is proportional to bar diameter in the local bond stress-slip relationship of braided Aramid fibre bars.

Khin, Matsumoto, Harada, and Takewaka (1994) performed pull-out tests on 100x100x100 mm cubes using the provisional testing procedures of Japan Society of Civil Engineers (JSCE). The three different types of FRP reinforcements examined were seven CFRP rods, four AFRP rods, and one Vinylon FRP rod. Test results indicate that the maximum bond stresses ranged from 4.4 to 15.3 MPa for carbon rods, 7.7 to 12.6 MPa for Aramid rods, and 9.2 for the Vinylon rod. It was concluded that the bond strength of FRP rods in concrete depends not only on the surface condition of the rods but also on the fibre type, fibre strength, spiral-rod adhesion, and the spiral strength of spiral FRP rods.

GFRP bars were tested by Malvar (1994) in pull-out tests with the presence of radial confining stresses. The bars were pultruded E-glass fibres embedded in a vinyl ester or polyester resin matrix. Specimens consisted of 3 inch diameter, 4 inch long concrete cylinders surrounding the bar. The bar had a contact length of 2 $^{5}/_{8}$ inches with the remaining length debonded. A split, threaded steel pipe was placed around the cylinders to provide the confining pressure. The pull-out load, for different confining

pressures, was measured as well as bar slippage and the radial deformations to plot a family of bond stress-slip curves. Confining pressures ranged from 3.5 to 31.0 MPa (500 to 4500 psi). It was concluded that small surface deformations (about 5.4% of the nominal bar diameter) are sufficient to develop bond stresses up to five times the concrete tensile strength, similar to that obtained by steel bars. Either surface deformations or indentations obtained by stressing an external helicoidal strand are acceptable for bond purposes. Deformations glued to the surface of the bars are unacceptable since they become unbonded. Large variations in the indentation depth resulted in large variations in bond strength. Bond strength can usually be increased threefold by increasing the confining pressure.

Nanni, Lui, Ash, and Nenninger (1994) performed 32 pull-out tests on hybrid FRP rods consisting of a steel core with a skin of either braided epoxy-impregnated Aramid or poly-vinyl alcohol (PVA). The variable in this experimental program include the type of FRP (Aramid or PVA fibres), FRP skin thickness, steel core type (High strength SBPR80 steel or low strength SR24 steel), steel core diameter, and concrete strength. It was concluded that the overall bond strength of hybrid rods is not significantly lower than that of steel bars. Also the free-end slip and loaded-end slip of hybrid rods at given values of pull-out load is significantly higher than that of standard deformed steel bars.

All of these different test procedures, specimens, and programs were developed to determine the bond stress-slip relationships for reinforced concrete to determine the flexural bond lengths.

2.3.2. Beam Testing

The flexural testing of beams is used to determine the flexural bond length and/or the transfer length of reinforcing bars and prestressing tendons. Nearly all of the literature which deals with this particular type of testing refers to the report from ACI Committee 208 as the accepted standard for the test.

2.3.2.1. Reinforced Concrete

ACI Committee 208 (1958) deals with deformed steel reinforcing bars and states that the beams shall be made for a two-point equal loading system and have a span of 72 in. (1800 mm). Half the beams are prescribed to be cast erect and half cast inverted to determine if any concrete segregation exists. The point loads should be of equal but variable distance from the beam supports. This distance is varied for different beams in order to vary the strand embedment lengths. Two 6 by 3 inch (150x75 mm) notches should be cast into the beam directly below the loading points at the bottom the beam in order to expose the reinforcement for instrumentation. A typical flexural test layout is shown in Figure 2.5 . The two-point loading pattern produces a constant moment region between the notches and linearly increasing moment regions over the embedment lengths.

2.3.2.1.1. Steel Reinforcements

This method was followed by Mathey and Watstein (1961) with the exception that the method of support was modified by widening the ends of the beams into a T-shape. This was done in order to move the reaction forces some distance away from the reinforcement to reduce the effect of confinement of the concrete at the supports. As well, the notches, which exposed the reinforcement, was reduced to 3 inches in length from 6 inches and the span was increased to 88 inches (2235 mm) to permit the use of longer embedment lengths. This study determined that the bond strength decreased with an increase in the length of embedment for a bar of a given size. The bond strength also decreased with an increase in the bar diameter for a given length-diameter ratio.

2.3.2.1.2. FRP Reinforcements

A similar study was conducted by Daniali (1992) on FRP reinforcing bars made from glass fibres and vinylester binder. The beams had a span of 112 inches (2845 mm). In order to eliminate the effect of reaction forces on the end of the bars over the supports, the ends of the bars were separated from the concrete by means of two 4 inch (104 mm) long oversized steel pipes. Daniali found that for larger diameter bars the specimens failed due to splitting of the concrete cover in the constant moment region. It was therefore required to place stirrups not only in the end regions of these beams but also in the constant moment region to prevent premature failure. He determined that the

development length varied from 200 mm for #4 bars to more than 762 mm for #8 bars.

A study by Kanakubo, Yonemaru, Fukuyama, Fujisawa, and Sonobe (1993) involved three different kinds of tests to investigate the bond performance of FRP bars. Three different types of FRP were examined (carbon, aramid, and glass) and six different shapes (straight, braided, deformed, strand, spiral, and double spiral). The first type of test was a simple pull-out test on eccentrically placed bars in concrete blocks. The objective of this test was to determine the bond splitting strength of FRP reinforced concrete without lateral reinforcement. The results indicated that the strength could be evaluated using the ratio of lug height to average diameter of the FRP bars. The second type of test involved cantilever type specimens which were modeled to have a similar stress condition as in a real structure. The objective of this test was to determine the increment of bond splitting strength caused by the presence of lateral reinforcement. These tests showed that the incremental bond strength can be evaluated using the elastic modulus of the lateral reinforcement and is influenced by the type of lateral reinforcement and the type of longitudinal bars. The third type of test was antisymmetrical loading tests on beams reinforced with FRP bars. the results of these tests indicated that the bond performance can be predicted using the results of the cantilever type bond tests.

Benmokrane, Tighiouart, and Chaallal (1994) performed bond testing on beams in accordance with the RILEM specifications (RILEM/CEB/FIB,1978) for reinforced concrete members. These beams consisted of two rectangular blocks of concrete joined at the top by a steel ball joint and at the bottom by the reinforcement. The concrete blocks were of 30 MPa compressive strength, were 240x150 mm in cross-section and the

anchorage length was a constant 10 times the bar diameter for all tests. Static loading was applied in two equal forces symmetrically on either side of the ball joint. The testing program in this case consisted of twenty beams with FRP and steel bars 12.7, 15.9, 19.1, and 25.4 mm in diameter. The FRP used in this experimental work was continuous longitudinal glass (E type) fibre strands bound together with a thermosetting polyester resin using a pultrusion process. As well, a sand coating was applied to the bars to enhance their bond properties. The GFRP had a tensile strength of 700 MPa with a modulus of elasticity of 45 GPa and an ultimate tensile strain of 1.8%. From these tests it was determined that the development length of the GFRP bars varied from 15 to 30 times the bar diameter depending on the bar diameter. It was also concluded that the bond strengths derived from these beam tests was lower than that from pull-out tests.

Ehsani, Saadatmanesh, and Tao (1994) tested reinforced concrete beam specimens, 18 pull-out specimens, and 36 hooked bar specimens with #3, #6, and #9 GFRP bars under monotonic loading conditions. The various parameters considered in this experimental program were concrete compressive strength, embedment length, concrete cover, bar diameter, concrete cast depth, radius of bond, and embedment length. The three observed modes of failure were splitting of the concrete, bar pull-out, and bar fracture. Splitting failure occurred when a small concrete cover was provided. For shorter embedment lengths, bar pull-out failure occurred, and under the conditions of longer embedment lengths and sufficient concrete cover the specimens failed by fracture of the bar. It was concluded that due to the absence of flexural cracks in pull-out test specimens, higher ultimate bond stress and greater slippage was developed. This clearly indicated that

it is not safe to rely on data from pull-out tests for determination of development lengths. It was determined that the basic development length of straight GFRP bars should be computed using the following formula.

$$L_d = 0.047 \frac{A_b f_y}{\sqrt{f_c'}} \qquad (2.2)$$

where $f_y = 0.9\ f_u$ for GFRP bars, and which should not be less than $L_d = 0.00035 d_b f_y$. Also to account for the influence of concrete cover, a factor of 1.0 can be used with a cover of not less than two bar diameters and a factor of 1.5 for a cover of one bar diameter or less. As well, for bars with a tensile strength other than 75 ksi (517 MPa), a modification factor of $f_y/75$ (in ksi) should be used.

2.3.2.2. Prestressed Concrete

The previous studies were performed on non-prestressed beams which have no transfer length. To determine the transfer length as well as the flexural bond length other studies have been done using prestressed beams with no notches in them.

2.3.2.2.1. Steel Reinforcements

Studies have been done by Cousins et al. (1990) which follow the same method as outlined by ACI Committee 208 except for the fact that the beams were prestressed and had no notches under the load points. The study was done using grit-impregnated

epoxy coated steel seven wire prestressing strands. It was determined that the development length for these strands was less than that based on ACI provisions. An additional study by Cousins et al. (1990) proposed an analytical model to determine the transfer and development lengths of the same type of strands which seemed to agree well with their test results.

2.3.2.2.2. FRP Reinforcements

A study by Nanni, Utsunomiya, Yonekura, and Tanigaki (1992) was performed on the transfer length of FRP tendons made of braided epoxy impregnated Aramid fibre. Beams 4000 mm (13.1 ft) long and cross-section of 120x210 mm (4.7x8.3 in) were made using different tendon size, number of tendons, surface condition (adhered sand), and initial prestressing force. The testing consisted of strain measurements in the strands and the concrete before and after release of the prestressing force. It was determined that the transfer length was lower for Aramid FRP tendons than for steel strands. This was explained by the fact that the swelling of the ends of the FRP strands in the transfer length (Hoyer effect) was higher than that of steel due to a higher Poisson's ratio for the FRP. However bursting stresses in these regions are consequently higher and may require special attention to avoid concrete cracking.

Another similar study was performed by Nanni and Tanigaki (1992) to determine the development length for Aramid FRP strands. The development length was determined using a three-point flexural test and the flexural bond length was determined using their

knowledge of the transfer length from their previous study. It was again found that the development length of Aramid FRP strands was low in comparison to equivalent steel strands.

Iyer and Khubchandani (1992) tested beams prestressed with seven-wire graphite cables 9.6 mm in diameter. The beams had 152x216 mm (6x8.5 in.) cross-section and were loaded statically up to failure. The transfer length of steel and graphite cables were 61 and 85 strand diameters respectively, which were higher than the ACI 318-89 recommended values, using a prestressing force of 45% of the ultimate strength of the graphite strand. The use of a sand coating doubled the bond strength of the graphite cables. The unsanded graphite cables slipped during transfer of the prestressing force showing poor bond strength with the concrete. Measured values of development length for the steel cables agreed with the ACI 318-89 recommended values, where sanded graphite cables showed lesser values and unsanded cables showed higher values than the ACI recommended values.

Pretensioned double-Tee beams prestressed by Arapree brand AFRP tendons were tested by Arockiasamy, Shahawy, Sandepudi, and Zhuang (1994). These tendons consisted of Twaron Aramid filaments embedded in an epoxy resin. The tendons had a rectangular cross-section of 6x20 mm, with an ultimate strength of 120 kN at 2.3% elongation, and a Young's modulus of 130 GPa. The beams tested were 33 feet long (10 m) with a central constant moment region 15 feet long (4.57 m). Each web of the double-tee had five tendons spaced at 2 inches on centre vertically for a total of ten Arapree tendons per beam. The experimental program is currently in progress and little results

have been reported yet. Test results on one beam indicate no sign of slippage of the tendon with the beam cracking at uniform spacing. This indicates that there is no bond failure between the tendons and concrete.

The serviceability of concrete beams prestressed by CFRP rods was investigated by Abdelrahman (1995). Although the prime objective was to study the serviceability of these beams, the transfer length of the CFRP rods was also evaluated. Eight concrete beams were cast, prestressed by 8 mm diameter Leadline CFRP rods. Six beams were prestressed up to 50% of the guaranteed strength of the rods and two beams were prestressed to 70% of the guaranteed strength. The transfer length for these two sets of tests was estimated to be 360 mm (46 rod diameters) and 500 mm (64 rod diameters) respectively. The average bond strength of the rods in the transfer zone was found to be 5.15 MPa which was comparable to steel (5.21 MPa).

Prestressed beam and slab tests were reported in the "State-of-the-art Report on Continuous Fibre Reinforcing Material" from the Japan Society of Civil Engineers in 1993. AFRP wound tendons of 6 mm diameter registered transfer lengths of 250 mm and 350 mm when the prestressing force is 55% and 76%, respectively, of the tendon tensile capacity. Flat-shaped AFRP tendons showed a transfer length of 60 mm. It was stated however that the flat tendons had a large surface area and were processed to provide irregularities, ensuring a high bond strength and an extremely short transfer length. An AFRP rope consisting of eight wires was used as a prestressing tendon and indicated a transfer length of 280 mm for a prestressing force of 62% of its tensile capacity, using 28 MPa concrete compressive strength. In the case of braided tendons, three different

types were reported all of 8 mm diameter. Braided AFRP tendons with a sand coating indicated a transfer length of 160 mm (20d) for a 65% prestressing force. AFRP tendons with no coating reported a transfer length of 240 to 280 mm (30 to 35 d). Braided CFRP tendons showed a transfer length of 130 mm (16d), however the prestressing force was not reported. Twisted continuous CFRP strands showed a transfer length of about 700 mm (65d) for 10.5 mm diameter strands at 60% prestressing force and 312 to 375 mm (25 to 30 d) for 12.5 mm diameter strands at 45% prestressing force. Indented CFRP tendons of 8 mm diameter showed a transfer length of 1000 mm but the level of prestressing was not reported.

2.3.3. Transfer Prisms

Another type of test, which is used to determine bond characteristics of reinforcements in concrete, is transfer prisms. This test can be used to determine the transfer length only, it can not be used to determine flexural bond length or overall development length of prestressing strands. Specimens are made by prestressing the tendons and casting concrete prisms of small cross-section concentrically with the strand. The prisms are usually square in cross-section and of long length.

2.3.3.1. FRP Reinforcements

Issa, Sen, and Amer (1993) performed this type of testing on GFRP strands. Seven

6 x 4 in. (102 x 152 mm) specimens were used for two concentric 3/8 in. (9.5 mm) diameter S-2 glass epoxy strands prestressed to 50% of their ultimate strength. The transfer length was found to be 10 to 11 inches (254 to 279 mm) or approximately 28 times the nominal diameter of the tendons.

Taerwe, and Pallemans (1993) also used this test to determine the transfer length of Aramid composite prestressing bars embedded in concrete prisms. Arapree AFRP bars of diameters 7.5 and 5.3 mm with a sand coating were used in this experimental program. The specimens used a concrete with compressive strength varied between 71.6 and 81.5 MPa and were prestressed to 55% of the bar ultimate tensile capacity. The transfer lengths determined were 16 to 38 times the bar diameter depending on the type of coating on the bars.

2.4. Temperature Effects

It seems that very little research has been done to determine the effect of elevated temperatures on bond behaviour. The only study which was found dealing specifically with this topic was reported by Diederichs and Schneider in Germany (1982). Their report investigates the bond stress-slip characteristics from pull-out tests. Variables included the type of steel reinforcement (deformed bars, plain round bars, and prestressing bars) and different concrete aggregate types. Two types of aggregates were used in the concrete specimens, basaltic and siliceous types. It was determined that differential thermal strain was the dominant factor affecting the bond strength. For siliceous type

concrete the bond strength reported to be deteriorating greatly for temperatures above 350 C. The bond strength of basaltic type slightly deteriorated for temperatures under 800 C. This can be explained by the fact that for siliceous concrete and steel the thermal strains are the same up to about 350 C. Above this level the concrete strains are higher than that of steel thus causing cracking at the interface bond zone. The basaltic concrete has lower thermal strains at all temperatures as compared to steel and therefore "shrinks" in relation to the steel ensuring adhesion.

Fibre reinforced plastics generally have a high transverse thermal expansion coefficient in comparison to steel. Therefore in terms of the interface behaviour between FRP and concrete it is logical to assume that the bond strength should not deteriorate at high temperatures for FRP. However no studies have been reported on the effect of high temperatures on the bond strength of FRP.

2.5. Code Requirements

The code requirements for the bond properties of concrete reinforcement are outlined in the following sections. Three different codes have been examined namely the CSA code (Canada), ACI code (USA), and CEB-FIP code (Europe).

2.5.1. CSA Code

According to the Canadian Standards Association (CSA) specification the basic

development length for non-prestressed deformed steel bars for No. 35 bars and smaller can be calculated, in SI units, as:

$$L_d = \frac{0.019\ A_b\ f_y}{\sqrt{f_c'}} \tag{2.3}$$

and for deformed wire:

$$L_d = \frac{0.36\ d_b\ f_y}{\sqrt{f_c'}} \tag{2.4}$$

where,

A_b = cross-sectional area of bar (mm^2)

d_b = nominal diameter of wire (mm)

f_y = yield strength of steel (MPa)

f_c' = concrete compressive strength (MPa)

L_d = basic development length (mm)

In addition to these equations there are modification factors applicable for top reinforcement, reinforcement with f_y greater than 400 MPa, low density concrete, reinforcement geometry, reinforcement in excess of that required by analysis, and reinforcement enclosed within spiral reinforcement. These modification factors may be found in CSA specification clauses 12.2.3, 12.2.4, and 12.2.5 .

For three or seven wire steel prestressing strand the transfer (L_T) and development length (L_d) can be calculated, in SI units, as:

$$L_T = 0.048\, f_{se}\, d_b \tag{2.5}$$

$$L_d = L_T + 0.145\, (f_{ps} - f_{se})\, d_b \tag{2.6}$$

2.5.2. ACI Code

For non-prestressed deformed steel bars and wires the basic development length for No. 11 bars and smaller and wires according to the American Concrete Institute (ACI) can be calculated, in imperial units, as:

$$L_d = \frac{0.04\, A_b\, f_y}{\sqrt{f_c'}} \tag{2.7}$$

where,

A_b = cross-sectional area of bar (in^2)

f_y = yield strength of steel (psi)

f_c' = concrete compressive strength (psi)

L_d = basic development length (in)

In additions to this equation there are modification factors which account for bar spacing, amount of cover, and enclosing transverse reinforcement which can be found in clauses 12.2.3.1 through 12.2.3.6 .

For three or seven wire steel prestressing strand the transfer and development length can be calculated in imperial units as:

$$L_T = \left(\frac{f_{se}}{3}\right) d_b \tag{2.8}$$

$$L_d = L_T + (f_{ps} - f_{se})\, d_b \tag{2.9}$$

2.5.3. CEB-FIP Code

The Comité Euro-International du Béton (CEB) design manual for steel reinforcement in concrete members specify the basic development length for non-prestressed smooth steel bars as:

$$L_d = \frac{1.04\, d_b\, f_y}{\sqrt{f_c'}} \tag{2.10}$$

and for high-bond (deformed) bars less than 32 mm in diameter as:

$$L_d = \frac{d_b\, f_y}{0.3\, f_r} \tag{2.11}$$

where,

d_b = nominal diameter of wire (mm)

f_y = yield strength of steel (MPa)

f_c' = concrete compressive strength (MPa)

f_r = concrete modulus of rupture (MPa)

L_d = basic development length (mm)

The manual states that for steel prestressing strand the transfer length should be determined either on the basis of values defined by approvals documents or by means of tests corresponding to the conditions of use. In the absence of these values the following limits are admissible:

$100\ d_b$ to $140\ d_b$ for a wire that is not smooth

$45\ d_b$ to $90\ d_b$ for 7-wire strand

It is also assumed, according to clause 7.2.4.2, that the transfer length consists of two zones. Firstly, a neutral zone near the end of the component of length 5 to 10 times the strand diameter. In this zone it is assumed that there is no force transfer from the strand to the concrete. The length of 5 diameters is applicable when prestressing is carried out by gradual release of the strands, and the length of 10 diameters is applicable when prestressing is carried out by severing of the strands. Beyond this, there is a second zone along which the stress in the prestressing strands varies linearly from zero to the design value.

2.6. Conclusions

It can be concluded from all of these studies that there are five main variables in determining the bond strength of any type of concrete reinforcement.

(i) Concrete strength: where bond strength is proportional to the tensile strength of the concrete and therefore proportional to the square root of the compressive strength

(ii) Concrete cover: where bond strength increases with increasing cover up to a limiting value

(iii) Bar size: where bond strength decreases with increasing bar size

(iv) Embedment length: where bond strength decreases with increasing embedment length

(v) Transverse reinforcement: where bond strength increases with the presence of transverse reinforcement

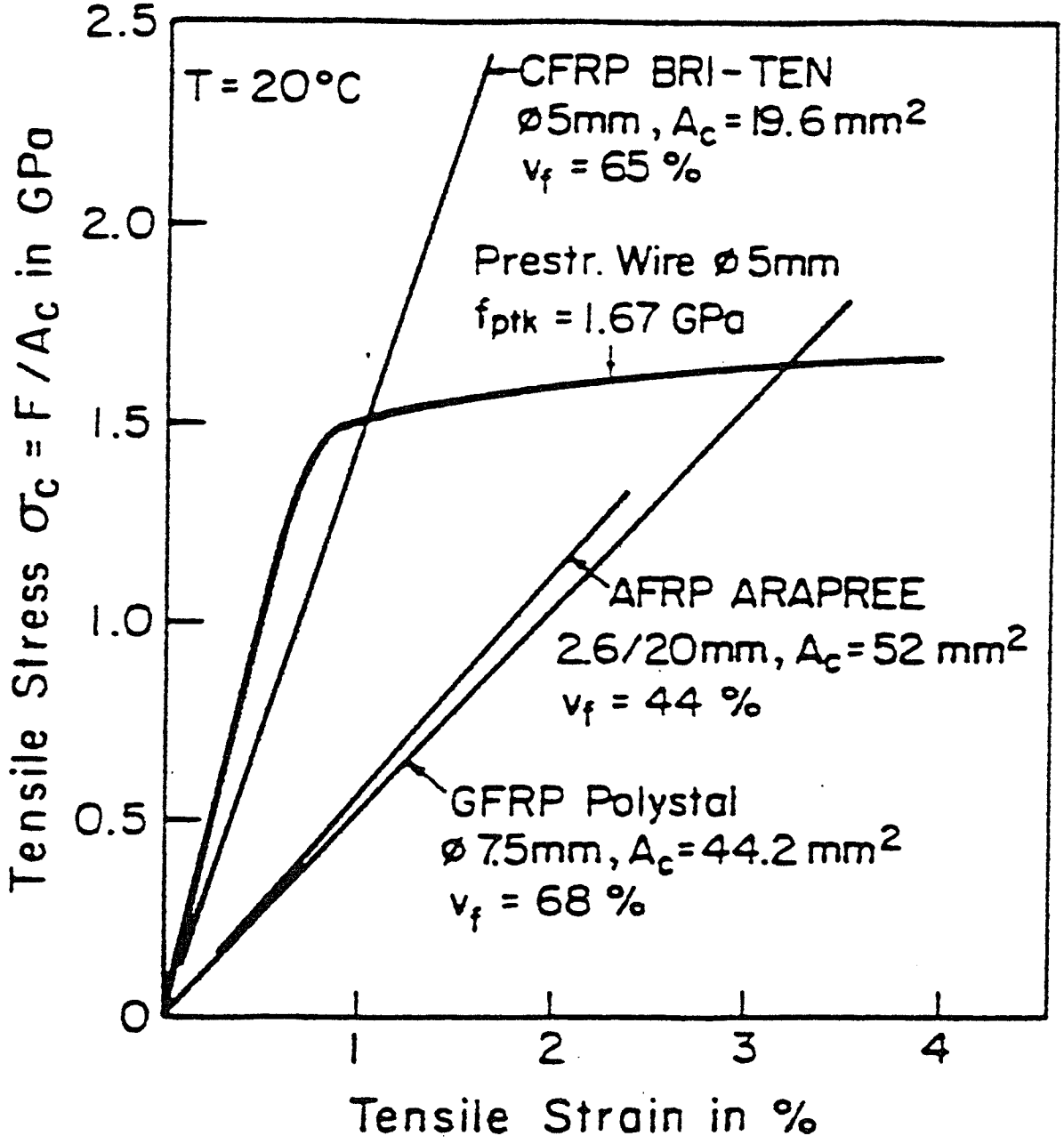

Figure 2.1 FRP Stress-strain Relationships

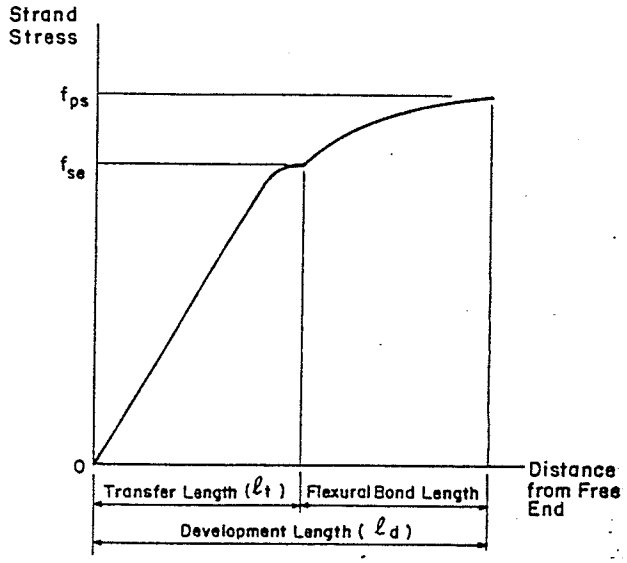

Figure 2.2 Variation of Strand Stress Within the Development Length

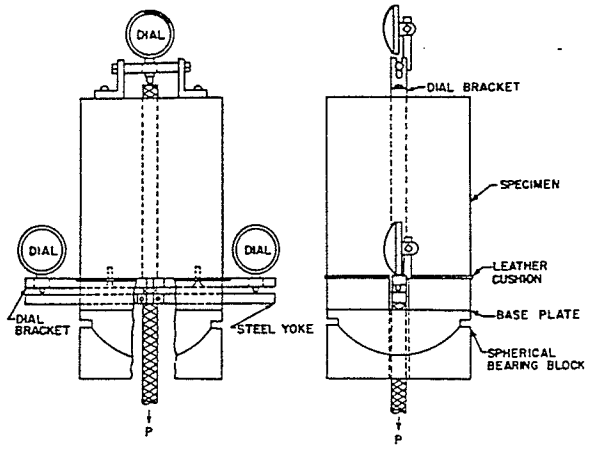

Figure 2.3 Details of Pull-Out Specimen and Test

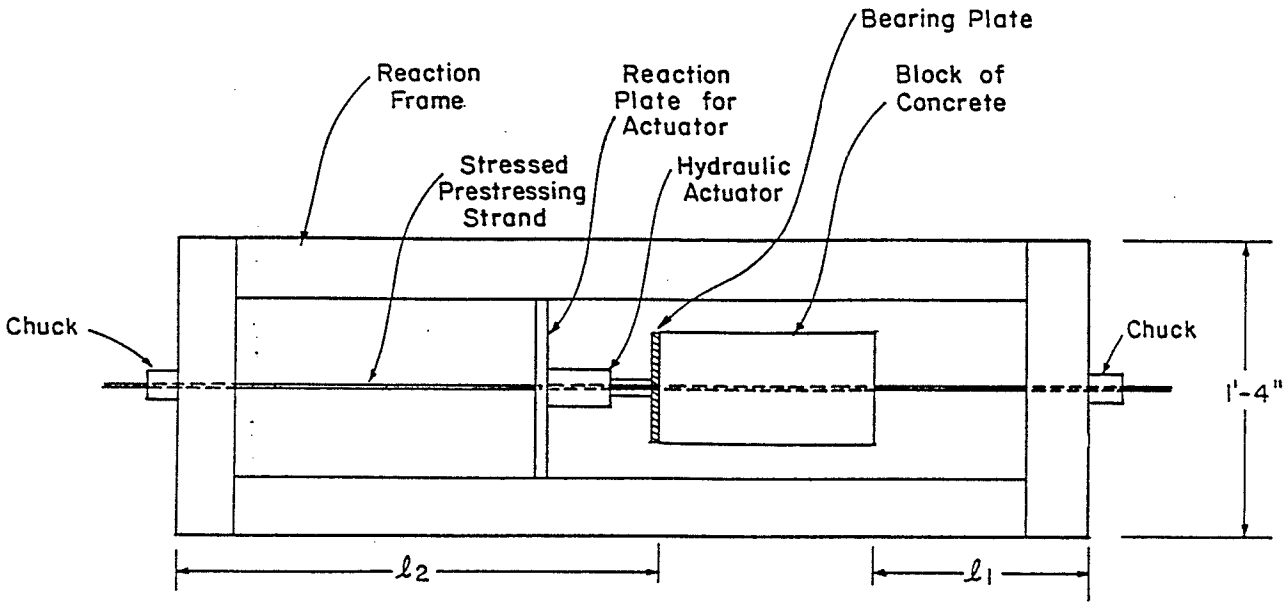

Figure 2.4 Cousins, et. al. Test Layout

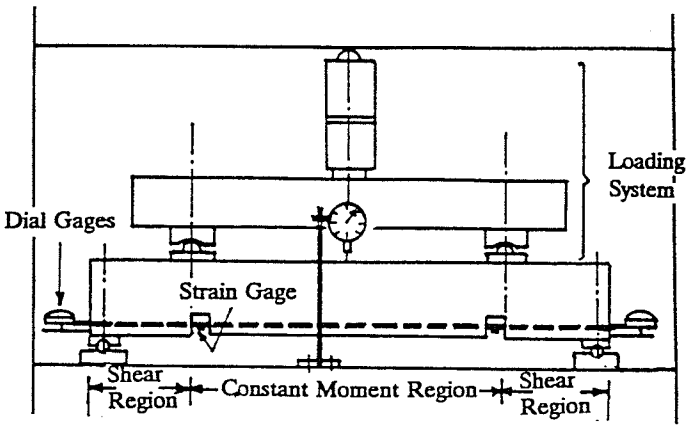

Figure 2.5 Typical Flexural Bond Test Layout

CHAPTER 3

THE EXPERIMENTAL PROGRAM

3.1. General

Bond characteristics of prestressing strands are of particular importance for pretensioned concrete members. It is considered to be the key characteristic in determining the effectiveness of any type of concrete reinforcement. Therefore, the evaluation of bond characteristics of FRP prestressing strands is of prime importance in the design of these members. Bond properties are influenced by many factors that depend on both the type of reinforcement and the concrete. These factors may be summarized as follows:

A- size and type of tendons (wires,strands, or rods)

B- surface conditions (smooth, deformed, braided, oiled)

C- tendon stress (prestressing force)

D- method of stress transfer (sudden or gentle release)

E- concrete strength

F- concrete confinement (transverse reinforcement and concrete cover)

G- type of loading (static, cyclic, impact)

H- tensile strength and modulus of reinforcement

I- Poisson's ratio (Hoyer effect)

J- type and volume of fibre and matrix of FRP reinforcements

The length of tendon at the end zone of a pretensioned member over which the prestress force develops and is transmitted to the concrete is called the transfer length, L_t. Within the transfer length the tendon stress increases from zero at the end of the member to an effective stress, f_{se}, at the end of the transfer length. In order to develop the full strength of a member an additional embedment length called the flexural bond length, L_f, is required. A summation of the transfer length, L_t, and the flexural bond length, L_f, leads to the overall development length, L_d, of the tendon.

3.2. Purpose

The purpose of this research program is to investigate the bond characteristics of carbon fibre reinforced plastic prestressing strands using pretensioned T-shaped concrete beams. The bond characteristics which will be examined are the transfer length, flexural bond length and the corresponding bond stresses for 15.2 mm diameter and 12.5 mm diameter seven-wire CFCC prestressing strands supplied by Tokyo Rope Manufacturing Company Ltd. in Japan.

Of all the different variables which may influence the transfer and development lengths of these strands it was decided that four parameters be investigated in this research program. These parameters are:

1. the prestressing strand diameter
2. the shear span of the test beams
3. the thickness of concrete cover

4. the initial prestressing force (degree of prestressing)

All other parameters were held constant throughout this study. The tendons were all seven-wire CFCC strands supplied by the manufacturer without any additional special surface treatments. The prestressing force was transferred to the concrete in a gentle manner under a gradual release, and the concrete strength was uniform using a common mix design. The amount of transverse reinforcement (two-legged steel stirrups) was constant, and the beams were loaded quasi-statically with the same load rate.

To determine the bond characteristics of CFCC prestressing strands, a total of ten prestressed flexural bond beams were cast and tested. Initially, two pilot beams were cast and tested first followed by the remainder. The specifications of the parameters are outlined in Table 3.1 .

3.3. Materials

This experimental program involves the manufacturing and testing of pretensioned prestressed concrete beams. The following sections describe the material characteristics of the CFCC prestressing strands and the concrete used.

3.3.1. CFCC Prestressing Strands

In this experimental program, Carbon Fibre Composite Cables (CFCC), produced

by Tokyo Rope Manufacturing Company Ltd., Japan, were used for pretensioning the concrete beams. The two different strand diameters used in this program were 15.2 mm and 12.5 mm nominal diameter with cross-sectional areas of 113.6 mm^2 and 76.0 mm^2 respectively. The guaranteed ultimate tensile strengths reported by the manufacturing company are 1750 MPa for the larger diameter strands and 1870 MPa for the smaller diameter strands. The elastic modulus is 137 GPa, and the ultimate tensile strain of the strands is 1.6% . Other characteristics of CFCC strands are reported in Table 3.2 .

The anchorage system used in prestressing the CFCC strands was a diecast method. In this method an alloy is diecast onto the end of the CFCC strand and is then anchored with a conventional wedge system. The disadvantage of this system is that the diecast is installed by the manufacturer and therefore the strands have to be ordered to a specified length. The advantage of this system is that the prestress losses incurred in its use are minimal, the wedge anchorage may be reused, and the alloy may be reused by remelting. The diecast is manufactured in lengths of 250 mm and 300 mm for 12.5 and 15.2 mm diameter strands respectively.

The stress-strain relationship of CFCC strand is linear up to failure as reported by the manufacturing company and measured at the Structural Engineering and Construction, Research and Development Facility at the University of Manitoba, Canada. A single static tension test was performed on 15.2 mm diameter CFCC strand. This test resulted in an ultimate tensile stress of 1955 MPa, an ultimate tensile strain of 1.27%, and an elastic modulus of 155.6 GPa. These values are higher than those reported by the

manufacturer with the exception of the ultimate strain which was approximately 20% less.

3.3.2. Concrete

The concrete used in the beam specimens was provided by Perimeter Concrete Ltd. , a local ready mix supplier in Oak Bluff, Manitoba, Canada. The concrete had a 14 mm maximum aggregate size, a water cement ratio of 0.37, and a slump of approximately 175 mm. The slump was achieved with the use of a superplasticizing admixture, " Reobuild 1000 ", in the quantity of approximately 3 l/m^3. The mix proportions by weight were 1 (Portland cement) : 2.9 (coarse aggregate) : 1.7 (fine aggregate).

Standard concrete cylinders were made at the time of casting of each beam. These were tested in compression at the time of the release of the prestressing forces and at the time of beam testing to determine the concrete properties. The compressive testing was performed according to ASTM C39-86. Concrete cylinders were also tested to determine the concrete elastic modulus according to the procedures in ASTM C469-87a. As well, small concrete beams 150x150 mm were made at the time of casting of each beam and were tested according to ASTM C78-84 to determine the concrete flexural tensile strength. A summary of concrete mix design can be seen in Table 3.3 .

3.4. Test Specimens

Ten pretensioned prestressed concrete T-shaped beams were tested in this experimental program. The beams are made 3200 mm long with a 330 mm depth and 260 mm effective depth. The beams are tested quasi-statically as simply supported with a span of 2800 mm and 200 mm overhanging the supports. The prestressing tendons were debonded over the 200 mm overhang at each end in order to minimize stress disturbances and confinement caused by the support reaction forces. A detailed description of the test program may be seen in Table 3.1. Cross-sections of the beam specimens may be seen in Figure 3.1a . All beam specimens have shear reinforcement in the form of two-legged steel stirrups with 6 mm diameter, spaced at 100 mm, and with a minimum yield stress of 400 MPa. Tests performed on the stirrup steel at the University of Manitoba indicated that the steel had a tensile strength on the order of 550 MPa. The stirrups were hung from 6 mm diameter plain steel longitudinal bars located in the beam flange. The flange was reinforced with steel mesh WWF 102 x 102, MW 25.8 x MW 25.8. To minimize stress disturbances caused by the reaction forces, two steel plates 101.6 mm (4") x 400 mm x 12.5 mm (1/2") thick were placed at the bottom of the web at the ends of the beams.

3.5. Jacking and Casting Set-up

A schematic plan view of the jacking and casting set-up for the beam specimens can be seen in Figure 3.2 . The beams were cast in pairs with the prestressing force

applied by two hydraulic jacks, 500 kN capacity each, with locking nuts to maintain the force after jacking. Photographs of the prestressing setup may be seen in Figures 3.8a and 3.8b . The jacks pushed against a fixed abutment and against a spreader beam. The spreader beam consisted of two C-channels bolted back-to-back. The CFCC cables were threaded through the channels to another set of channels at the dead end of the set-up and anchored. The dead end channels were held stationary by another abutment fixed to the floor. Plywood forms were placed around the cables to form the concrete beam specimens. During jacking, the forces were monitored by 1000 kN capacity load cells placed between the jacks and the spreader beam. The tendon elongation and strain was monitored by Linear Variable Displacement Transducers (LVDT's) placed at the jacking end of the set-up and electrical resistance strain gauges placed along the cables themselves. Three days after the beam casting the prestressing forces were released gradually using the jacks and the forms were stripped from the specimens. The beams were removed using a 45 kN (5 ton) capacity overhead crane attached to two lifting points approximately 0.5 m from the ends of the beam.

3.6. Testing Setup

A schematic drawing of the first testing setup for the first two pilot beams may be seen in Figure 3.3 . For the two pilot beam tests a closed-loop MTS testing machine of 5000 kN (1.2 million pounds) capacity was used to apply the loading to the beam. Range cards of 1000 kN load and 200 mm stroke were used in the MTS machine for the

tests. Load was applied to the beam by the machine under stroke control with a rate of 1 mm/min. up to the cracking load and then was changed to 2 mm/min. after cracking up to failure. The beams were simply supported during testing with roller supports provided at each end. The bottom portion of each roller support was attached to concrete blocks which were fixed to the floor.

The load was applied at the specified loading points by the use of a load spreader beam. This scheme allows the load to be transferred from the load piston of the machine to the desired load points on the beam evenly. The spreader beam consisted of a steel HSS section 10 x 150 x 150 x 1600 mm, two roller supports, and two steel HSS sections 100 x 100 x 300 mm. The purpose of the two smaller HSS sections was to distribute the load evenly, laterally across the flange of the beam.

The concrete surfaces of the beams tended to be slightly rough. Therefore to distribute the loads evenly, Plaster of Paris pads were placed between all of the interfaces between the concrete and the roller supports or spreader beam.

A schematic drawing of the second testing setup for the remaining beams may be seen in Figures 3.4 and 3.5 . For these beam tests a smaller closed-loop MTS testing machine of 1000 kN (225 kips) capacity was used to apply the loading to the beam. Range cards of 1000 kN load and 100 mm stroke were used in the MTS machine for the tests. Photographs of the test setup may be seen in Figures 3.10a through 3.10e . Load was applied to the beam by the machine under stroke control with a rate of 0.2 mm/min up to the cracking load and then was changed to 0.4 mm/min after cracking up to failure. The beams were also simply supported with roller supports provided at each end. The

bottom portion of each roller support was attached to concrete blocks which rested on the floor.

A spreader beam was again used to apply the load at the specified loading points. The spreader beam consisted of a steel section W310x39 x 2050 mm long, two roller supports, and two steel HSS sections 100 x 100 x 300 mm. Plaster of Paris pads were placed between all of the interfaces between the concrete and the roller supports or spreader beam.

3.7. Instrumentation

The mid-span deflection of the beam was recorded using two LVDT's (Linear Voltage Displacement Transducer) of 125 mm stroke on both sides of the beam. For beams A1, A2, and A3 vertical displacements of the beam at the supports was also recorded using an LVDT of 25 mm stroke at each end of the beam. Strain in the CFCC cable was monitored using electronic strain gauges along the entire length of the cable. The gauges used were purchased from the Showa Measuring Instruments Company Ltd. of Tokyo Japan, were type N11-FA-5-120-11 with a gauge length of 5 mm and electrical resistance of 120 Ω. The strain gauge layout for each beam is shown in Figure 3.6 .

Additional measurements were made of concrete strain using demec gauges of 200 mm and 50 mm gauge length. The accuracy of the demec gauge readings was 0.8×10^{-5} mm/mm. The demec point layout for each beam is shown in Figures 3.7, 3.10c, and 3.10d . Longitudinal concrete strains were measured at the height of the

CFCC strand along the entire length of the beams using the 200 mm and 50 mm demec gauges. Strain at the extreme concrete compressive fibre at midspan was measured using the 200 mm demec gauge. For beams A1 and A2 the 50 mm demec gauge was used to measure bursting strains around the CFCC strand in the development length region. Demec point readings were taken in increments of 5 or 10 kN of applied load for beams A1 and A2, and increments of 10 or 20 kN of applied load for the remaining beams, depending on the load range. Dial gauges were used to measure any slip in the CFCC strand at the beam ends during loading. The dial gauges were fixed to each end of the beams and rested on the exposed ends of the strand.

The data acquisition system used in the testing consisted of 48 input channel capacity, sample rate capacity of 40 samples per second,and a Data Scan 7000 digital card of 16 bit resolution at a range of 10 volts $\pm$ 0.3 millivolts. The software package "Labtech Notebook" was used on an IBM compatible personal computer. The software was programmed to store the data at a rate of one sample every two seconds. The load and stroke of the MTS machine head were also recorded.

Table 3.1. Beam Specifications

Beam No.	Strand diameter (mm)	Concrete Cover (mm)	Prestress Force (%)	Shear Span (mm)	Study	Beam X-sec. Type
A1	15.2	50	50	1200	A	a
A2				1000	A	a
A3				700	A,C,D	a
C4			70	700	C	a
D5		75	50	700	D	b
B6	12.5	50	50	700	B	a
B7				550	B	a
B8				450	B,C,D	a
C9			60	450	C	a
D10		75	50	450	D	b

Study A - Determine transfer and developement length for 15.2 mm diameter strand
Study B - Determine transfer and developement length for 12.5 mm diameter strand
Study C - Determine the transfer length and bond stress for different prestressing forces
Study D - Determine the influence of side concrete cover on transfer length and bond stress

Type a - Beam cross-section with 100 mm web width
Type b - Beam cross-section with 150 mm web width

Table 3.2. Characteristics of CFCC Strands as Reported by the Manufacturer

Characteristic		Size of CFCC Strand	
		1x7 12.5 mm	1x7 15.2 mm
Tensile strength (MPa)		2120	2150
Breaking load (kN)		160	244
Elongation at break (%)		1.57	1.6
Tensile modulus (GPa)		137	137
Unit weight (g/m)		153	227
Cross-section area (mm^2)		76.0	113.6
Shearing strength (MPa)		181	--
Relaxation	20 C x 0.8Pu x 10h	0.66	1.05 (1)
	60 C x 0.8Pu x 16h	2.46	3.50 (2)
Creep (%) 130 C x 60% x 1000h		0.04	--
Coeff. of linear expansion		0.6x10^-6	0.6x10^-6
Specific resistance (micro-ohm cm)		3000	--
Efficiency of impact loading (%)		88	--
Bending stiffness (N mm^2)		5.7	6.0
Adhesive force to concrete (MPa)		7.23	6.67

Note: (1) 22 C x 0.65Pu x 100h

(2) 22 to 80 C x 10h to 22 C x 30h x 0.65Pu

Table 3.3 Concrete Mix Design

	Quantity (kg/m^3)	% by weight
Portland cement	400	16.8
coarse aggragate (14 mm maximum diameter)	1149.6	48.3
fine aggregate (passing #4 seive)	679.8	28.6
water	148.5	6.2
superplasticizer (Reobuild 1000)	3 *	-

Notes:

- * approximate value
- water/cement ratio = 0.37

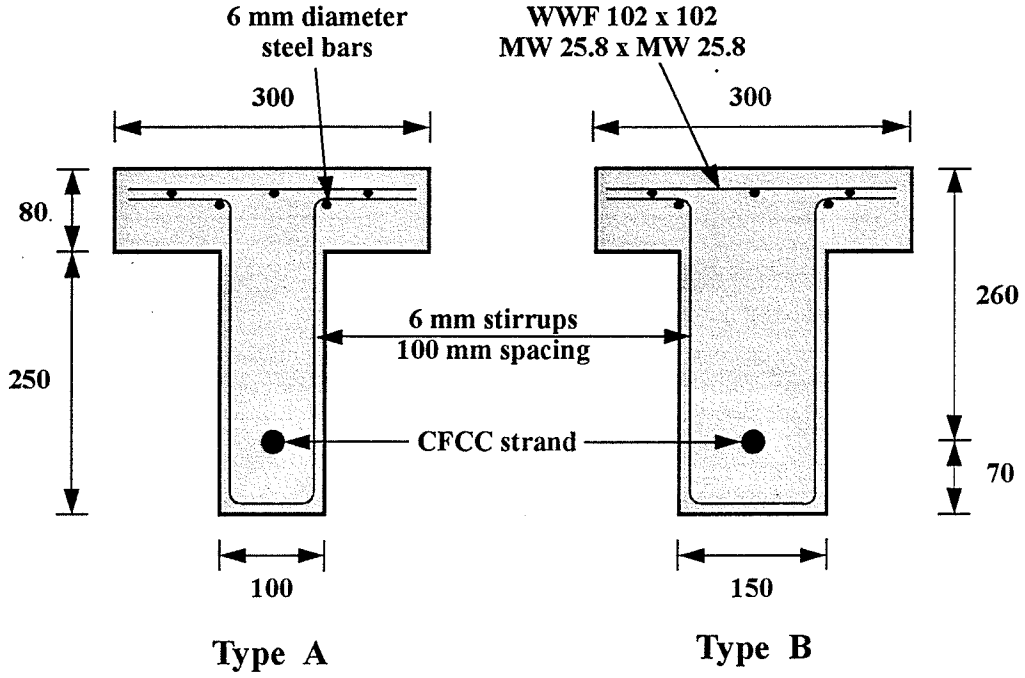

Figure 3.1a Cross-Sections of Beam Types A and B

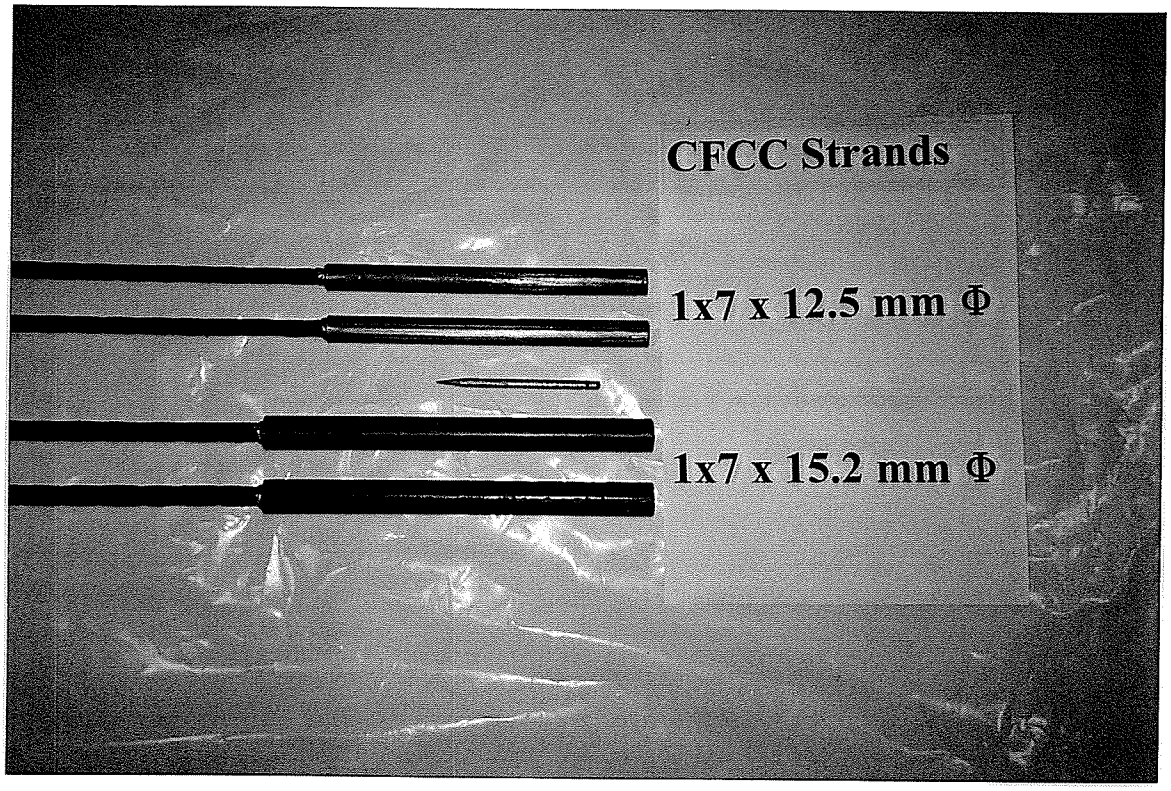

Figure 3.1b CFCC Prestressing Strands

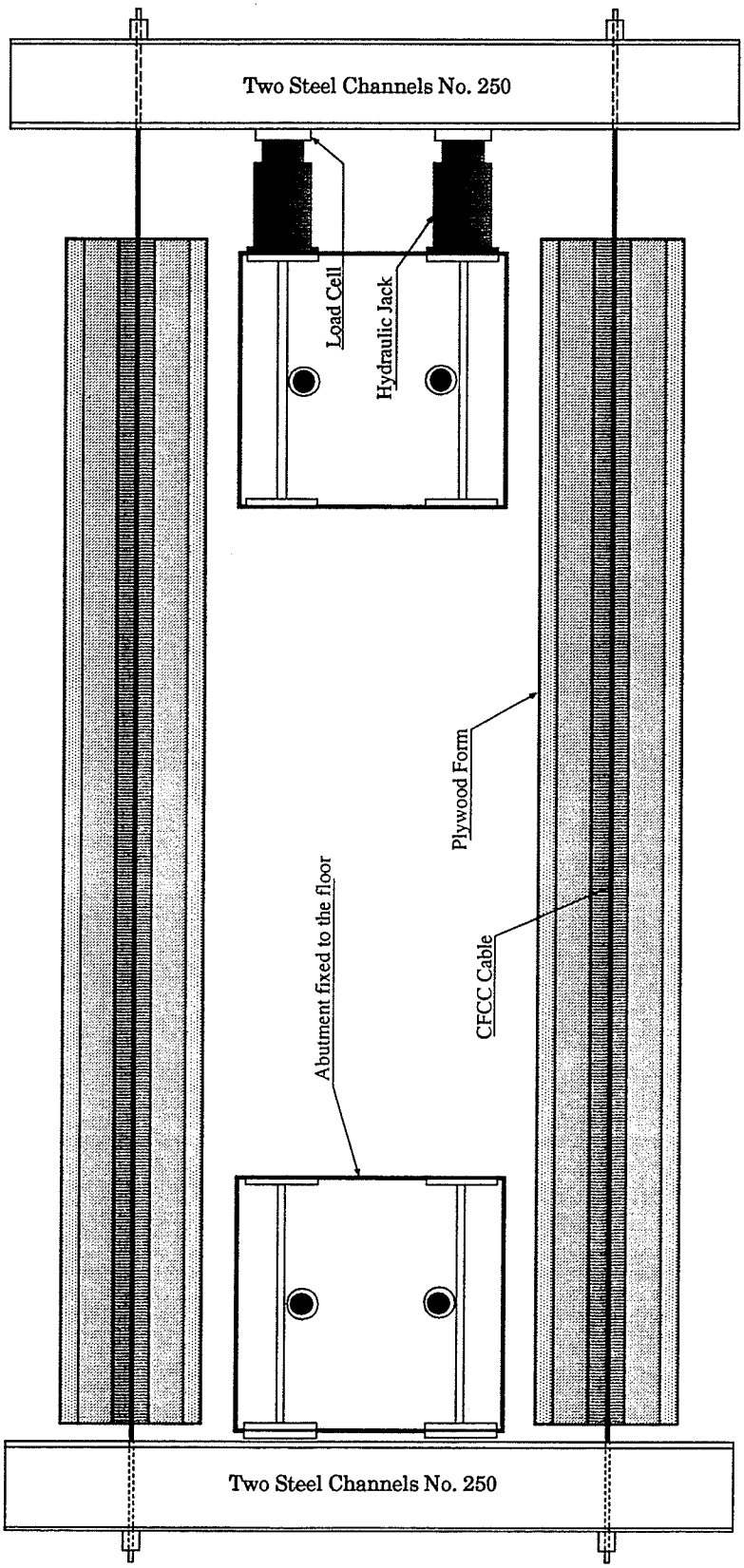

Figure 3.2. Plan of Prestressing and Casting Setup For Two Beam Specimens

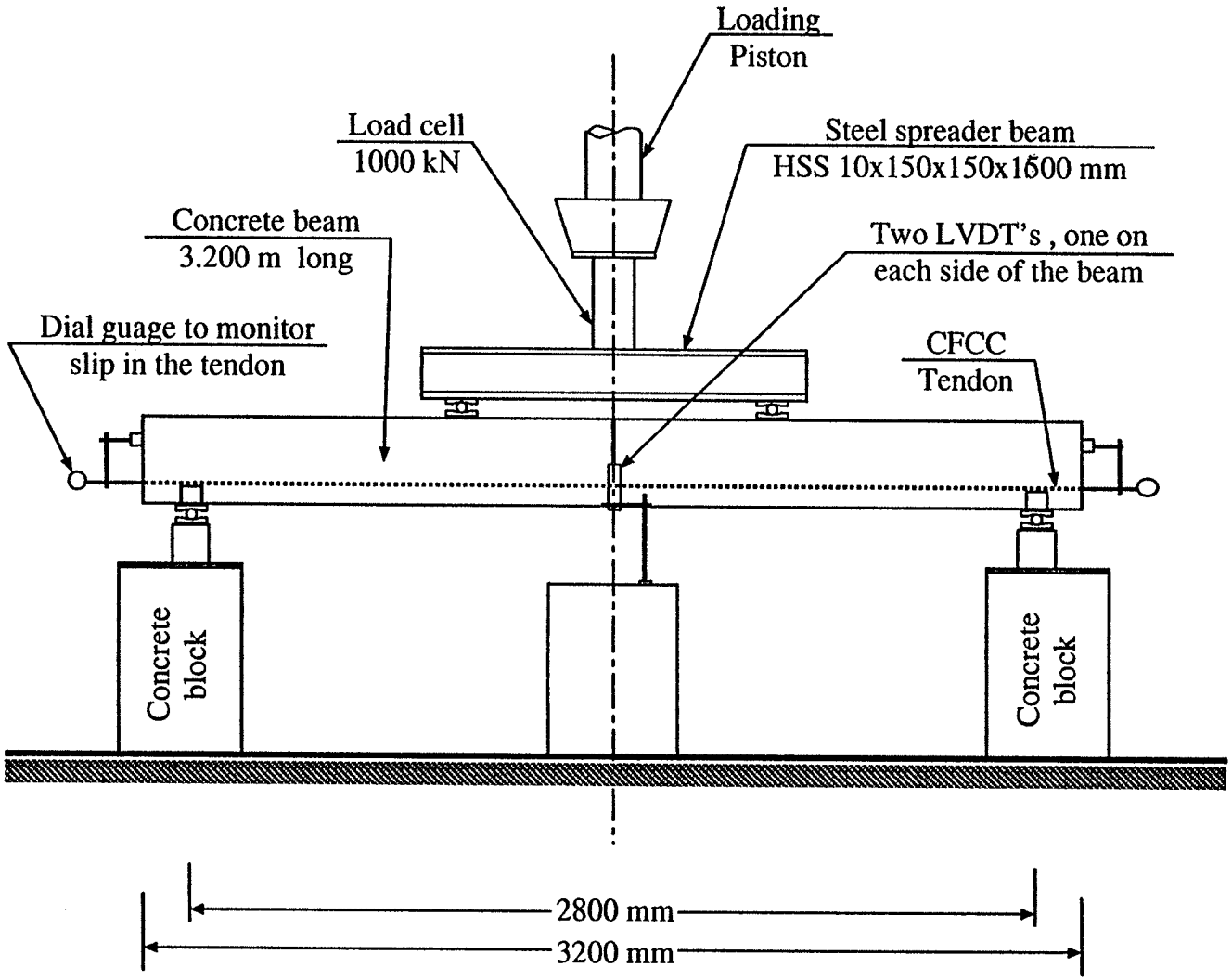

Figure 3.3 Elevation of First Test Setup

Elevation of Test Setup

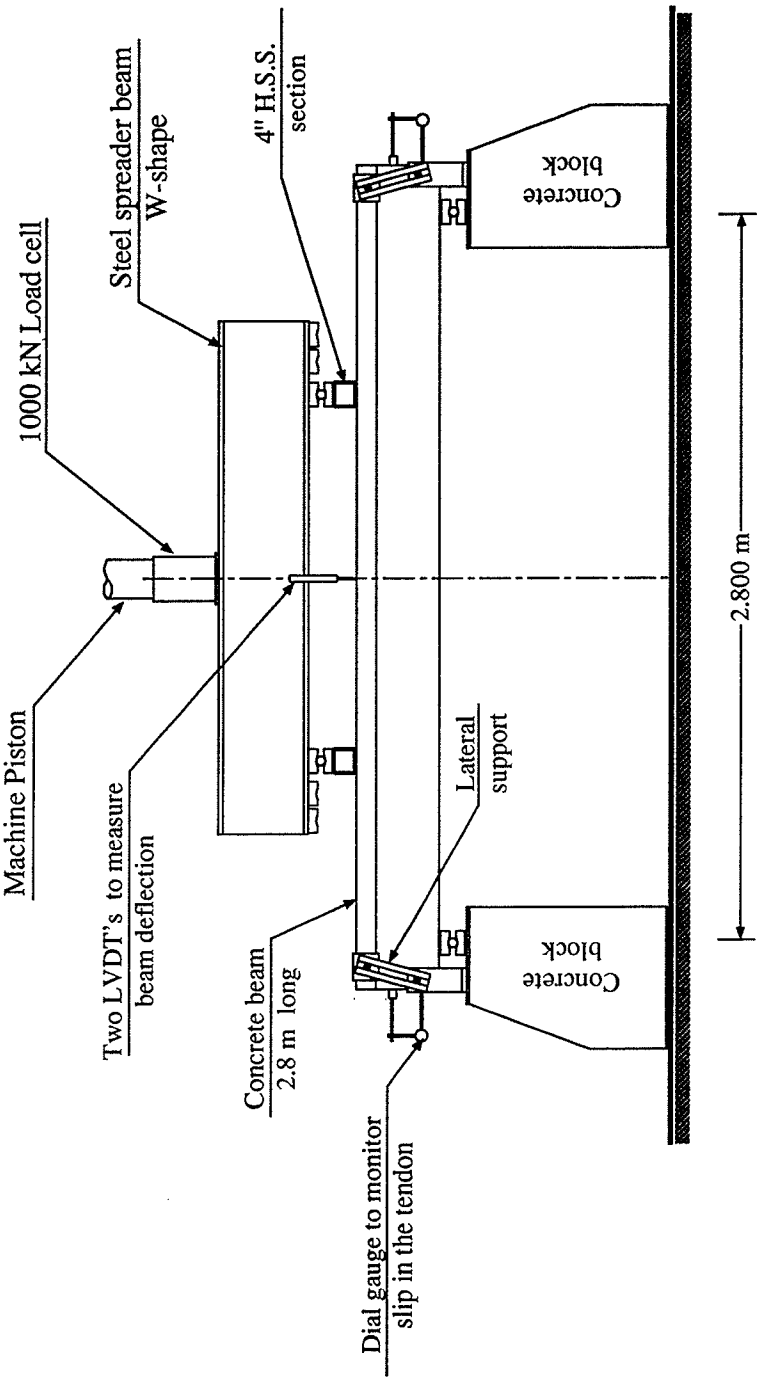

Figure 3.4. Front View Schematic of test set-up

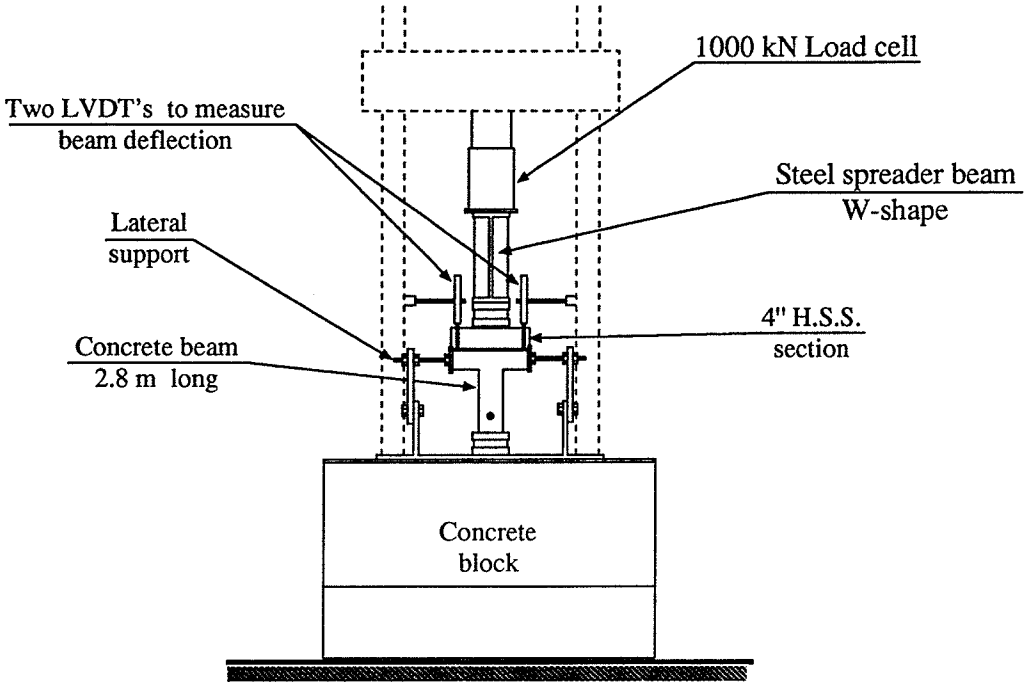

Figure 3.5. Side View Schematic of test set-up

Beams A1, A2, A3, C4, D5 :

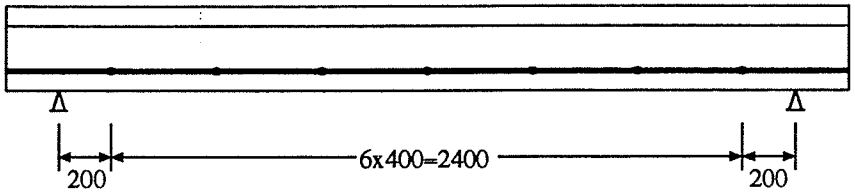

Beam B6 :

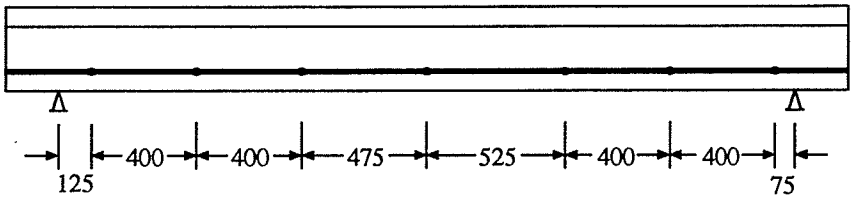

Beam B7 :

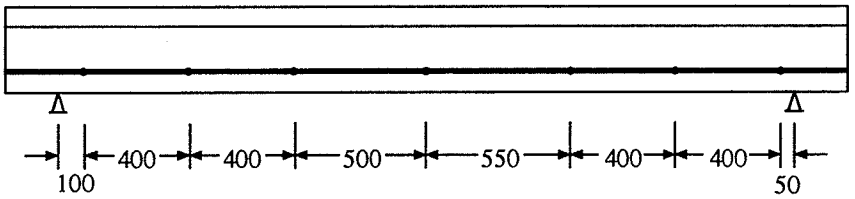

Beam B8 :

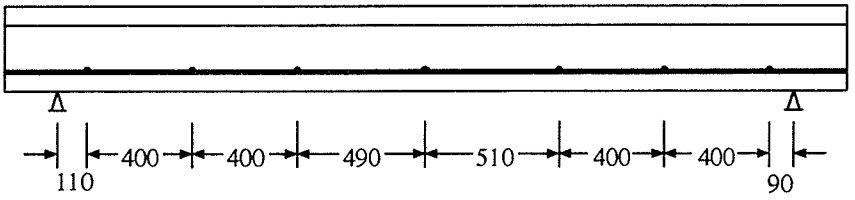

Beam C9 :

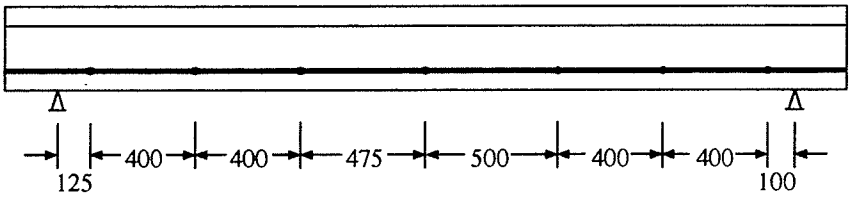

Beam D10 :

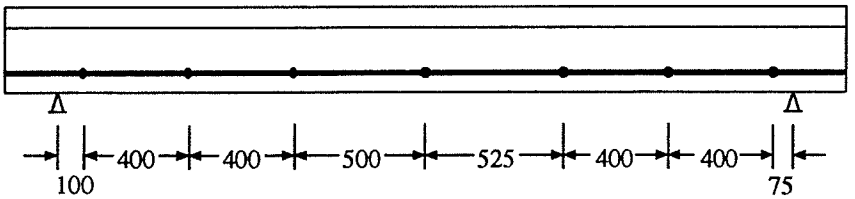

Figure 3.6. Locations of Strain Gauges

Figure 3.7. Locations of Demec Points
(all dimensions in mm)

Beams A1, A2 :

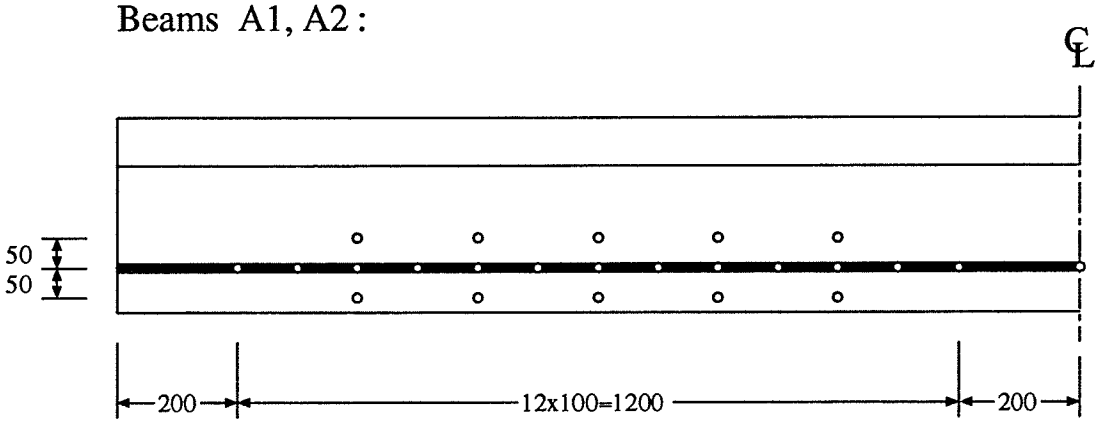

Beams A3, C4, D5, B6, B7 :

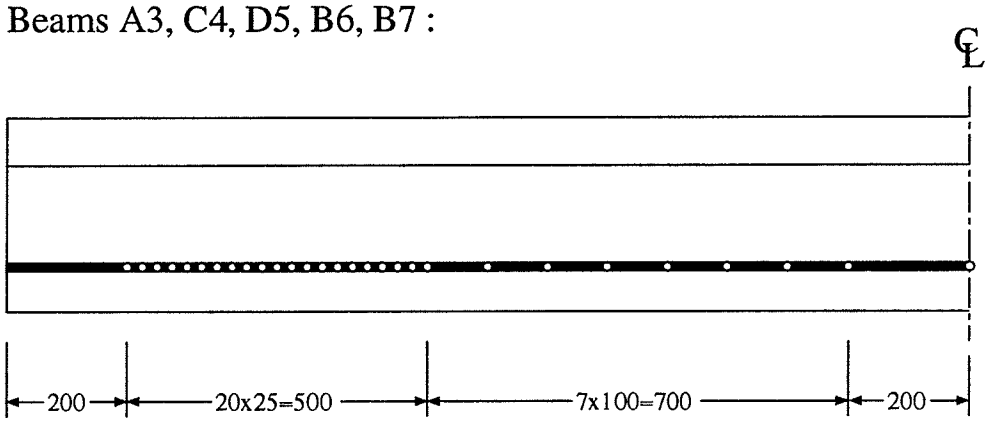

Beams B8, C9, D10 :

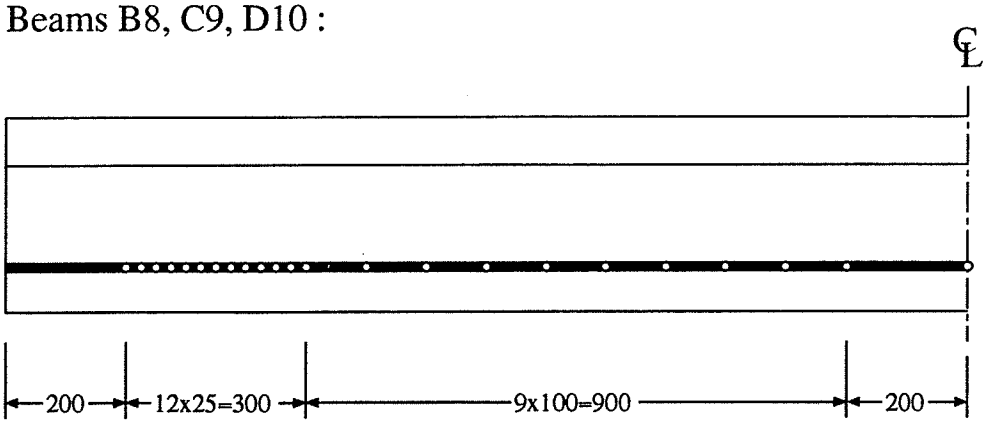

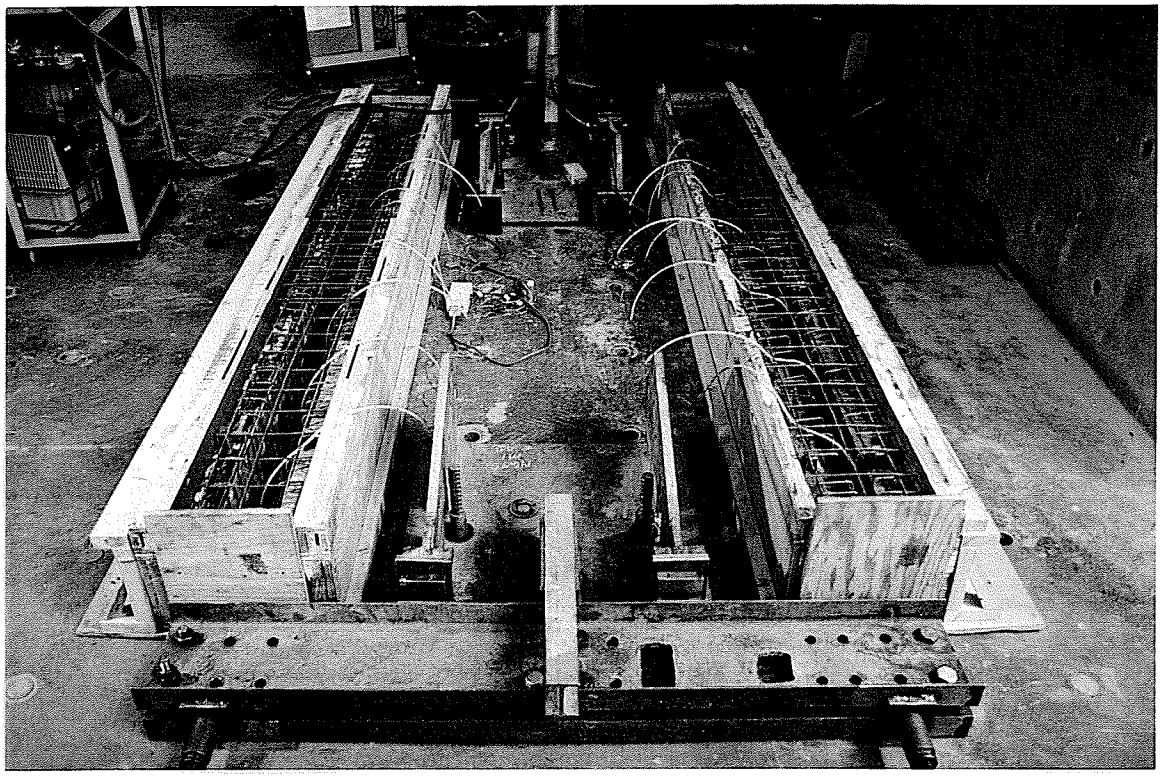

Figure 3.8a Prestressing and Casting Setup

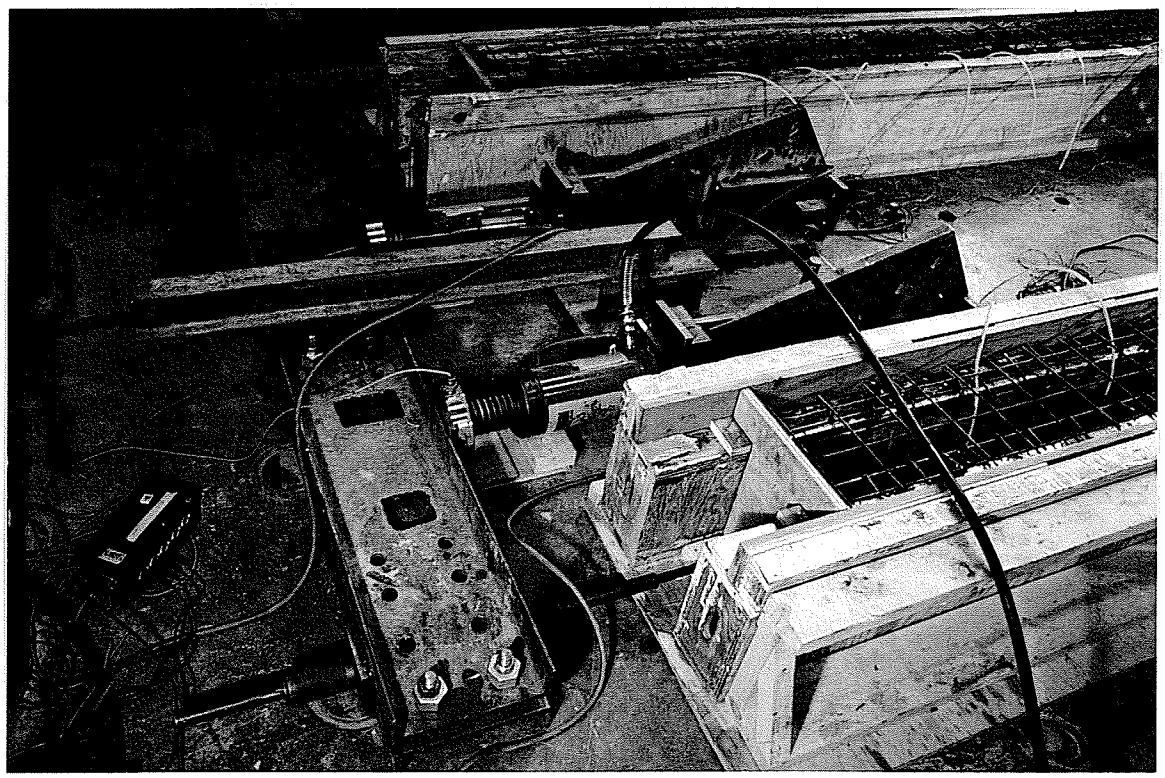

Figure 3.8b Close-up of Jacking End

Figure 3.9 Reinforcement at End of Beam

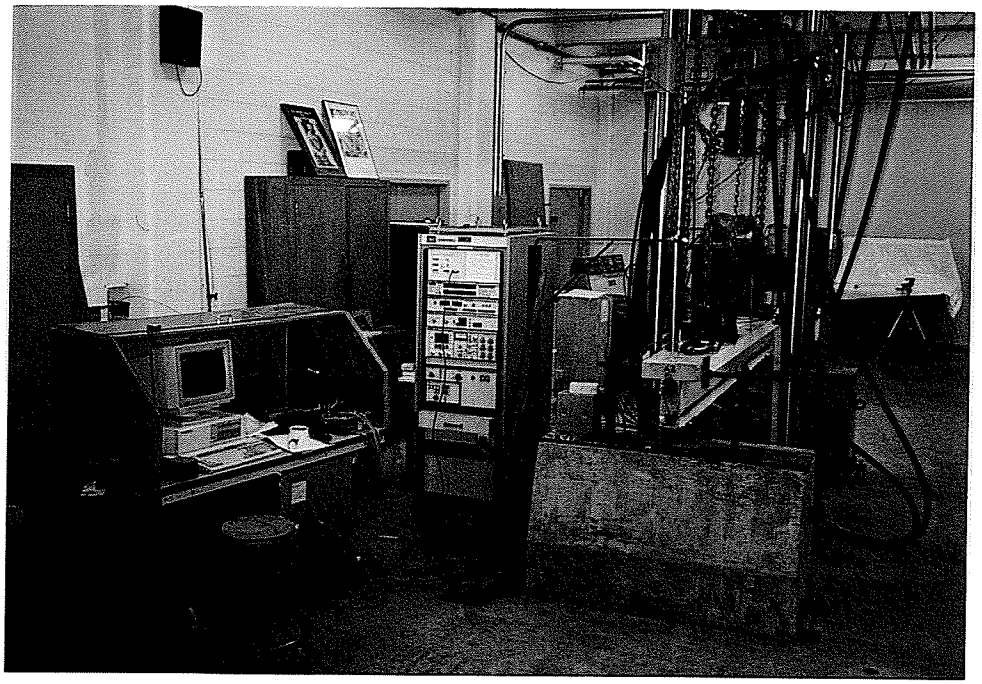

Figure 3.10a Test Setup

Figure 3.10b Loading Spreader Beam

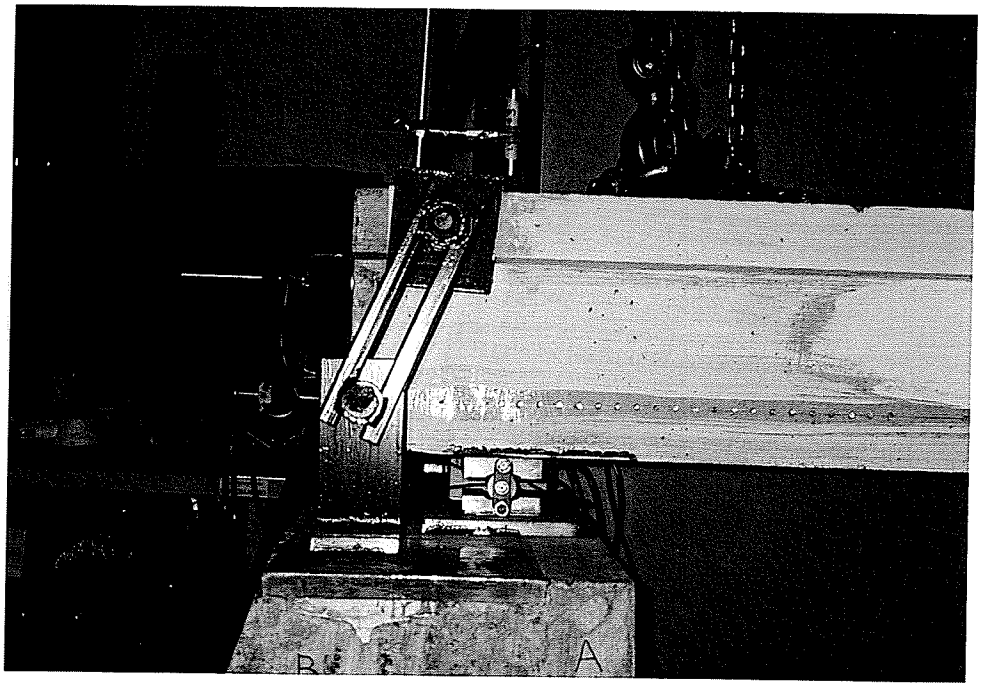

Figure 3.10c Test Setup - Left End Lateral Support

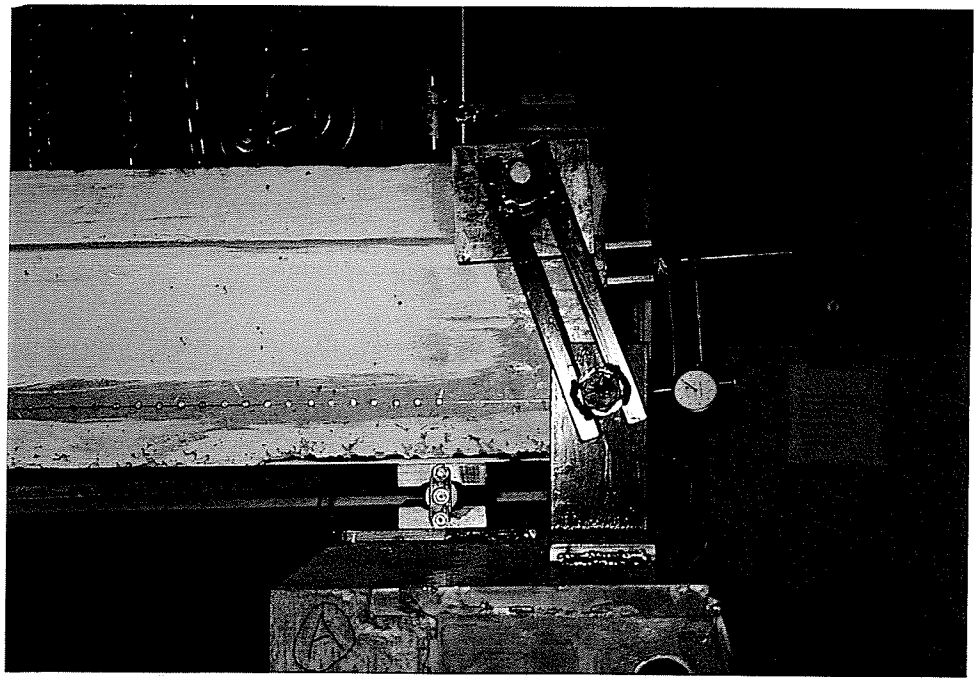

Figure 3.10d Test Setup - Right End Lateral Support

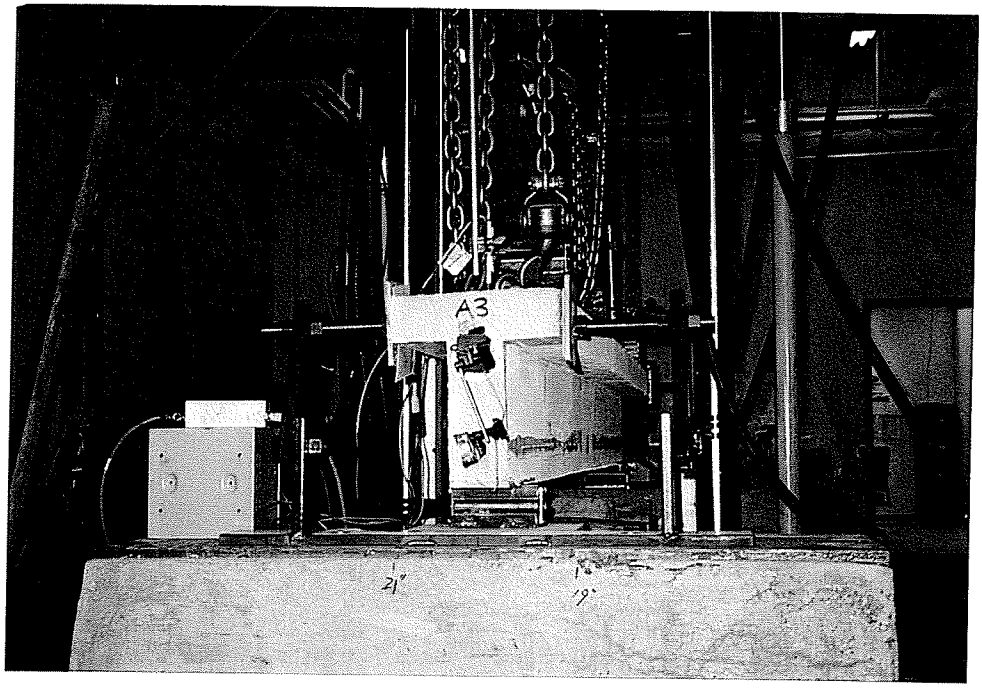

Figure 3.10e End View of Test Setup

CHAPTER 4

EXPERIMENTAL RESULTS

4.1. General

Ten prestressed concrete beams designated A1,A2,A3,C4,D5,B6,B7,B8,C9, and D10 were tested. In the designation, letters A through D indicate the parameter considered for each beam, and numbers 1 through 10 are the beam numbers. The beam cross-sections may be seen in Figure 4.1 . Each beam was prestressed by one CFCC strand stressed to a percentage of its guaranteed ultimate tensile strength. Prestressing was monitored by measuring the strain changes in the strands using electrical resistance strain gauges. As well, demec point gauges were used to monitor strain changes in the concrete at the level of the strand and at the extreme compressive fibre at mid-span after hardening of the concrete.

4.2. Prestress Losses

The prestress losses were measured for the ten beams based on strain gauge and demec point measurements. Strain in the cables was measured at different embedment lengths from each end of the beam for a total of seven strain gauge locations per beam. Strain in the concrete was measured by demec point readings starting at the beginning of the transfer length for each end of the beam and ending at the beam centre. Table 4.1

summarizes the elastic losses, creep losses up to the time of testing, and total losses for all beams. Figures 4.2 through 4.11 show the creep and relaxation losses as measured by the strain gauges and demec gauges along each beam. The losses due to elastic shortening ranged from 1.5 to 2.7 % according to demec point readings and from 1.3 to 2.3 % according to the strain gauge readings. The losses due to creep and relaxation ranged from 5.7 to 9.4 % according to demec point readings and from 6.4 to 14.3 % according to the strain gauge readings. Therefore, the total losses ranged from 7.2 to 12.1% according to demec point readings and from 8.2 to 17.0 % according to the strain gauge readings.

4.3. Transfer Length

The transfer length is defined as the cable embedment length required to develop the full prestress force in the concrete section. The transfer length was estimated by measuring strain changes before and after release of the prestressing force to the concrete section.

Three days after casting of the concrete the prestressing force was released to the beams slowly by releasing the pressure in the jacks. At this time the concrete strength was determined by standard concrete cylinder compressive tests. The tendon strains along the entire beam span before and after release may be seen in Figures 4.12 through 4.21 . In these figures the top line is the measured strains before release and the bottom line is the measured strains after release.

It should be noted that the variation in the magnitude of the tendon strain along the cables in Figures 4.12 to 4.21 is most likely due to two factors. The first is the fact that the strain gauges are placed on individual wires within the seven-wire strand. Any wire within the cross-section may be stressed slightly different than the adjacent wires and therefore the strain gauge reading may be slightly different. Secondly, the strain gauges themselves are not exactly aligned with the longitudinal axis of the wire. Any misalignment would result in strain gauge readings slightly less than the actual strain in the wire. It is due to these two factors that the strain gauge readings vary along the tendon when it is known that the strain should be constant beyond the transfer length. However, the strain changes before and after release recorded by the gauges can be trusted as being accurate.

For the strain gauge data the transfer lengths were determined for each beam or set of beams by the following method. Firstly, the cable strains after prestress release were expressed in terms of a percentage of the strains before release for normalization purposes. Secondly, all of the data which was clearly beyond the transfer zone was averaged to determine the elastic prestressing losses. Then a linear regression analysis was performed on the data inside the transfer zone. The transfer length was then determined as the point of intersection of the regression line and a horizontal line at the average of the interior gauges.

From the strain gauge data Figures 4.22 through 4.29 show the tendon strains expressed as a percentage of the strain before release. In these figures the strain gauges are at different locations for each beam in order to best determine the transfer lengths.

As well, in each figure the linear regression line and the horizontal line placed at the average of the interior gauges is shown. Again, the point intersection of these two lines is concluded to be the transfer length.

The concrete strain at the tendon level after release may be seen in Figures 4.30 through 4.37 as determined by demec gauges on the concrete surface at the height of the strand. In these figures the same method was used to determine the transfer lengths as in the strain gauge figures. A linear regression line is passed through the data in the transfer zone and a horizontal line is placed at the average of the interior data. The point intersection of these two lines is then concluded to be the transfer length.

The concrete strain data in the transfer zone obtained from demec point gauges was highly scattered. This was due to the fact that the strain being measured was on the order of 10^{-4} while the sensitivity of the demec gauge was 2.5×10^{-5} , in other words the error was approximately 25%.

According to Taerwe (1993) the transfer length measured by demec point gauges is not fully accurate and should be corrected. The difference being that the measured transfer length is the distance over which a linear distribution of the longitudinal concrete stresses is developed while the actual transfer length is the distance over which the full initial prestress is developed. This difference is due to a shear lag effect from the prestressed cable to the outer face of the concrete. Therefore the transfer lengths measured by demec point gauges are corrected by subtracting the concrete cover. The concrete cover being the distance from the centre of the prestressing cable to the face of the concrete where the strain is being measured. After this correction is applied to the

demec gauge transfer lengths, they are in closer agreement with the strain gauge transfer lengths. A summary of the measured transfer lengths can be seen in Table 4.2.

4.4. Flexural Bond Length

The development length is defined as the summation of the transfer length and the flexural bond length. The flexural bond length is defined as the cable embedment length beyond the transfer length required to develop the full tensile strength of the prestressing strand. Therefore in order to determine the flexural bond length of a prestressing strand one must first find the transfer length, then measure the entire development length from testing, and subtract the two. The transfer lengths were determined by the methods described in the previous section. The development length was measured by flexural testing of the beams of series A and B with different shear spans. A summary of the test results from series A and B may be seen in Table 4.3 .

Series A beams, that is beams A1, A2, and A3, were all made to be identical. The prestressing strands were 15.2 mm in diameter, the concrete cover was 50 mm, the prestress force was 50% of the guaranteed ultimate strength of the strands, and the beam cross-sections were all the same. The only difference between these beams was that for testing, the shear span was varied. For beam A1 the shear span was 1200 mm or 0.43 of the beam span, for beam A2 the shear span was 1000 mm or 0.36 of the beam span, and for beam A3 the shear span was 700 mm or 0.25 of the beam span. Both beams A1 and A2 failed by rupturing of the strand in tension while beam A3 failed by strand

slippage or bond failure. However, the ultimate load carried by beam A3 was nearly identical the load carried by beam A2. Therefore it can be concluded that the development length for these size strands is very close to the shear span of beam A3. By linear interpolation it was determined to be 707 mm as shown in Figure 4.38 .

Series B beams, that is beams B1, B2, and B3, were also all made to be identical. The prestressing strands were 12.5 mm in diameter, the concrete cover was 50 mm, the prestress force was 50% of the guaranteed ultimate strength of the strands, and the beam cross-sections were the same. Series B beams were the same as series A beams except that the strand diameter was smaller in series B. For beam B6 the shear span was 700 mm or 0.25 of the beam span, for beam B7 the shear span was 550 mm or 0.20 of the beam span, and for beam B8 the shear span was 450 mm or 0.16 of the beam span. Both beams B6 and B7 failed by rupturing of the prestressed strand while beam B8 failed by strand slippage or bond failure. Therefore, by interpolation between the shear spans of beams B7 and B8 as shown in Figure 4.39, it can be concluded that the development length for 12.5 mm diameter strands is 522 mm.

4.5. Flexural Behaviour

A summary of the test results for all beams may be seen in Table 4.4 . For all beams standard ASTM testing procedures were followed to determine the concrete properties. The concrete compressive strength at the time of prestressing release and at the time of testing was determined according to ASTM C39-86 "Standard Test Method

for Compressive Strength of Concrete Cylinder Specimens". The concrete elastic modulus at the time of testing was determined according to ASTM C469-87a "Standard Test Method for Static Modulus of Elasticity and Poisson's Ratio of Concrete In Compression". The concrete tensile strength at the time of testing was determined for all beams except beams A1 and A2 according to ASTM C78-84 "Standard Test Method for Flexural Strength of Concrete (Using Simple Beam With Third-Point Loading)". For beams A1 and A2 the concrete tensile strength was determined according to ASTM C496-90 "Standard Test Method for Splitting Tensile Strength of Concrete Cylinder Specimens". A summary of the concrete properties is shown in Table 4.5 .

The moment versus midspan deflection relationship from the testing of all beams may be seen in Figures 4.40 through 4.49 . In these figures one line shows the experimental data and the other shows the predicted behaviour which includes tension stiffening based on the I-E method. The solid prediction lines shows the beam behaviour up to the average CFCC strand strength reported by the manufacturer and the dotted extensions of the lines are the behaviour up to the actual strand strengths obtained from the tests. In general most beams showed a bilinear relationship with one linear portion up to the cracking load and a second linear portion from the cracking load up to failure. This behaviour is due to the linear elastic characteristic of the CFCC strands.

4.5.1. Beam A1

Beam A1 behaved in the common bilinear moment-deflection relationship as

previously described. The cracking load was 25.1 kN·m, the ultimate load was 57.0 kN·m, and the calculated ultimate strand stress was 2027 MPa. The mode of failure was strand rupture in the constant moment region with no strand slippage at the end of the beam prior to failure. The predicted ultimate load bases on the ultimate strand strength reported by the manufacturer was 60 kN·m and was calculated using rectangular stress block factors outlined by Collins and Mitchell (1987).

Prior to failure extensive flexural cracking and some flexural-shear cracking was observed which extended up to the top flange of the beam. Beam failure occurred by rupture of the CFCC cable at a primary vertical crack directly at midspan. The average crack spacing in the constant moment zone was 115 mm and there was lots of horizontal splitting of the concrete at the tendon level after failure. Some of this splitting occurred before failure but most occurred at failure. This was due to the sudden release of strain energy in the cable after rupture causing it to recoil.

At the ultimate load of the beam the strain at midspan in the extreme compression fibre was approximately 0.0021 as measured from demec point readings. This was well below the ultimate compressive strain of the concrete. The curve of moment versus top concrete strain at midspan may be seen in Figure 4.50 .

4.5.2. Beam A2

In general beam A2 showed a similar bilinear moment-deflection relationship as with beam A1. The cracking load was 25.5 kN·m, the ultimate load was 61.0 kN·m, and

the calculated ultimate strand stress was 2168 MPa. The mode of failure was strand rupture in the constant moment region with no strand slippage at the end of the beam prior to failure. The predicted ultimate load was 60 kN·m the same as for beam A1.

Prior to failure extensive flexural cracking and some flexural-shear cracking was observed which extended up to the top flange of the beam. Beam failure occurred by rupture of the CFCC cable at a primary vertical crack under the right load point 1200 mm from the right end of the beam. The average crack spacing in the constant moment zone was 118 mm and again there was lots of horizontal splitting of the concrete at the tendon level after failure.

At the ultimate load of the beam the strain at midspan in the extreme compression fibre was approximately 0.0018 as measured from demec point gauges. This was well below to ultimate compressive strain of the concrete. The curve of moment versus top concrete strain at midspan may be seen in Figure 4.51 .

4.5.3. Beam A3

Beam A3 also showed a bilinear moment-deflection relationship as with the previous beams. The cracking load was 28.0 kN·m, the ultimate load was 61.2 kN·m, and the calculated ultimate strand stress was 2166 MPa. The mode of failure was strand slip or bond failure. The predicted ultimate load was 60 kN·m the same as for beam A1 and A2.

Prior to failure an interesting phenomenon was observed in the moment-deflection

relationship. At a mid-span deflection of about 26 mm a peak occurred on the moment-deflection curve. After this peak the load dropped off suddenly by about 5 kN·m, then continued to rise as before the peak but at a shallower angle, indicating a reduced stiffness. A reasonable explanation for this event is as follows. It is possible that after extensive cracking the bond between the prestressing cable and the concrete was lost within the constant moment zone. But, since the transfer length for these cable is short and therefore the bond strength in the transfer zone is high, the beam was still able to carry load with the transfer zones acting as anchorages and the beam acting as a post-tensioned member. At this stage, the beam acting as a member with an unbonded tendon will have a lower stiffness than it had with a bonded tendon. This accounts for the reduced stiffness after the peak in the curve. The peak itself was most likely caused by the fact that when the cable suddenly becomes debonded it had a tendency to straighten the beam as a tie for an arch action. This created a sudden upward force on the concrete and since the tests were conducted under displacement control, was measured as a peak in the applied load during the test.

Prior to failure extensive flexural cracking and some flexural-shear cracking was observed which extended up to the top flange of the beam. Beam failure occurred by slippage of the CFCC cable at a primary vertical crack under the left load point 900 mm from the left end of the beam. The average crack spacing in the constant moment zone was 113 mm and lots of horizontal splitting of the concrete (almost 100%) was observed at the tendon level after failure.

At the ultimate load of the beam the strain at midspan in the extreme compression

fibre was approximately 0.0014 as measured by demec point gauges. This was well below to ultimate compressive strain of the concrete. The curve of moment versus top concrete strain at midspan may be seen in Figure 4.52 .

4.5.4. Beam C4

In general beam C4 showed the same bilinear moment-deflection relationship as with the previous beams. The cracking load was 39.4 kN·m, the ultimate load was 57.4 kN·m, and the calculated ultimate strand stress was 2047 MPa. The mode of failure was a combination strand slip and shear failure. The predicted ultimate load was 60 kN·m the same as for the previous beams.

Prior to failure extensive flexural cracking and some flexural-shear cracking was observed which extended up to the top flange of the beam. Beam failure occurred by slippage of the CFCC cable at a primary shear crack 400 mm from the left end of the beam. When failure occurred a large shear crack formed 200 mm from the left support point and instantaneously the CFCC cable slipped at this point. The average crack spacing in the constant moment zone was 125 mm and lots of horizontal splitting of the concrete was observed at the tendon level after failure.

At the ultimate load of the beam the strain at midspan in the extreme compression fibre was approximately 0.0013 as measured by demec point gauges. This was well below to ultimate compressive strain of the concrete. The curve of moment versus top concrete strain at midspan is shown in Figure 4.53 .

4.5.5. Beam D5

In general beam D5 showed the bilinear moment-deflection relationship. The cracking load was 30.0 kN·m, the ultimate load was 67.7 kN·m, and the calculated ultimate strand stress was 2394 MPa. The mode of failure was strand rupture in the constant moment region with no strand slippage at the end of the beam prior to failure. The predicted ultimate load was 60 kN·m.

Prior to failure extensive flexural cracking and some flexural-shear cracking was observed which extended up to the top flange of the beam. Beam failure occurred by rupture of the CFCC cable at a primary vertical crack 100 mm to the right of mid-span. The average crack spacing in the constant moment zone was 236 mm but there was very little horizontal splitting of the concrete at the tendon level after failure.

At the ultimate load of the beam the strain at midspan in the extreme compression fibre was approximately 0.0017 as measured from demec point gauges. This was well below to ultimate compressive strain of the concrete. The curve of moment versus top concrete strain at midspan may be seen in Figure 4.54 .

4.5.6. Beam B6

In general beam B6 showed the bilinear moment-deflection relationship. The cracking load was 22.1 kN·m, the ultimate load was 50.2 kN·m, and the calculated ultimate strand stress was 2632 MPa. The mode of failure was strand rupture in the

constant moment region with no strand slippage at the end of the beam prior to failure. The predicted ultimate load was 40 kN·m.

Prior to failure the same phenomenon as for beam A3 was observed in the moment-deflection relationship. At a mid-span deflection of about 28 mm a peak occurred on the moment-deflection curve. After this peak the load dropped off suddenly by about 8 kN·m, then continued to rise as before the peak but at a shallower angle, indicating a reduced stiffness. The explanation for this phenomenon is the same as that of beam A3.

Prior to failure extensive flexural cracking and some flexural-shear cracking was observed which extended up to the top flange of the beam. Beam failure occurred by rupture of the CFCC cable at a primary vertical crack 100 mm to the right of the left load point or 1000 mm from the left end of the beam. The average crack spacing in the constant moment zone was 135 mm and lots of horizontal splitting of the concrete (almost 100%) was observed at the tendon level after failure.

At the ultimate load of the beam the strain at midspan in the extreme compression fibre was approximately 0.0015 as measured by demec point gauges. This was well below to ultimate compressive strain of the concrete. The curve of moment versus top concrete strain at midspan is given in Figure 4.55 .

4.5.7. Beam B7

Beam B7 showed the bilinear moment-deflection relationship. The cracking load was 21.3 kN·m, the ultimate load was 51.0 kN·m, and the calculated ultimate strand

stress was 2674 MPa. The mode of failure was strand rupture in the constant moment region with no strand slippage at the end of the beam prior to failure. The predicted ultimate load was 40 kN·m.

Prior to failure the same phenomenon as for beams A3 and B6 was observed in the moment-deflection relationship. At a mid-span deflection of about 37 mm a peak occurred on the moment-deflection curve. After this peak the load dropped off suddenly by about 5 kN·m, then continued to rise as before the peak but at a shallower angle, indicating a reduced stiffness.

Prior to failure extensive flexural cracking and some flexural-shear cracking was observed which extended up to the top flange of the beam. Beam failure occurred by rupture of the CFCC cable at a primary vertical crack 150 mm to the right of mid-span or 1450 mm from the right end of the beam. The average crack spacing in the constant moment zone was 143 mm and lots of horizontal splitting of the concrete (almost 100%) was observed at the tendon level after failure.

At the ultimate load of the beam the strain at midspan in the extreme compression fibre was approximately 0.0019 as measured by demec point gauges. This was reasonably well below to ultimate compressive strain of the concrete. The curve of moment versus top concrete strain at midspan may be seen in Figure 4.56 .

4.5.8. Beam B8

Beam B8 also showed a bilinear moment-deflection relationship as with the

previous beams. The ultimate load was 43.9 kN·m and the calculated ultimate strand stress was 2305 MPa. The mode of failure was strand slip or bond failure. The predicted ultimate load was 40 kN·m the same as for beams B6 and B7.

Prior to testing this beam was accidentally precracked at two points along its span. One crack was at the mid-span and the other one was under the left load point with both cracks extending across the entire cross-section of the beam. However, the same trends in the moment-deflection relationship are exhibited by this beam as compared to the other beams. The only difference being that in the initial loading stage the beam is less stiff than the others due to the precracking.

Prior to failure extensive flexural cracking and some flexural-shear cracking was observed which extended up to the top flange of the beam. Beam failure occurred by slippage of the CFCC cable at a primary vertical crack 100 mm to the right of the right load point or 550 mm from the right end of the beam. The average crack spacing in the constant moment zone was 133 mm and a moderate amount of horizontal splitting of the concrete was observed at the tendon level after failure.

At the ultimate load of the beam the strain at midspan in the extreme compression fibre was approximately 0.0014 as measured by demec point gauges. This was well below to ultimate compressive strain of the concrete. The curve of moment versus top concrete strain at midspan may be seen in Figure 4.57 .

4.5.9. Beam C9

In general beam C9 showed the same bilinear moment-deflection relationship as with the previous beams. The cracking load was 24.4 kN·m, the ultimate load was 46.6 kN·m, and the calculated ultimate strand stress was 2448 MPa. The mode of failure was a combination strand slip and shear failure. The predicted ultimate load was 40 kN·m the same as for the previous beams.

Prior to failure extensive flexural cracking and some flexural-shear cracking was observed which extended up to the top flange of the beam. Beam failure occurred by slippage of the CFCC cable at a primary shear crack 450 mm from the right end of the beam. When failure occurred a large shear crack formed 250 mm from the right support point and instantaneously the CFCC cable slipped at this point. The average crack spacing in the constant moment zone was 127 mm and a moderate amount of horizontal splitting of the concrete was observed at the tendon level after failure.

At the ultimate load of the beam the strain at midspan in the extreme compression fibre was approximately 0.0014 as measured by demec point gauges. This was well below to ultimate compressive strain of the concrete. The curve of moment versus top concrete strain at midspan may be seen in Figure 4.58 .

4.5.10. Beam D10

Beam D10 showed the common bilinear moment-deflection relationship. The

cracking load was 27.3 kN·m, the ultimate load was 48.8 kN·m, and the calculated ultimate strand stress was 2560 MPa. The mode of failure was a combination strand slip and shear failure. The predicted ultimate load was 40 kN·m the same as for the previous beams.

Prior to failure extensive flexural cracking and some flexural-shear cracking was observed which extended up to the top flange of the beam. Beam failure occurred by slippage of the CFCC cable at a primary shear crack 400 mm from the left end of the beam. When failure occurred a large shear crack formed 200 mm from the left support point and instantaneously the CFCC cable slipped at this location. The average crack spacing in the constant moment zone was 238 mm and no horizontal splitting of the concrete was observed at the tendon level after failure.

At the ultimate load of the beam the strain at midspan in the extreme compression fibre was approximately 0.0014 as measured by demec point gauges. This was well below to ultimate compressive strain of the concrete. The curve of moment versus top concrete strain at midspan is shown in Figure 4.59 .

Table 4.1. Prestressing Losses For All Beams

Beam	Age at Test (days)	Prestress Force (kN)	Elastic Loss (%)				Creep Loss (%)				Total Loss (%)		
			Demec Gauges	Strain Gauges	Avg.	fci' (MPa)	Demec Gauges	Strain Gauges	Avg.	fc' (MPa)	Demec Gauges	Strain Gauges	Avg.
A1	42	95.2	2.70	2.32	2.51	35.8	9.42	10.70	10.06	55.0	12.12	13.02	12.57
A2	67	96.7	2.50	2.34	2.42	35.8	6.91	9.27	8.09	55.0	9.41	11.61	10.51
A3	167	96.7	1.86	2.77	2.32	40.2	8.45	14.25	11.35	57.8	10.31	17.02	13.67
C4	137	137.7	2.16	2.19	2.18	45.1	8.12	10.18	9.15	60.5	10.28	12.37	11.33
D5	169	99.6	1.50	1.79	1.65	40.2	5.68	6.44	6.06	57.8	7.18	8.23	7.71
B6	111	70.9	1.48	1.39	1.44	56.3	7.24	7.97	7.61	68.3	8.72	9.36	9.04
B7	114	72.6	1.46	1.34	1.40	56.3	6.23	7.64	6.94	68.3	7.69	8.98	8.34
B8	98	68.0	1.70	1.63	1.67	41.4	8.44	10.70	9.57	59.0	10.14	12.33	11.24
C9	70	77.8	1.71	1.87	1.79	50.0	9.06	10.38	9.72	64.0	10.77	12.25	11.51
D10	105	69.1	1.53	1.50	1.52	41.4	6.38	N.A.	6.38	59.0	7.91	N.A.	7.91

Table 4.2. Measured Transfer Lengths For All Beams (mm)

Beam	Measured Transfer Lengths Based on:		
	Electric Strain Gauges	Demec Gauges	
		Measured	Corrected According to Eqn. 5.1
A3	196	250	200
C4	239	N.A.	N.A.
D5	201	N.A.	N.A.
B6	128	N.A.	N.A.
B7	122	175	125
B8	124	175	125
C9	145	N.A.	N.A.
D10	135	200	125

Table 4.3 Test Results for Series A and B

Beam	Strand Diam. (mm)	Shear Span (mm)	Ultimate Moment (kNm)	Ultimate Strand Stress (kNm)	Failure Mode
A1	15.2	1200	57.0	2027	strand rupture
A2	15.2	1000	61.0	2168	strand rupture
A3	15.2	700	61.2	2166	bond slip
B6	12.5	700	50.2	2632	strand rupture
B7	12.5	550	51.0	2674	strand rupture
B8	12.5	450	43.9	2305	bond slip

Table 4.4 Test Results for All Beams

Beam	Shear Span (mm)	Ultimate Load (kN)	Ultimate Moment (kNm)	Observed Failure Mode
A1	1200	95	57.0	strand rupture
A2	1000	122	61.0	strand rupture
A3	700	175	61.2	bond slip
C4	700	164	57.4	shear / bond slip
D5	700	193	67.7	strand rupture
B6	700	144	50.2	strand rupture
B7	550	186	51.0	strand rupture
B8	450	195	43.9	bond slip
C9	450	207	46.6	shear / bond slip
D10	450	217	48.8	shear / bond slip

Table 4.5 Concrete Properties for All Beams

Beam	Compressive Strength			Tensile Strength (MPa)	Elastic Modulus (GPa)
	At Transfer (MPa)	At Test (MPa)	Age at Test (days)		
A1	35.8	55.0	42	*4.06	28.0
A2	35.8	55.0	67	*4.06	28.0
A3	40.2	57.8	167	6.07	33.4
C4	45.1	60.5	137	N.A.	35.7
D5	40.2	57.8	169	6.07	33.4
B6	56.3	68.3	111	7.24	34.1
B7	56.3	68.3	114	7.24	34.1
B8	41.4	59.0	98	6.79	32.7
C9	50.0	64.0	70	6.62	33.8
D10	41.4	59.0	105	6.79	32.7

* from splitting tensile test

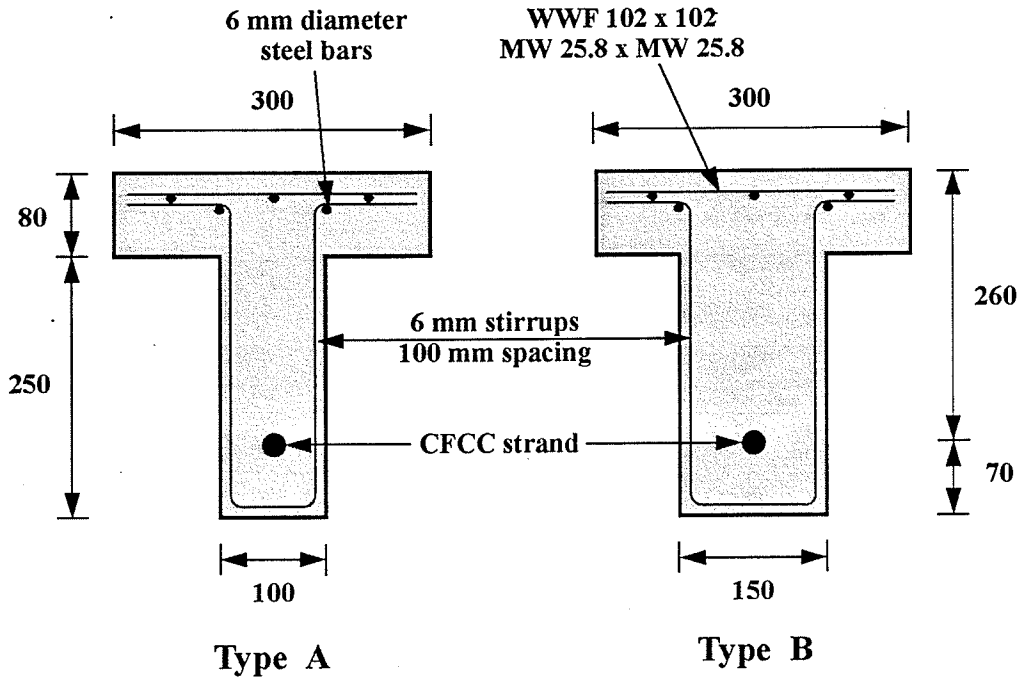

Figure 4.1 Beam Cross-Sections

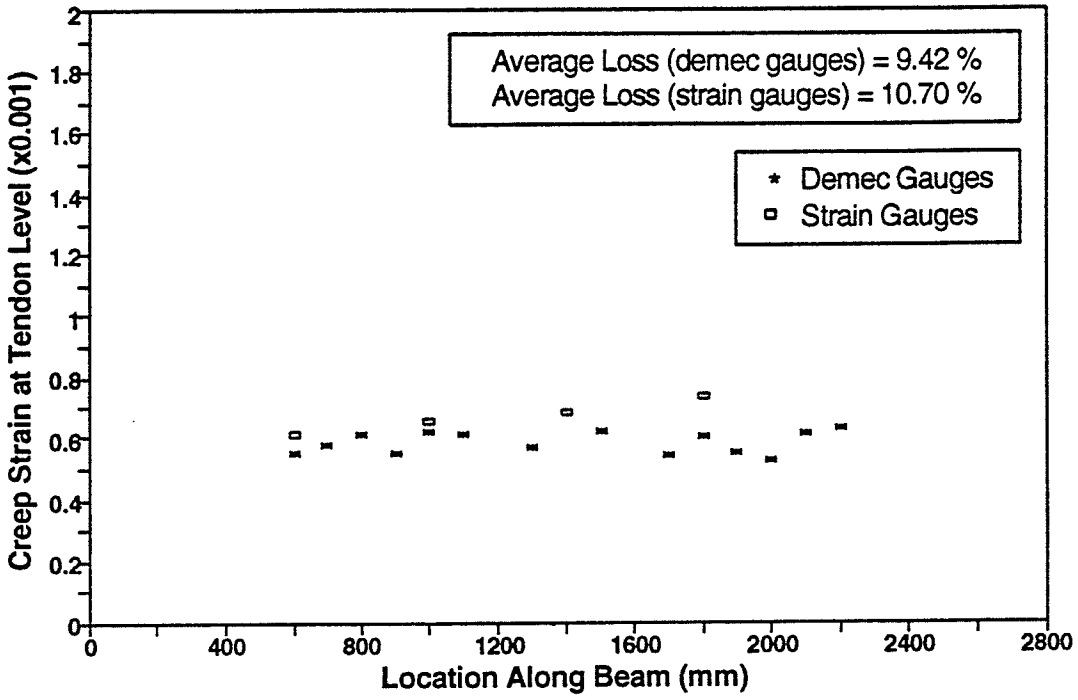

Figure 4.2 Creep and Relaxation Losses For Beam A1

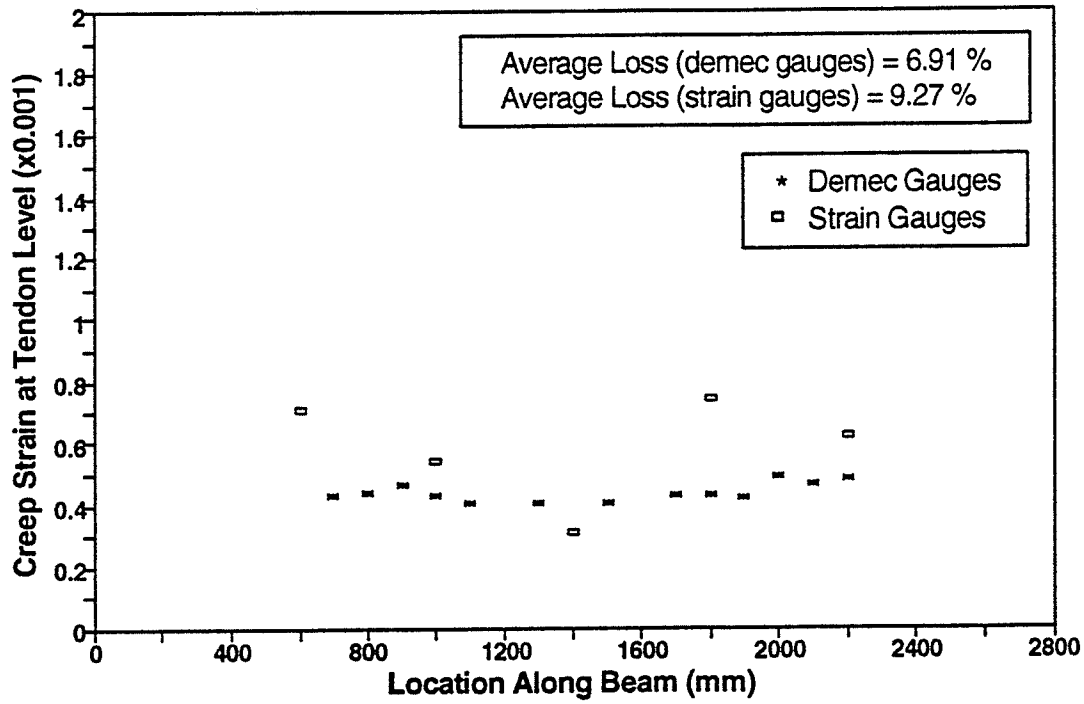

Figure 4.3 Creep and Relaxation Losses For Beam A2

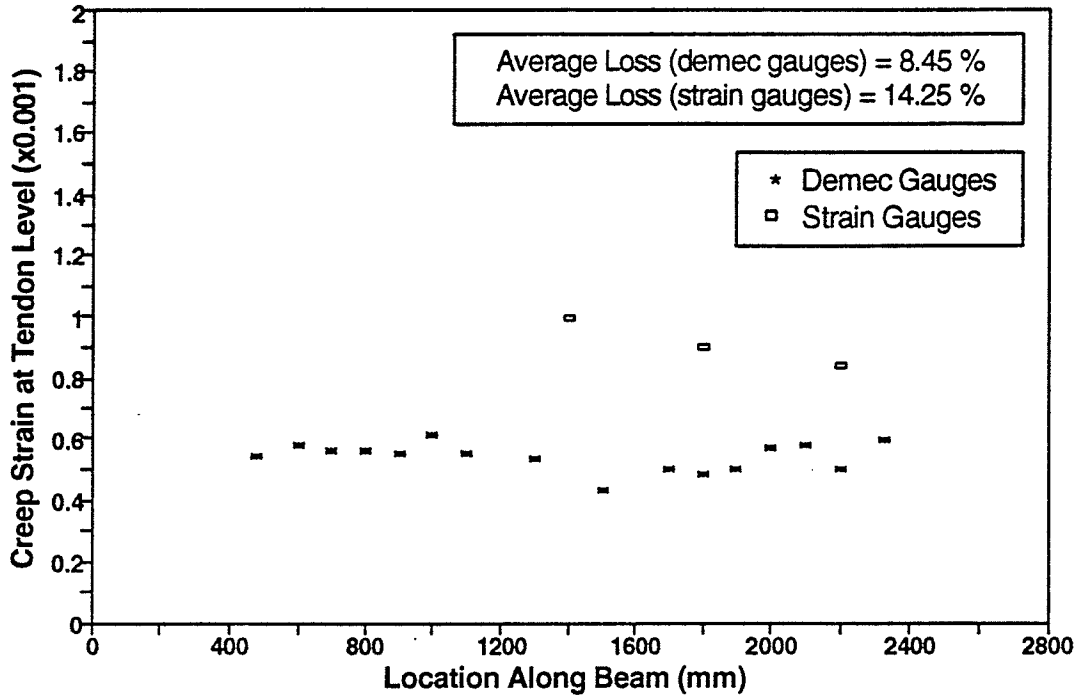

Figure 4.4 Creep and Relaxation Losses For Beam A3

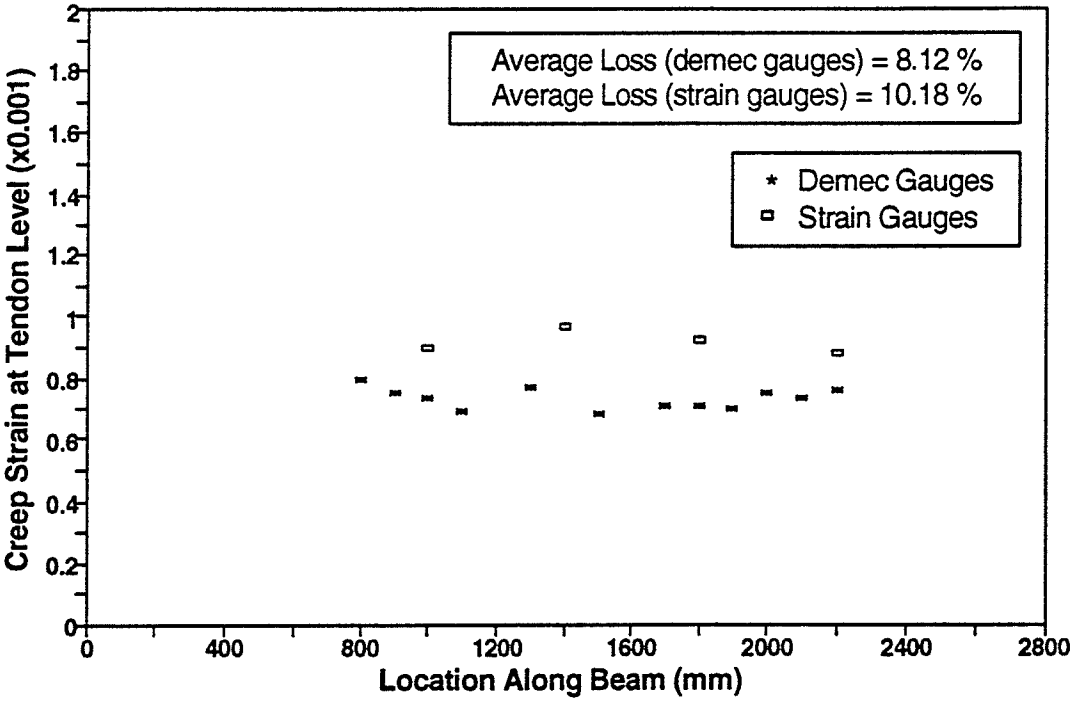

Figure 4.5 Creep and Relaxation Losses For Beam C4

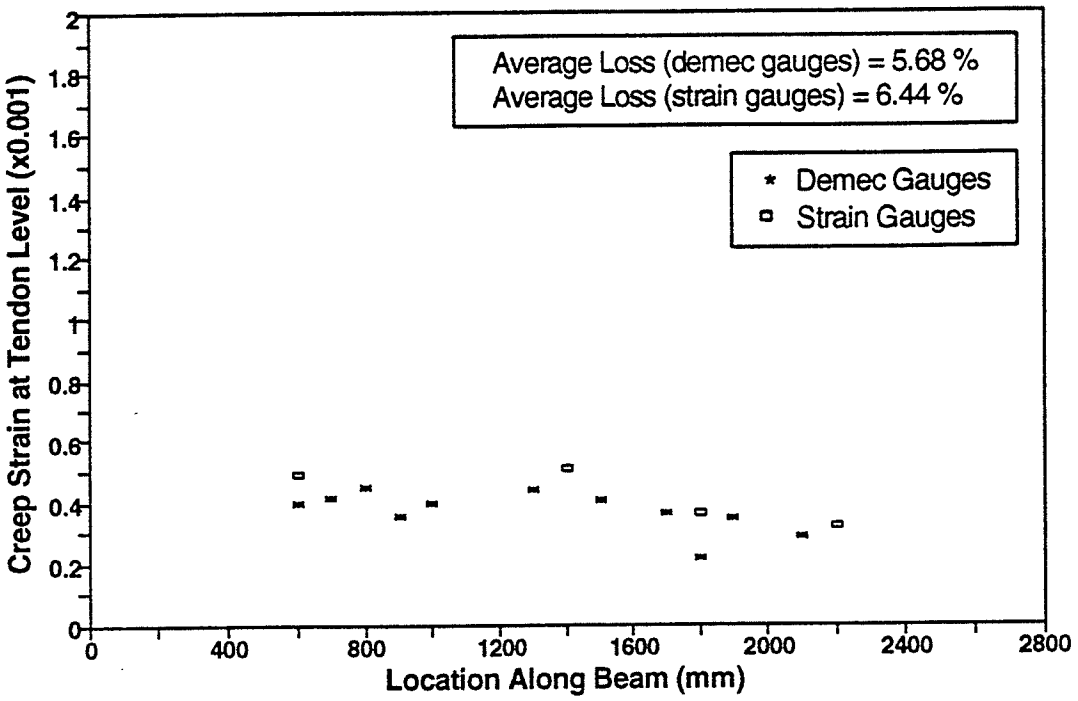

Figure 4.6 Creep and Relaxation Losses For Beam D5

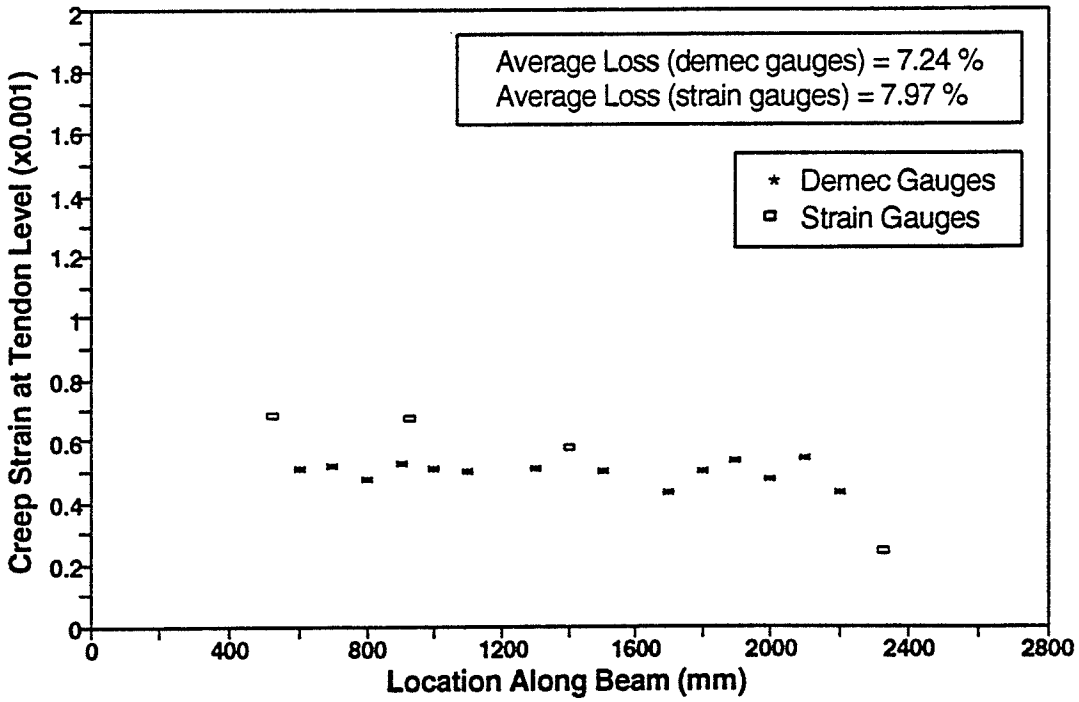

Figure 4.7 Creep and Relaxation Losses For Beam B6

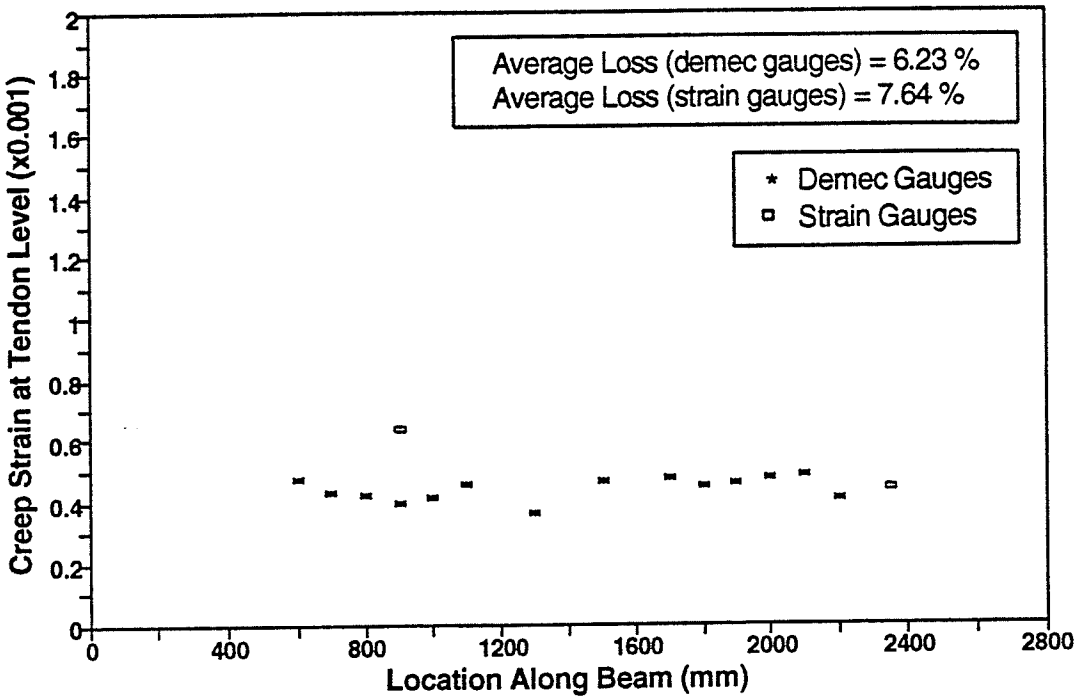

Figure 4.8 Creep and Relaxation Losses For Beam B7

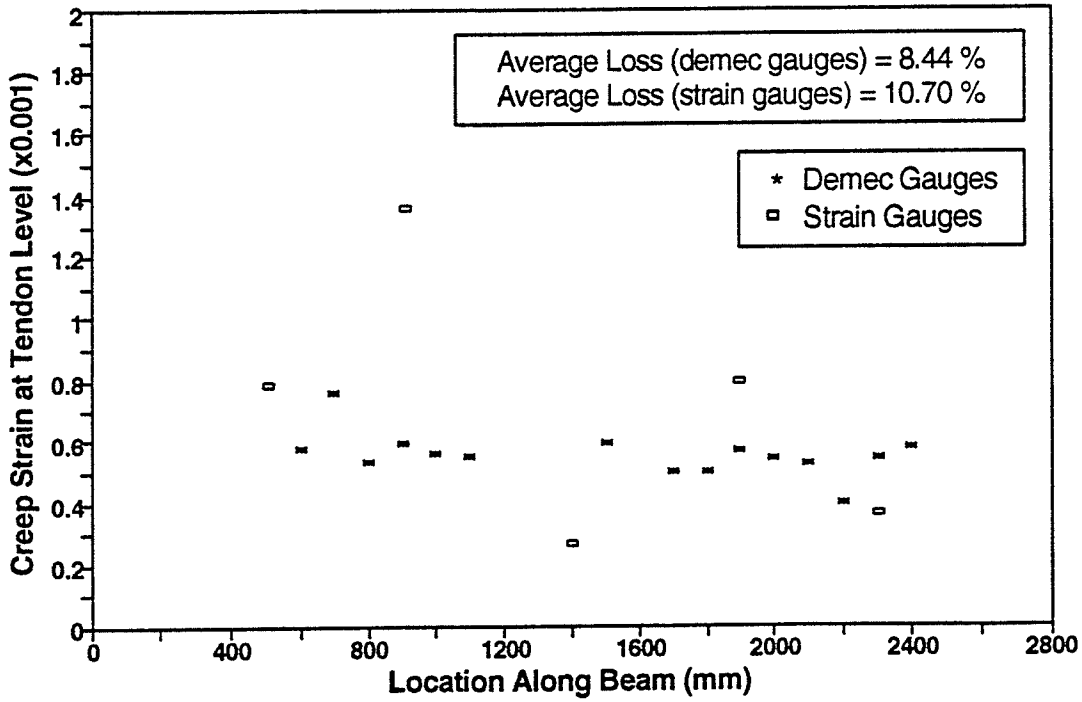

Figure 4.9 Creep and Relaxation Losses For Beam B8

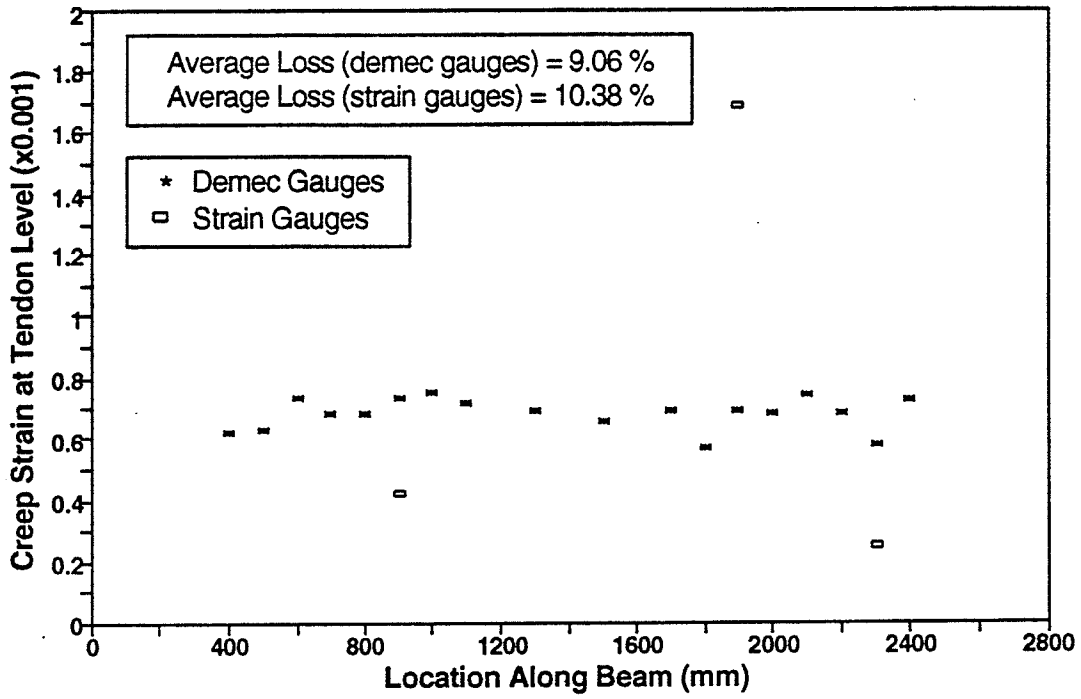

Figure 4.10 Creep and Relaxation Losses For Beam C9

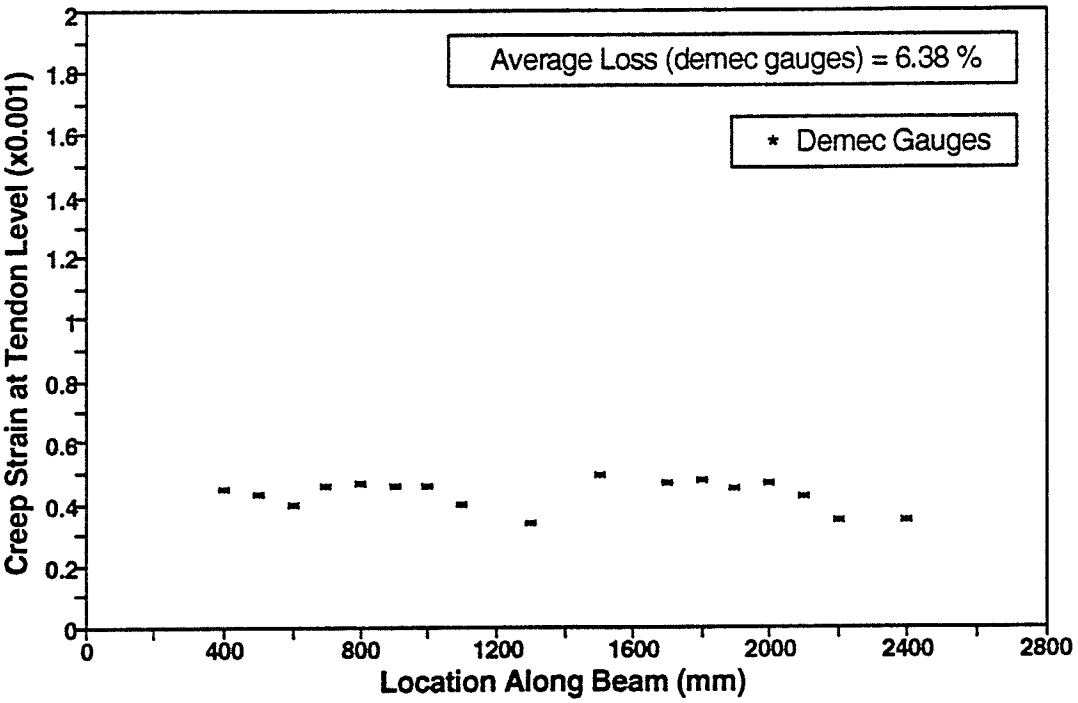

Figure 4.11 Creep and Relaxation Losses For Beam D10

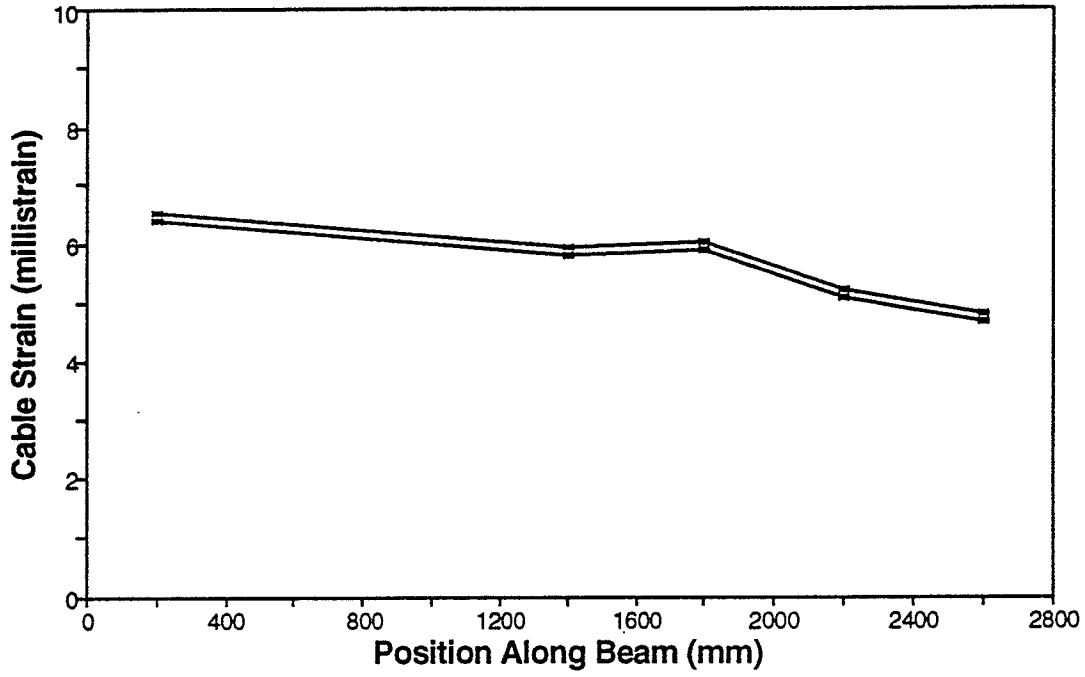

Figure 4.12 Cable Strain Before and After Release for Beam A1

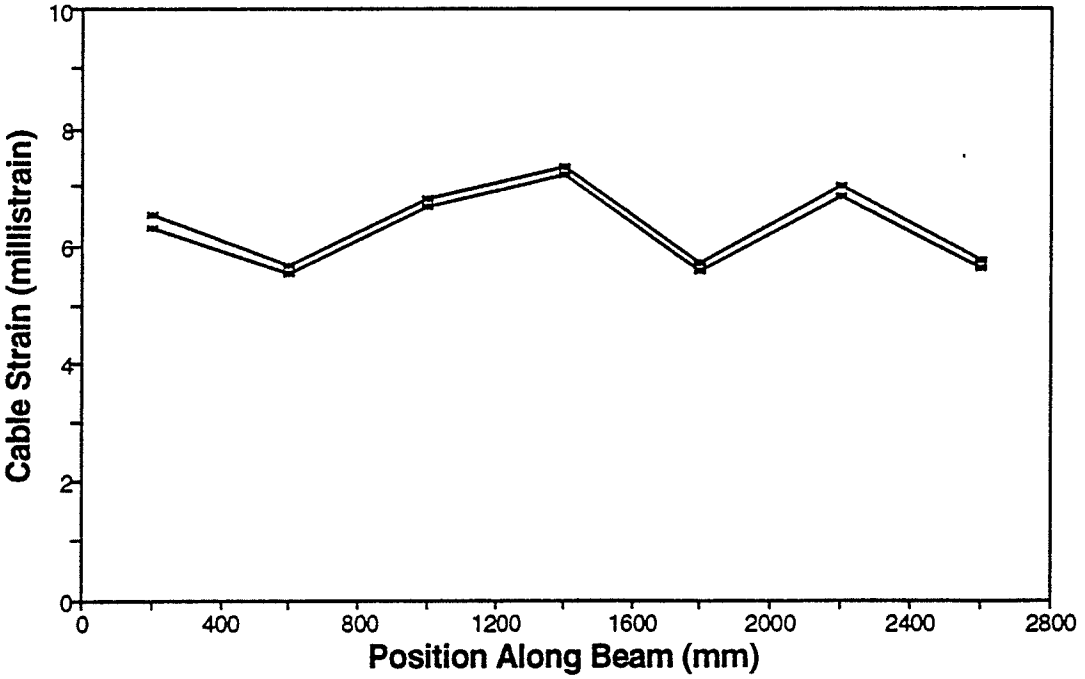

Figure 4.13 Cable Strain Before and After Release for Beam A2

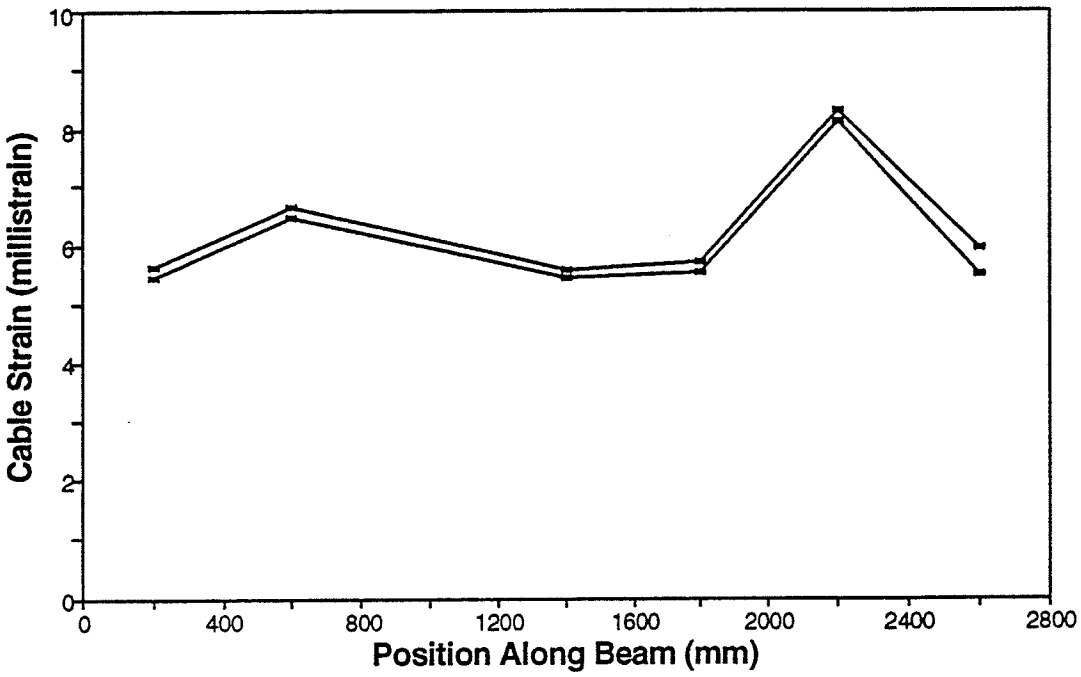

Figure 4.14 Cable Strain Before and After Release for Beam A3

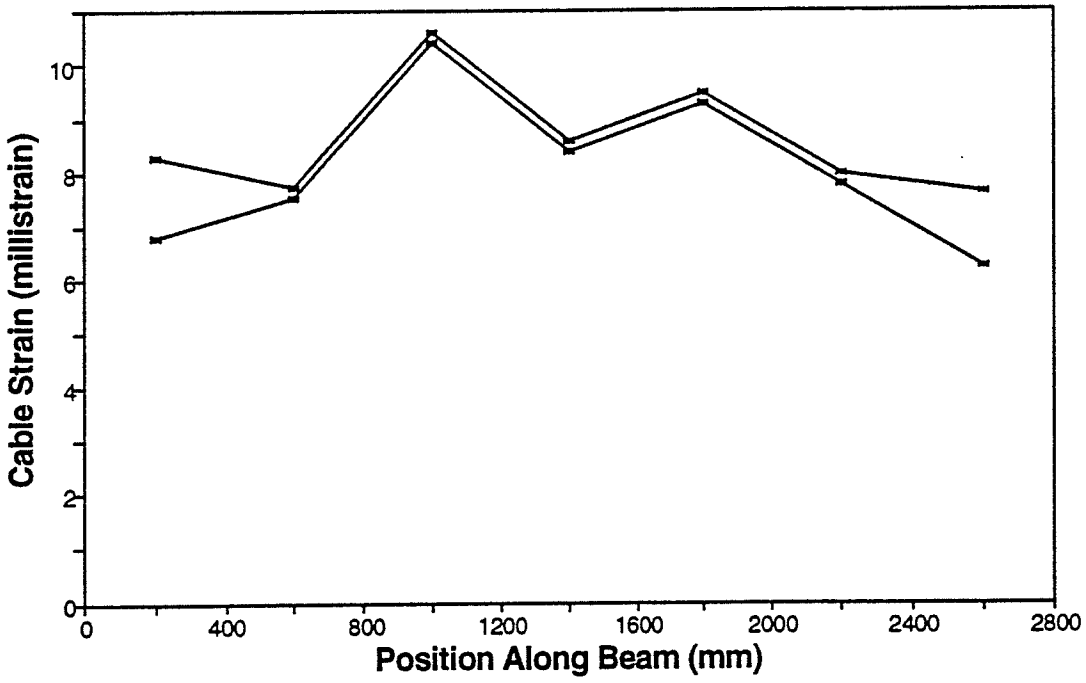

Figure 4.15 Cable Strain Before and After Release for Beam C4

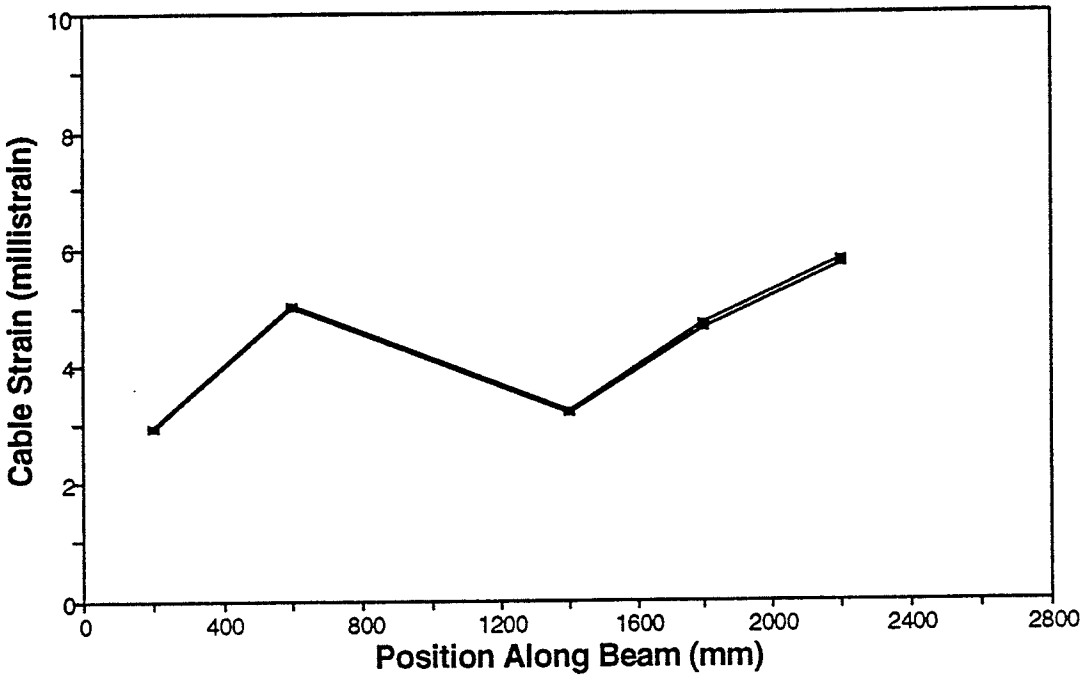

Figure 4.16 Cable Strain Before and After Release for Beam D5

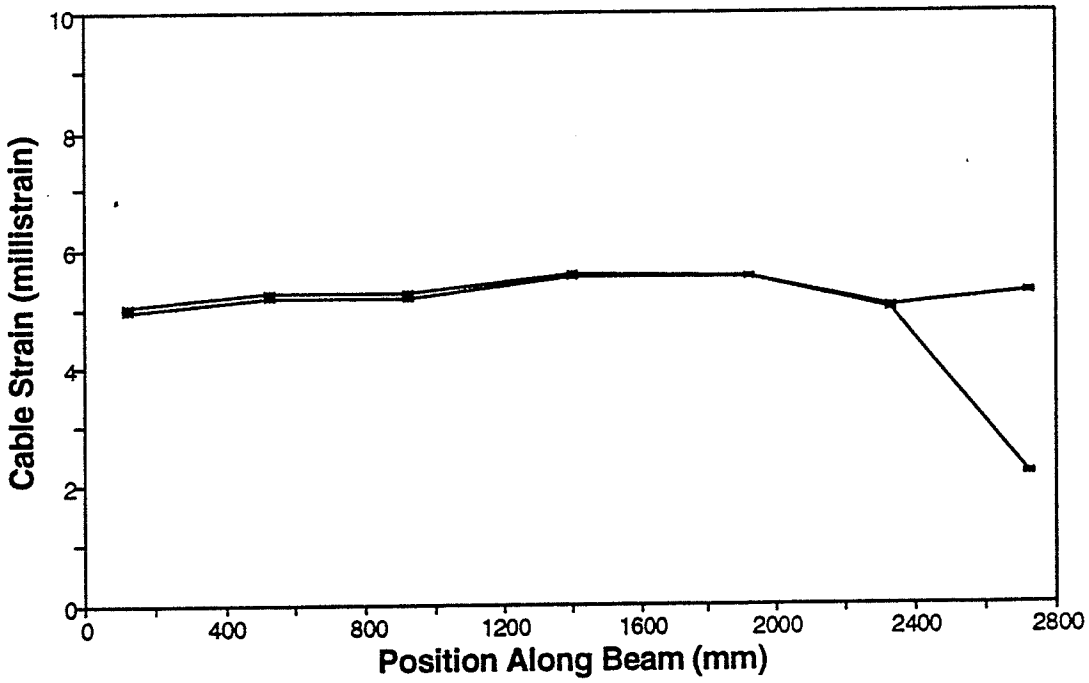

Figure 4.17 Cable Strain Before and After Release for Beam B6

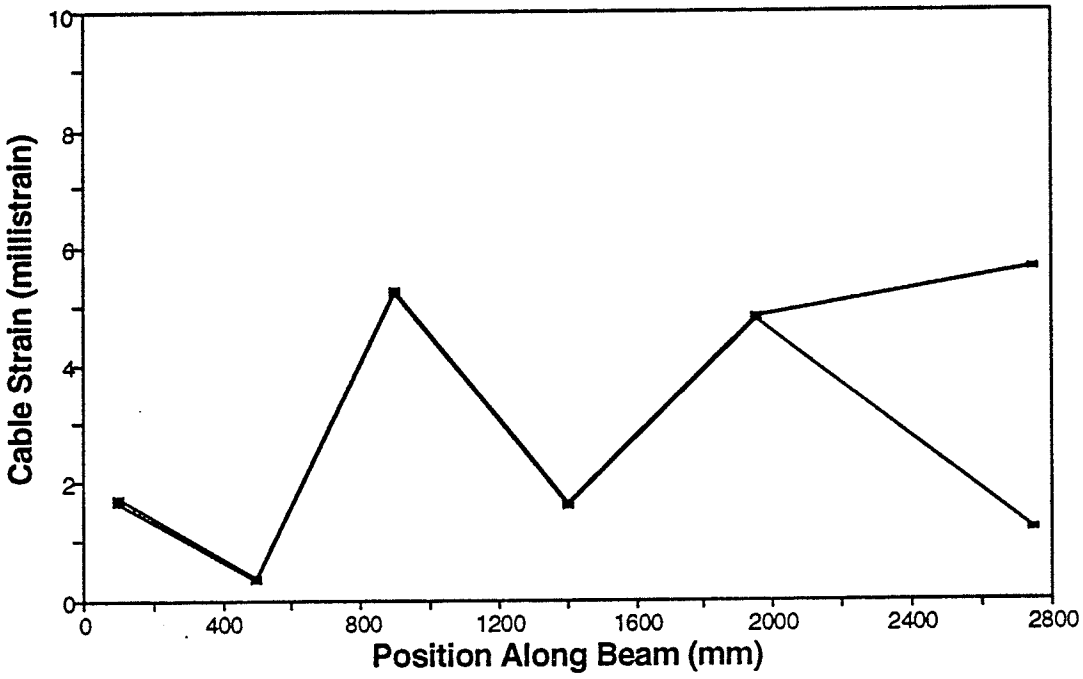

Figure 4.18 Cable Strain Before and After Release for Beam B7

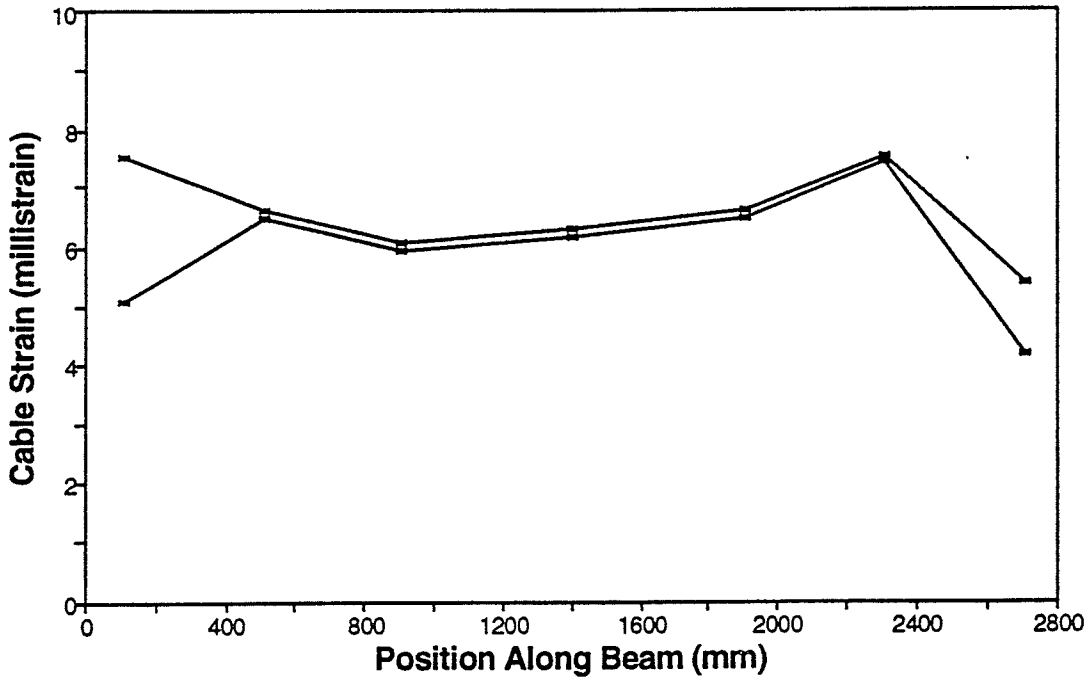

Figure 4.19 Cable Strain Before and After Release for Beam B8

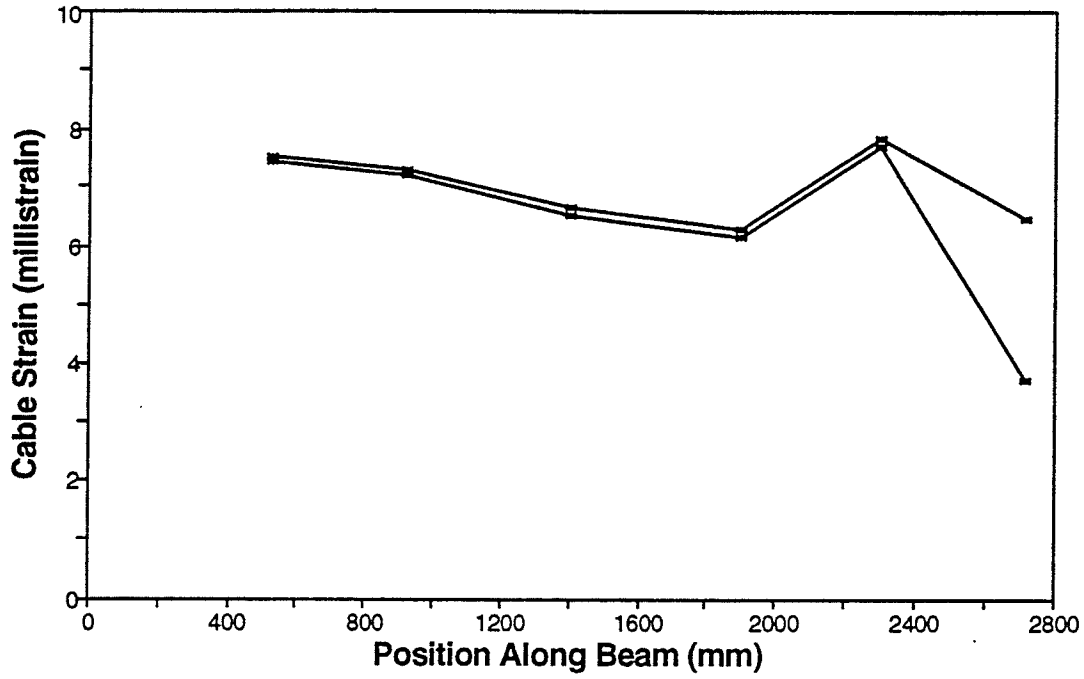

Figure 4.20 Cable Strain Before and After Release for Beam C9

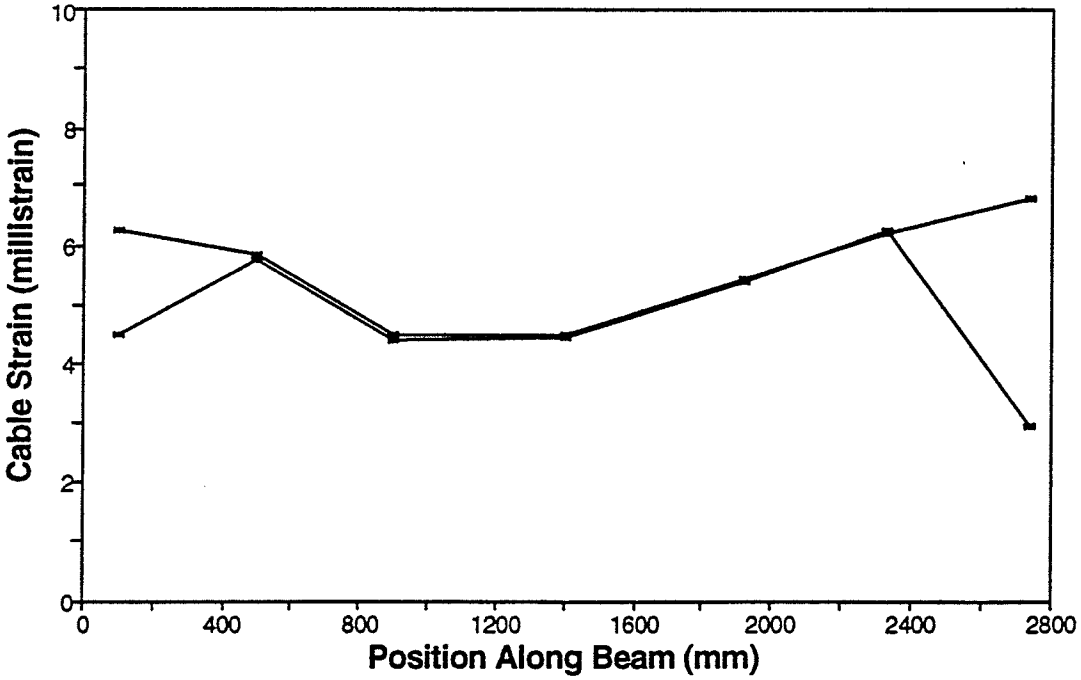

Figure 4.21 Cable Strain Before and After Release for Beam D10

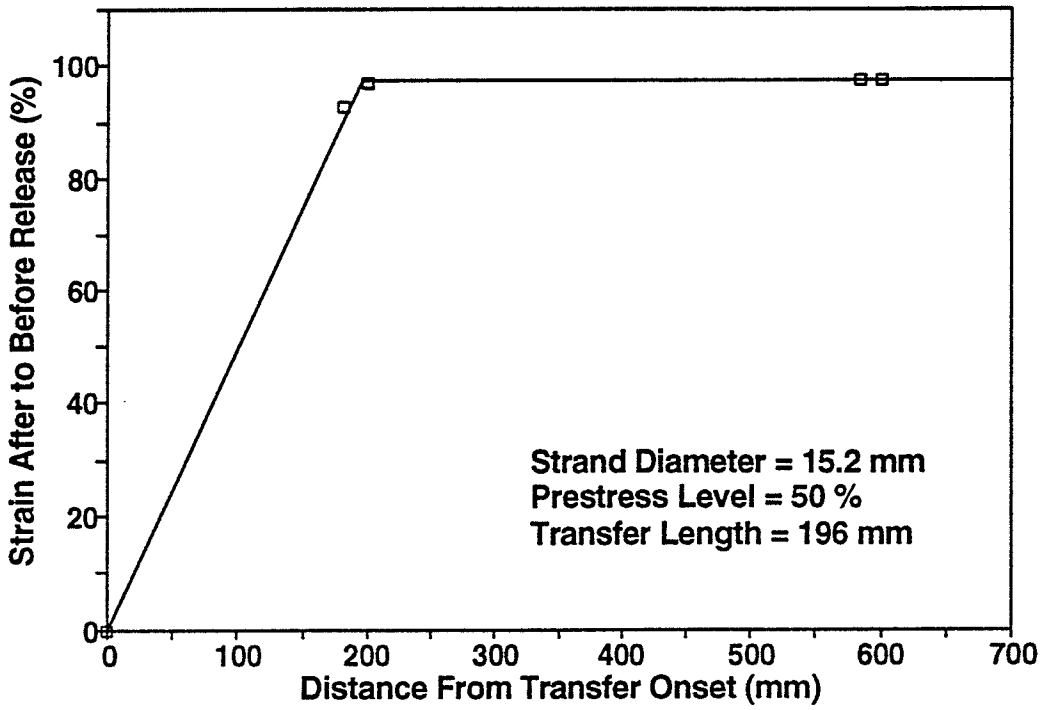

Figure 4.22 Cable Strain in Transfer Zone For Beam A3

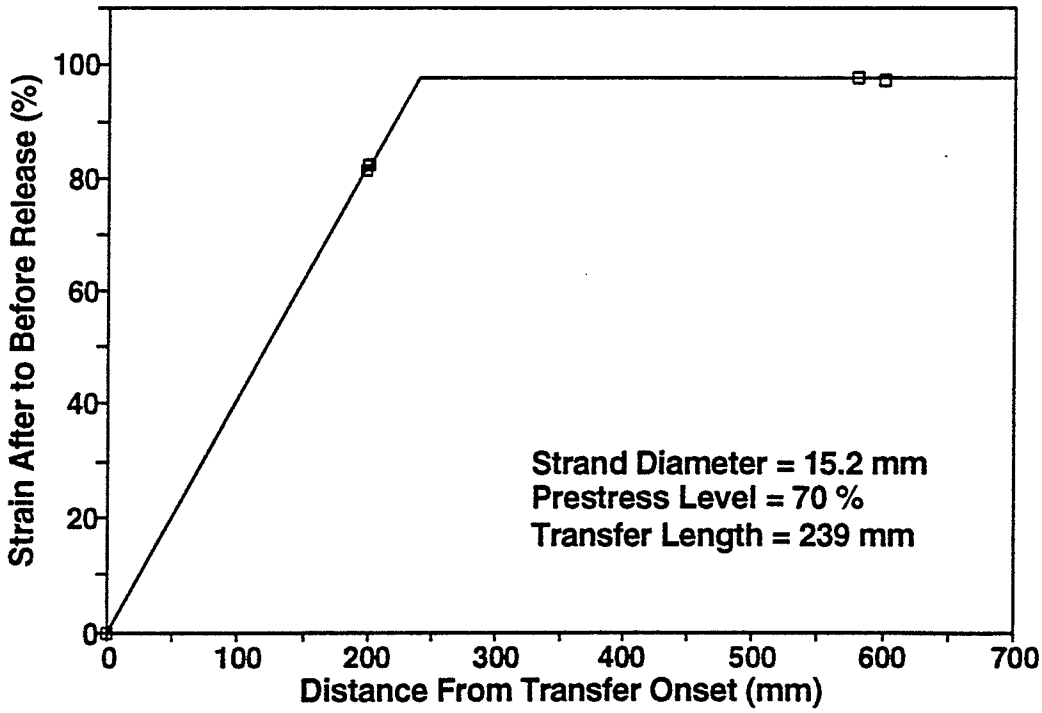

Figure 4.23 Cable Strain in Transfer Zone For Beam C4

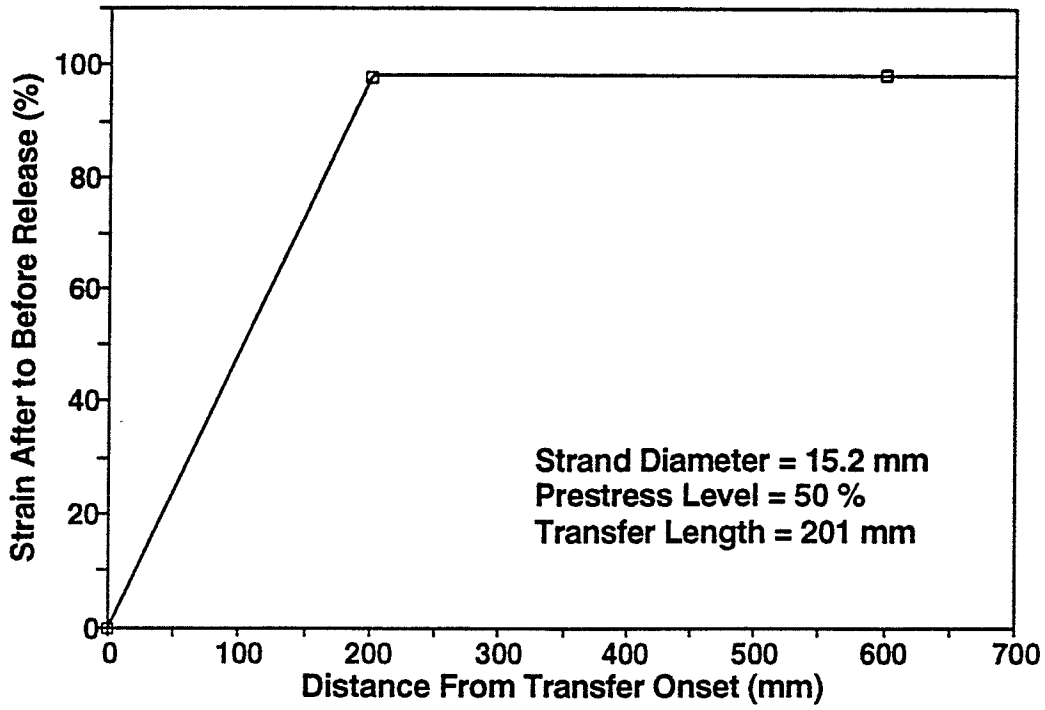

Figure 4.24 Cable Strain in Transfer Zone For Beam D5

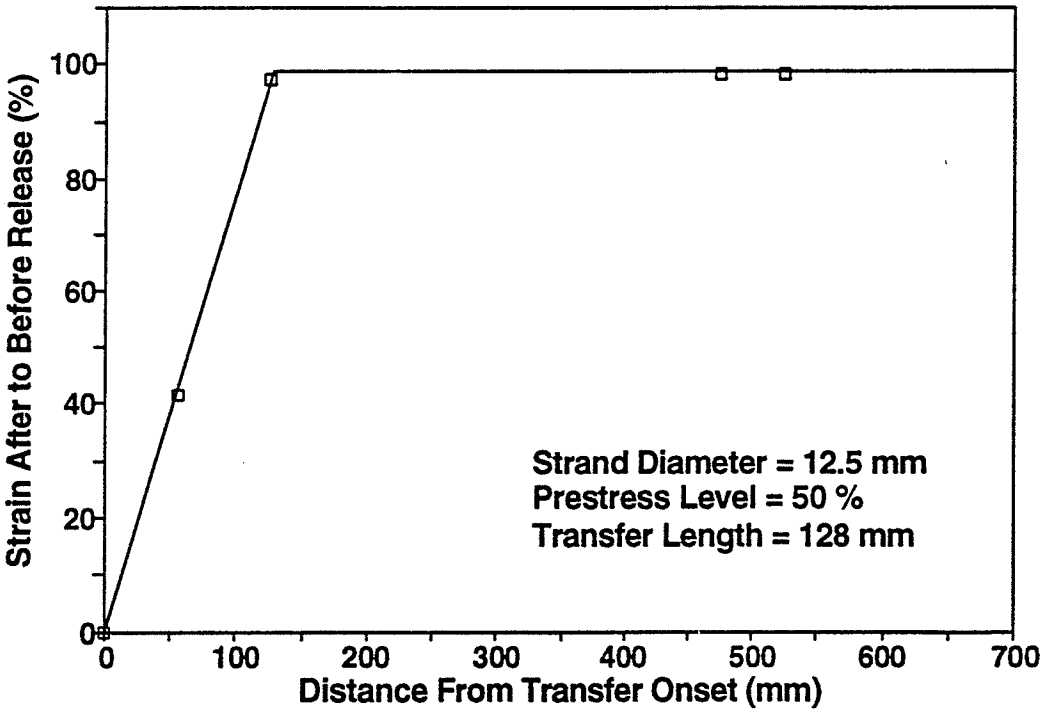

Figure 4.25 Cable Strain in Transfer Zone For Beam B6

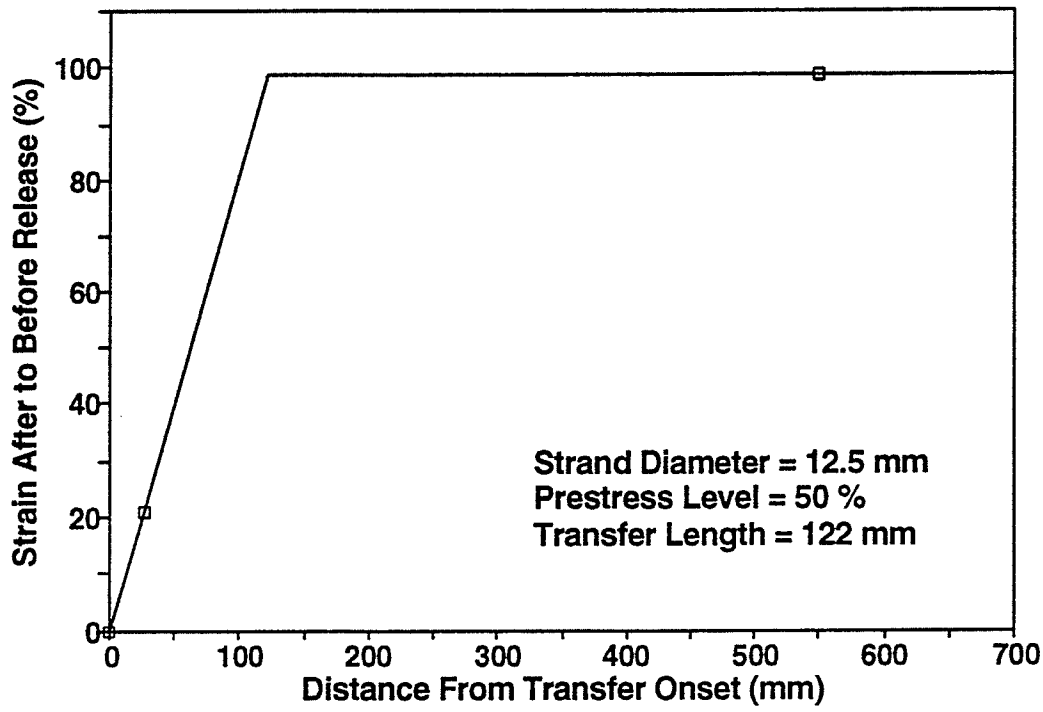

Figure 4.26 Cable Strain in Transfer Zone For Beam B7

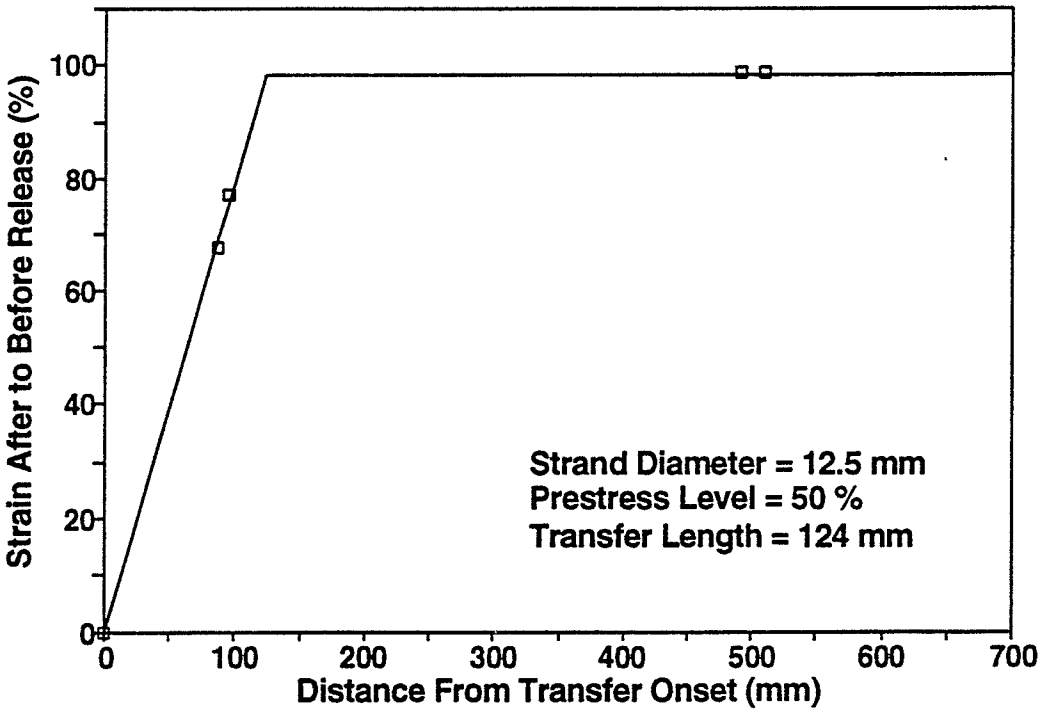

Figure 4.27 Cable Strain in Transfer Zone For Beam B8

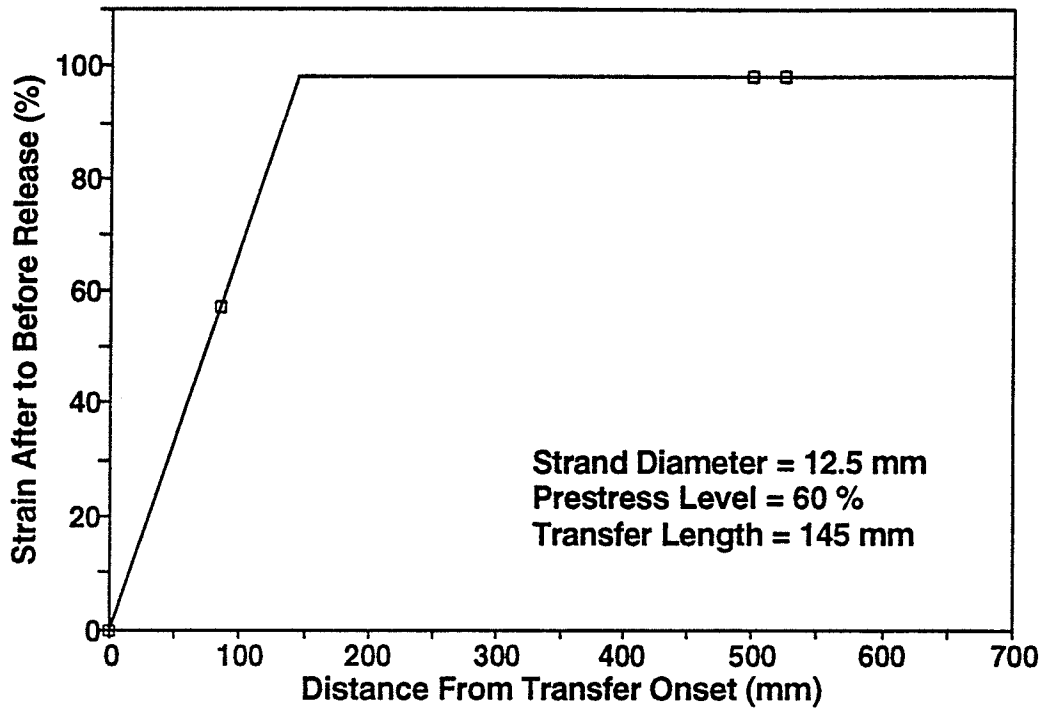

Figure 4.28 Cable Strain in Transfer Zone For Beam C9

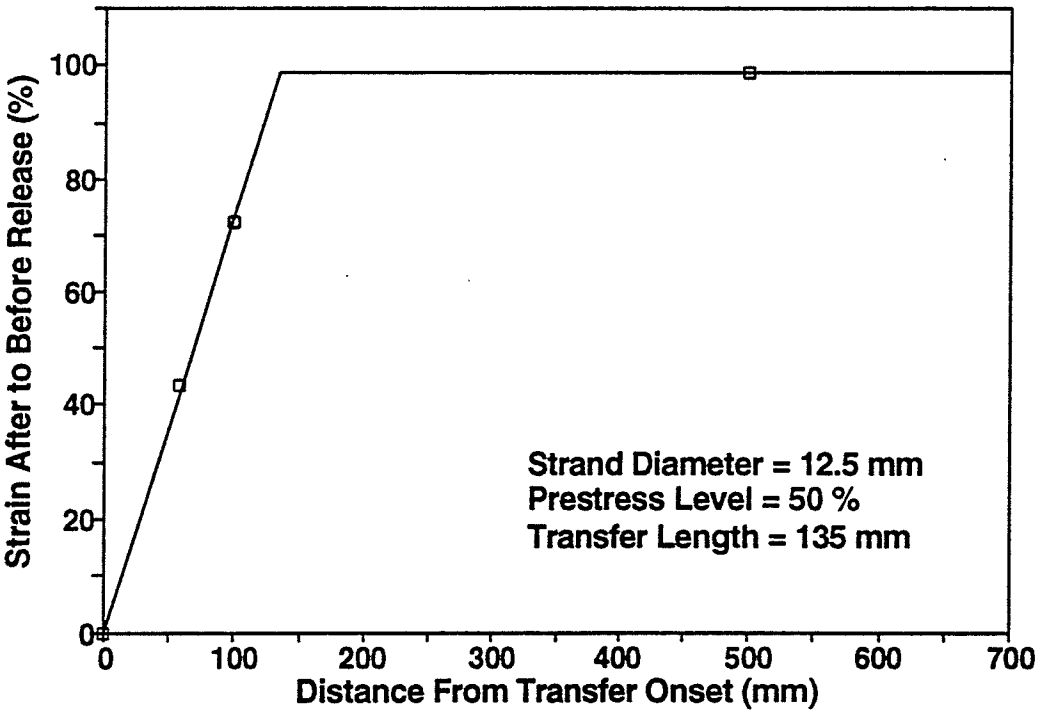

Figure 4.29 Cable Strain in Transfer Zone For Beam D10

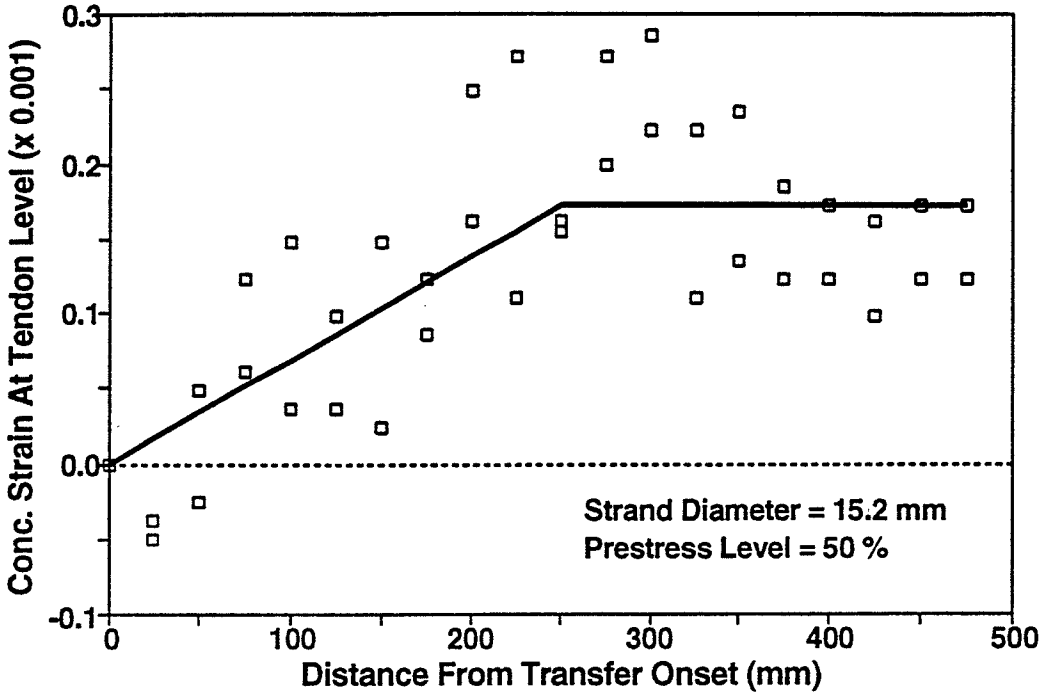

Figure 4.30 Concrete Strain After Transfer For Beam A3

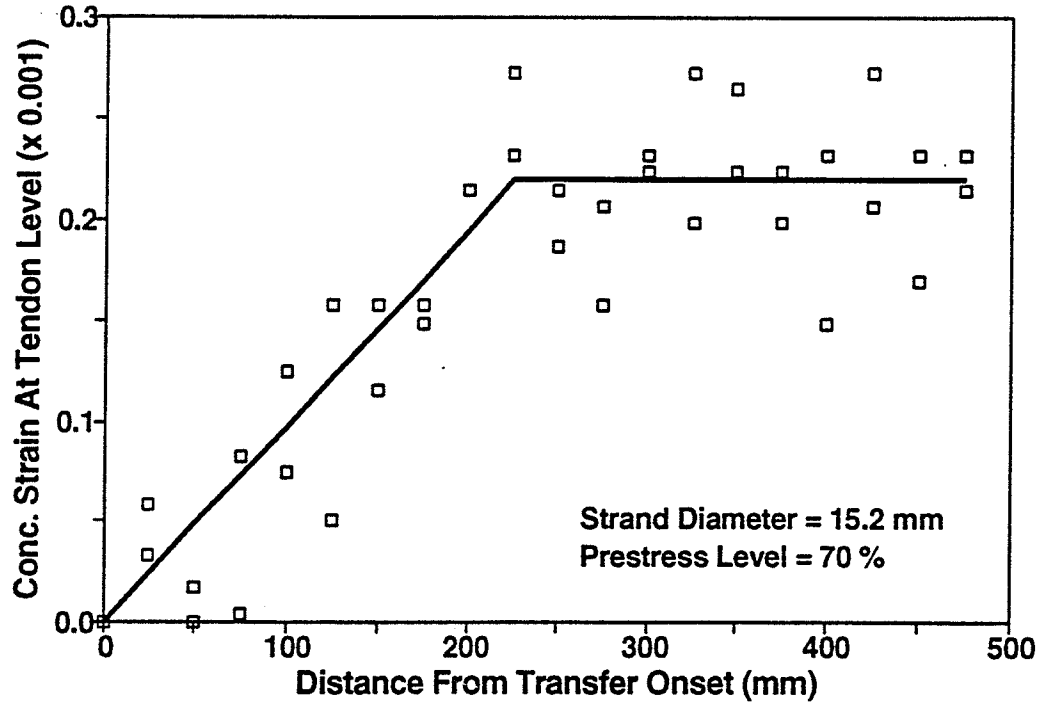

Figure 4.31 Concrete Strain After Transfer For Beam C4

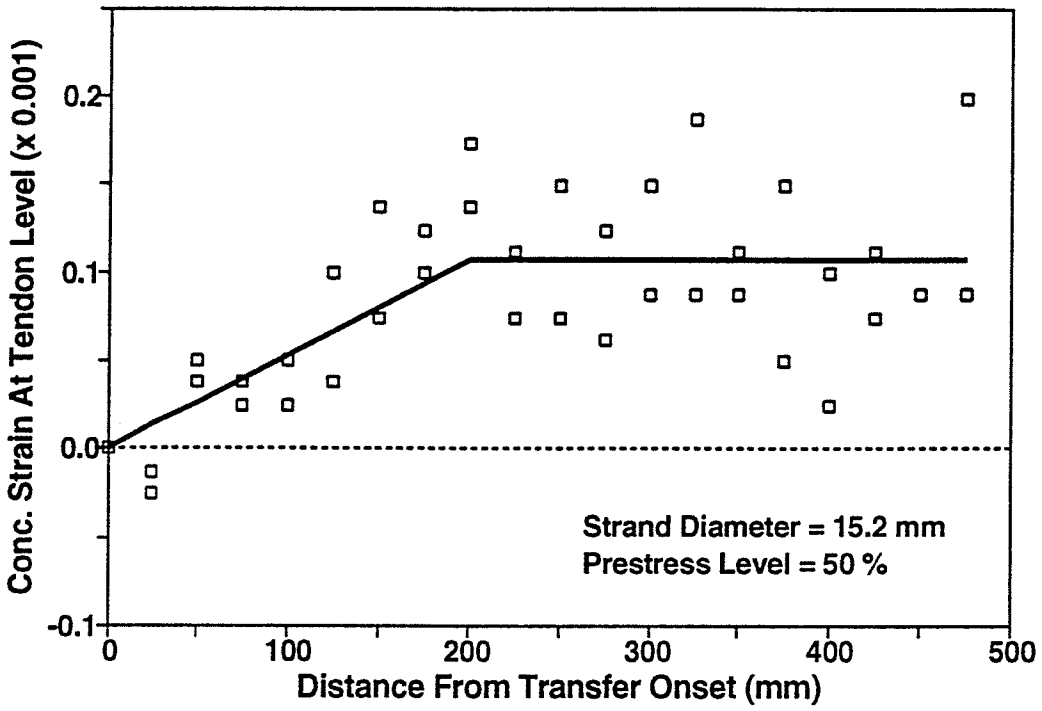

Figure 4.32 Concrete Strain After Transfer For Beam D5

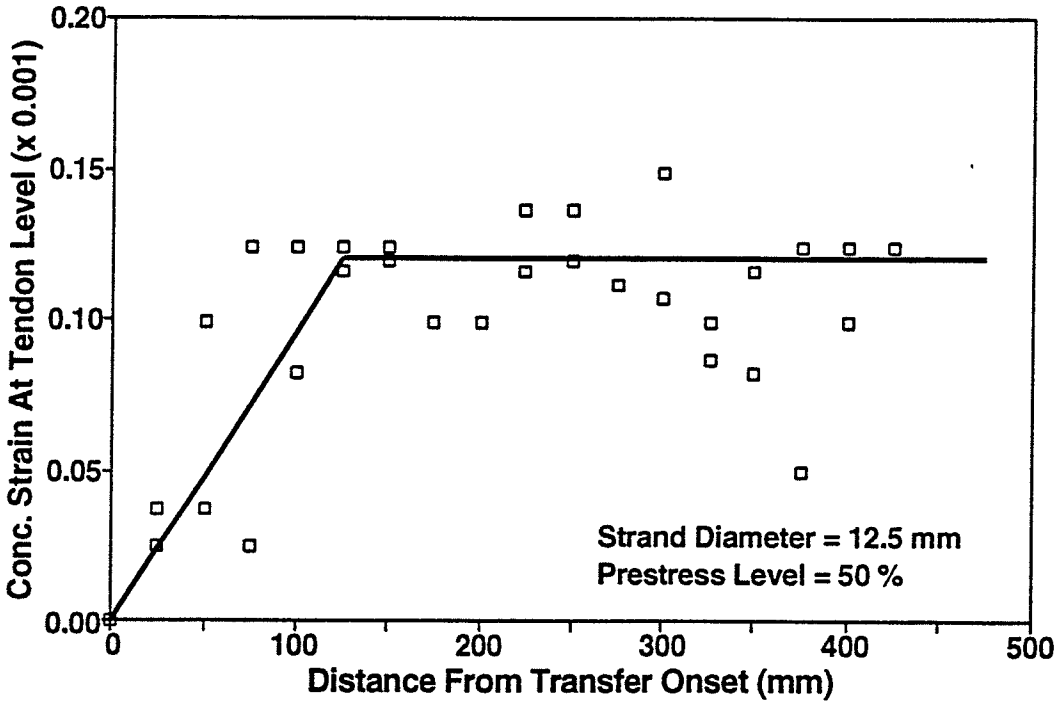

Figure 4.33 Concrete Strain After Transfer For Beam B6

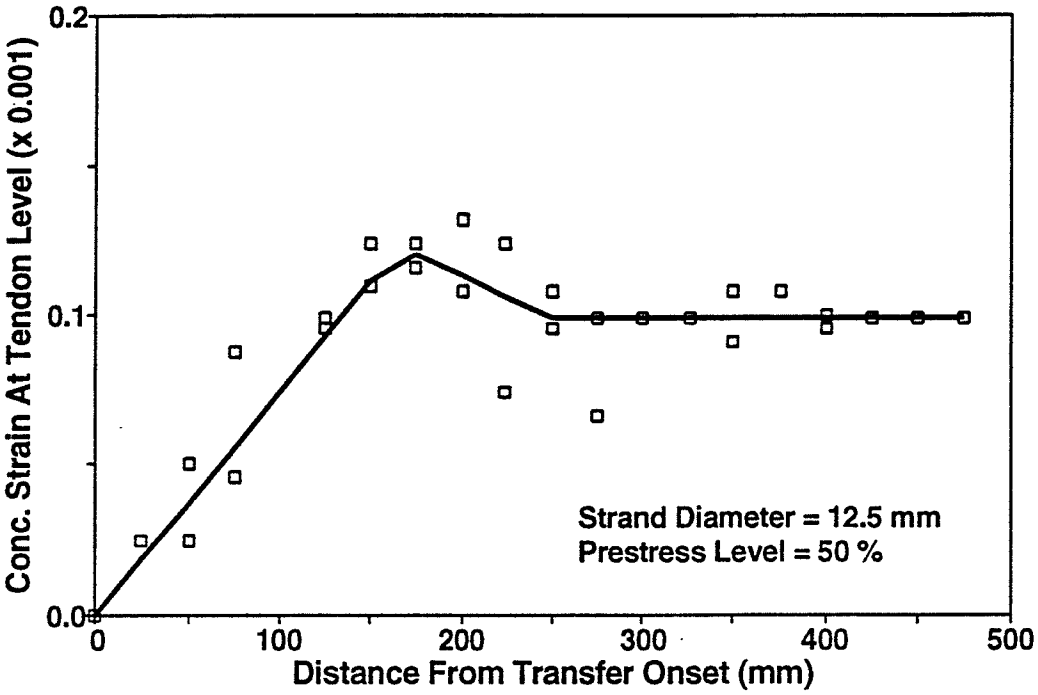

Figure 4.34 Concrete Strain After Transfer For Beam B7

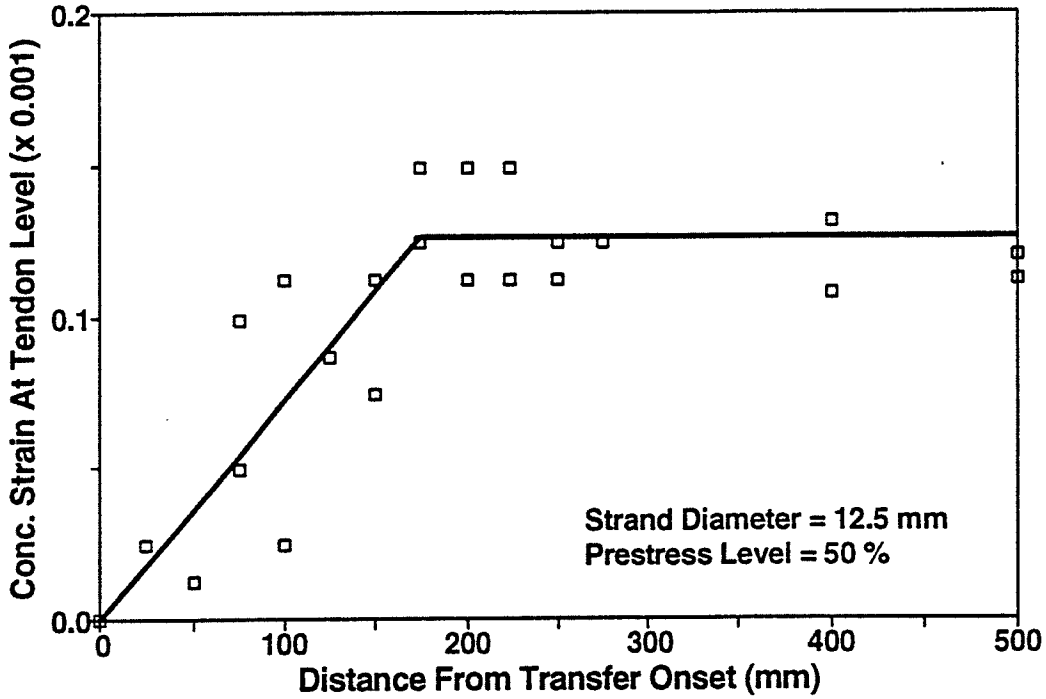

Figure 4.35 Concrete Strain After Transfer For Beam B8

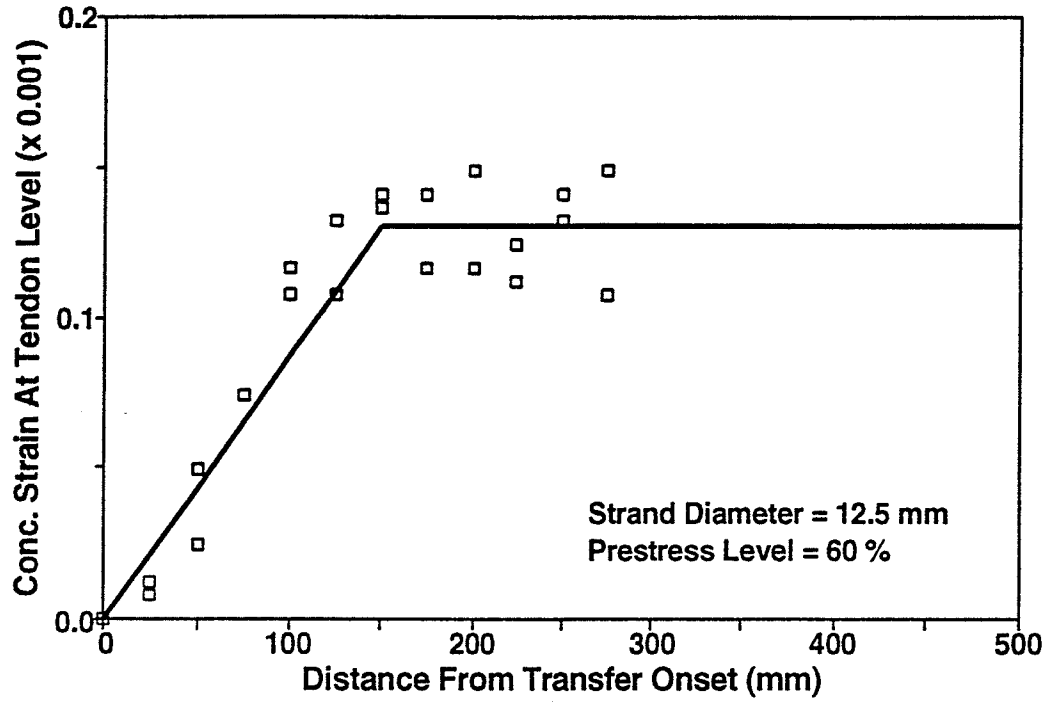

Figure 4.36 Concrete Strain After Transfer For Beam C9

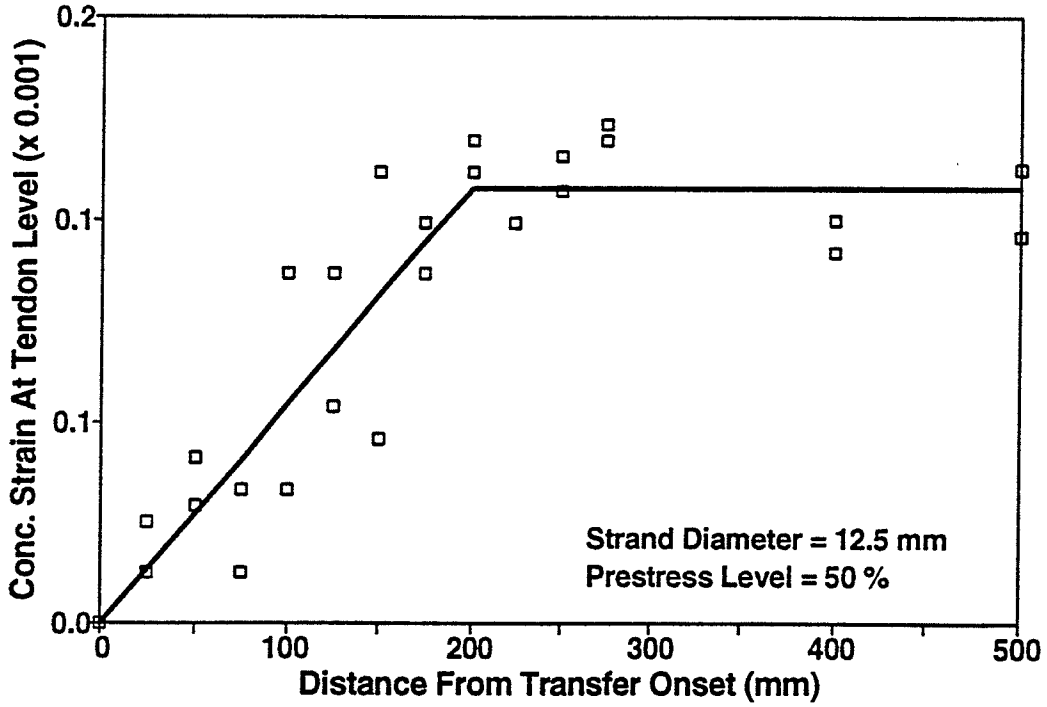

Figure 4.37 Concrete Strain After Transfer For Beam D10

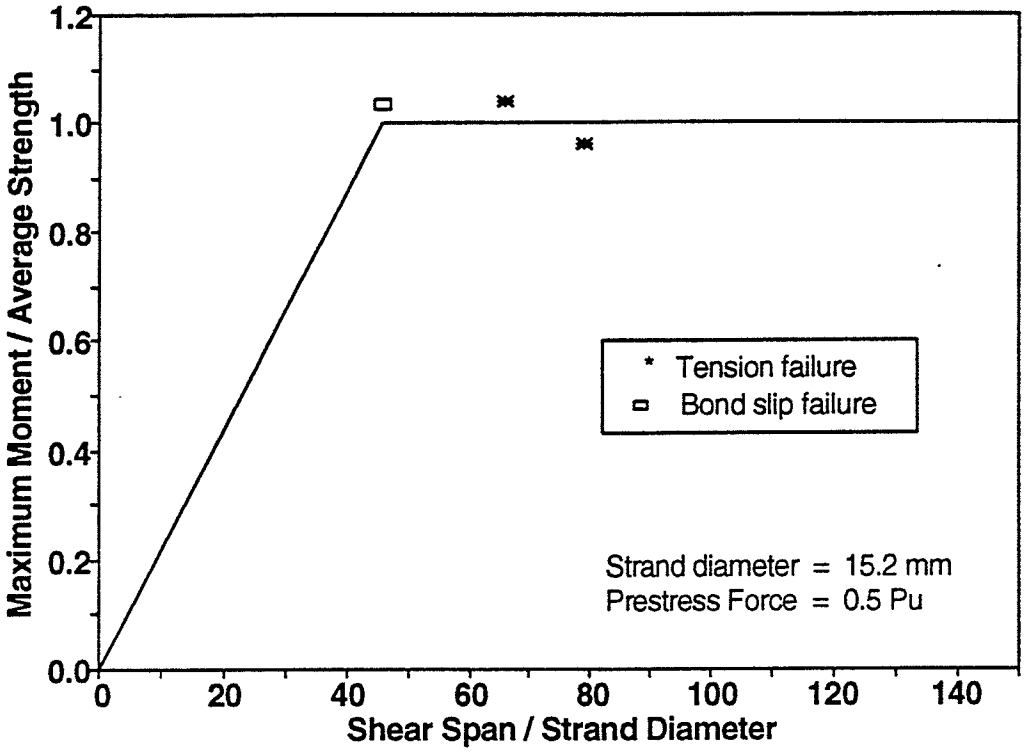

Figure 4.38 Series A Test Results

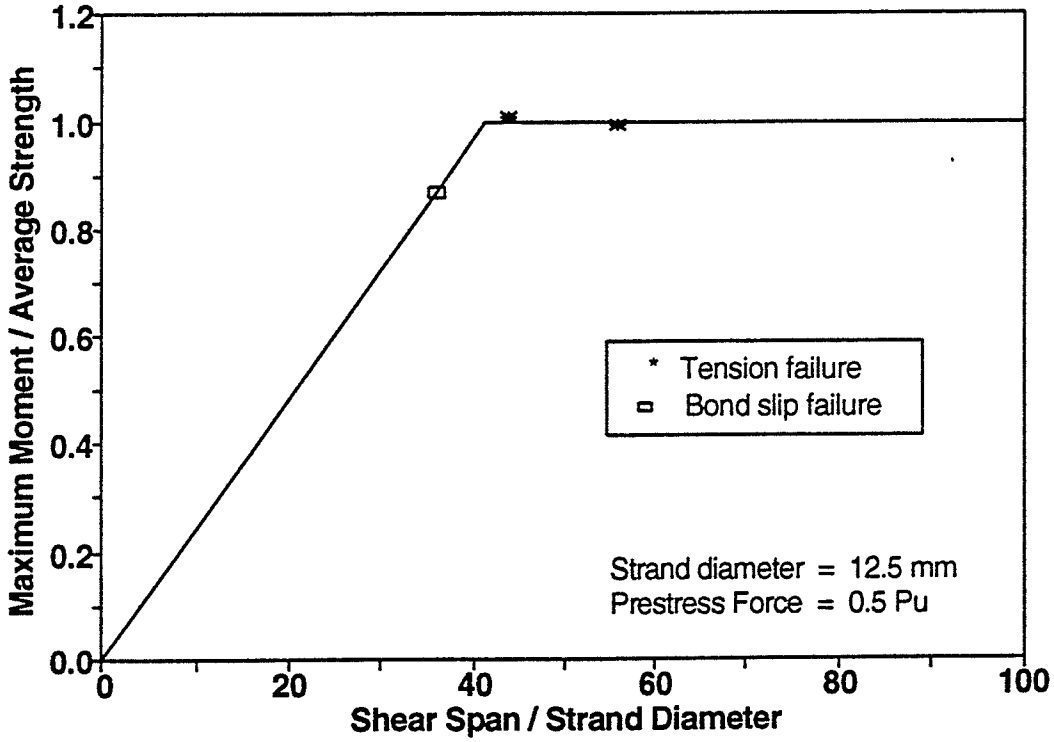

Figure 4.39 Series B Test Results

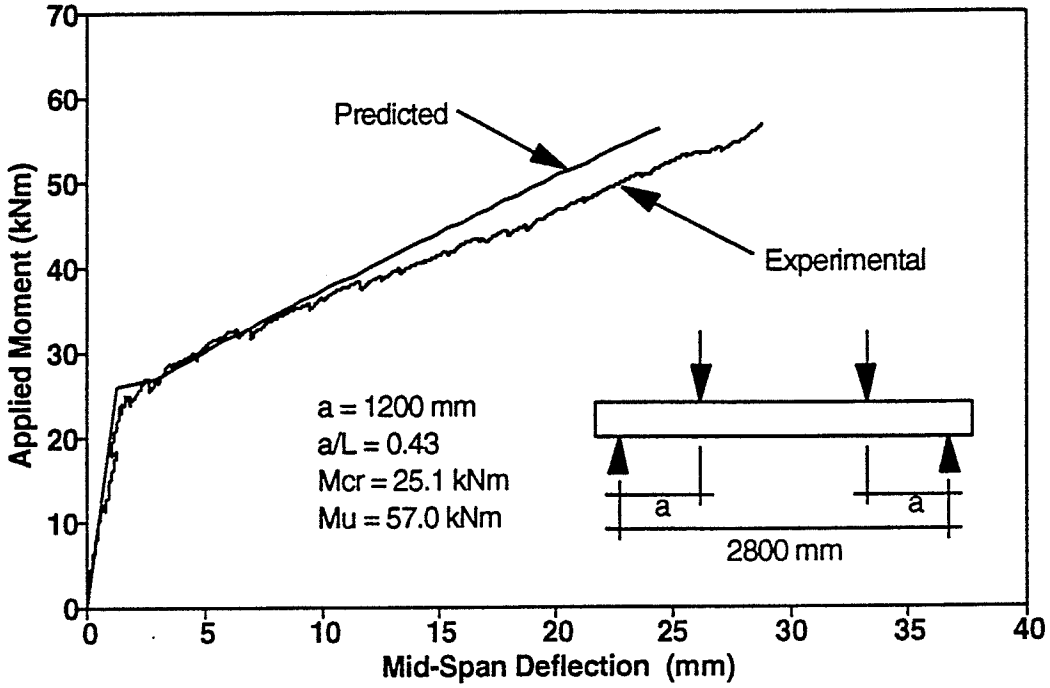

Figure 4.40 Moment-Deflection Relationship For Beam A1

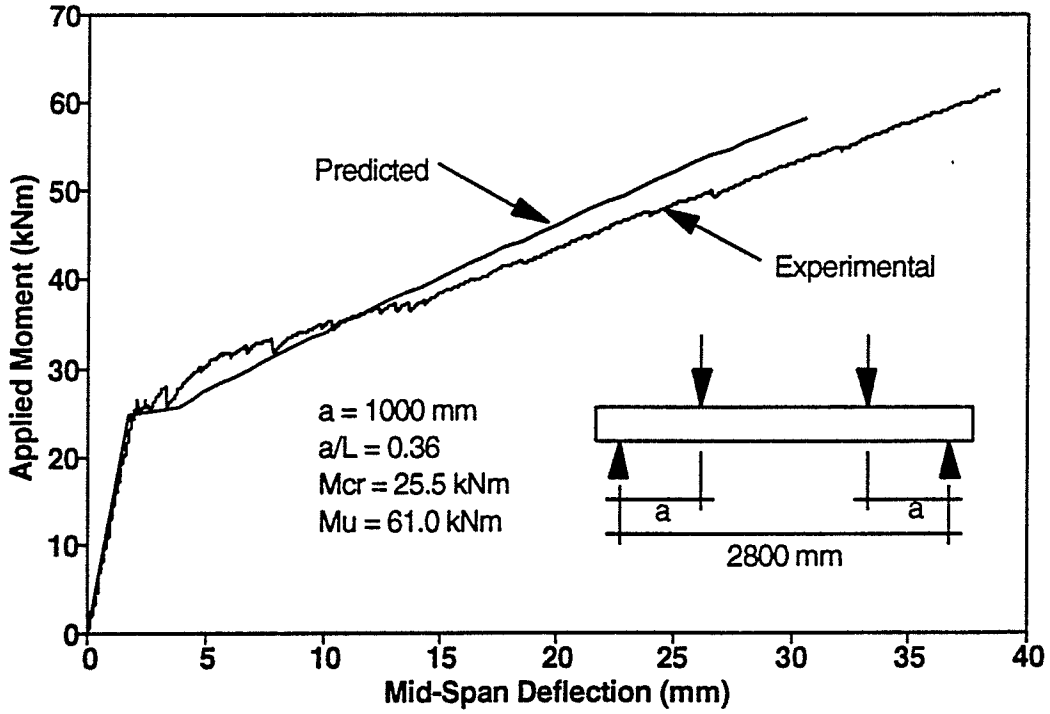

Figure 4.41 Moment-Deflection Relationship For Beam A2

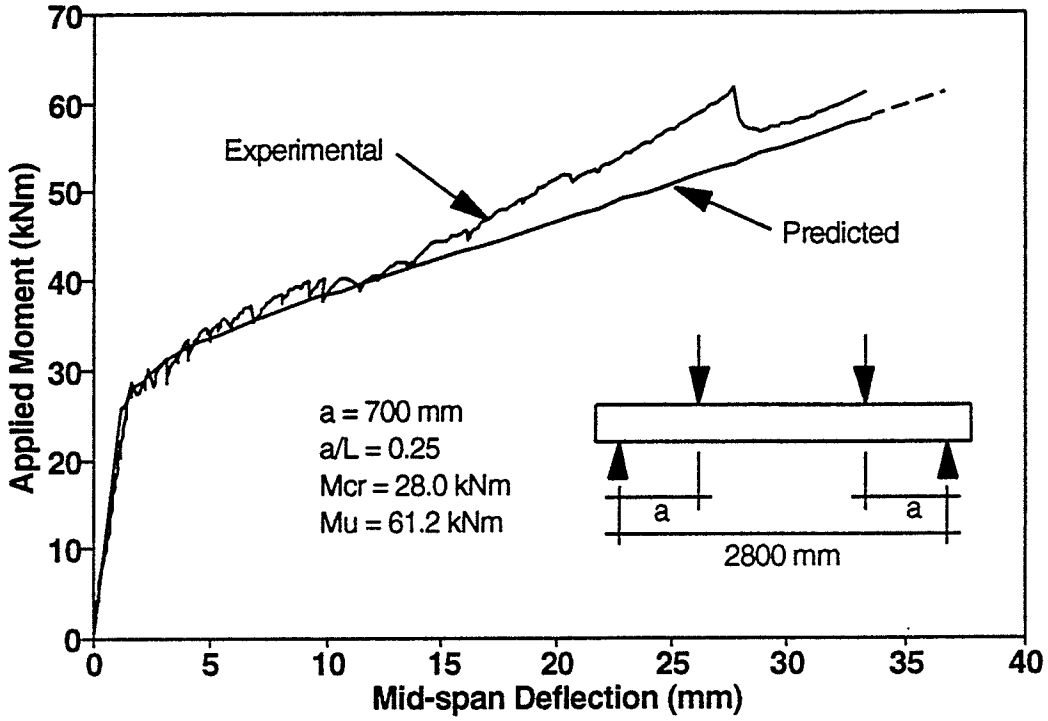

Figure 4.42 Moment-Deflection Relationship For Beam A3

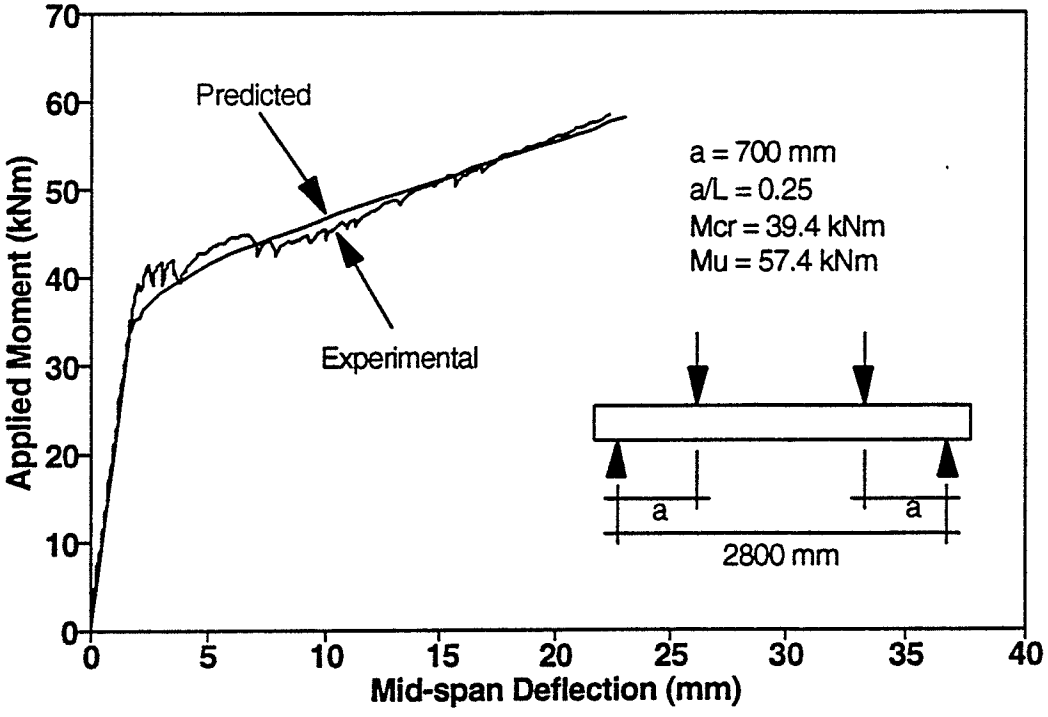

Figure 4.43 Moment-Deflection Relationship For Beam C4

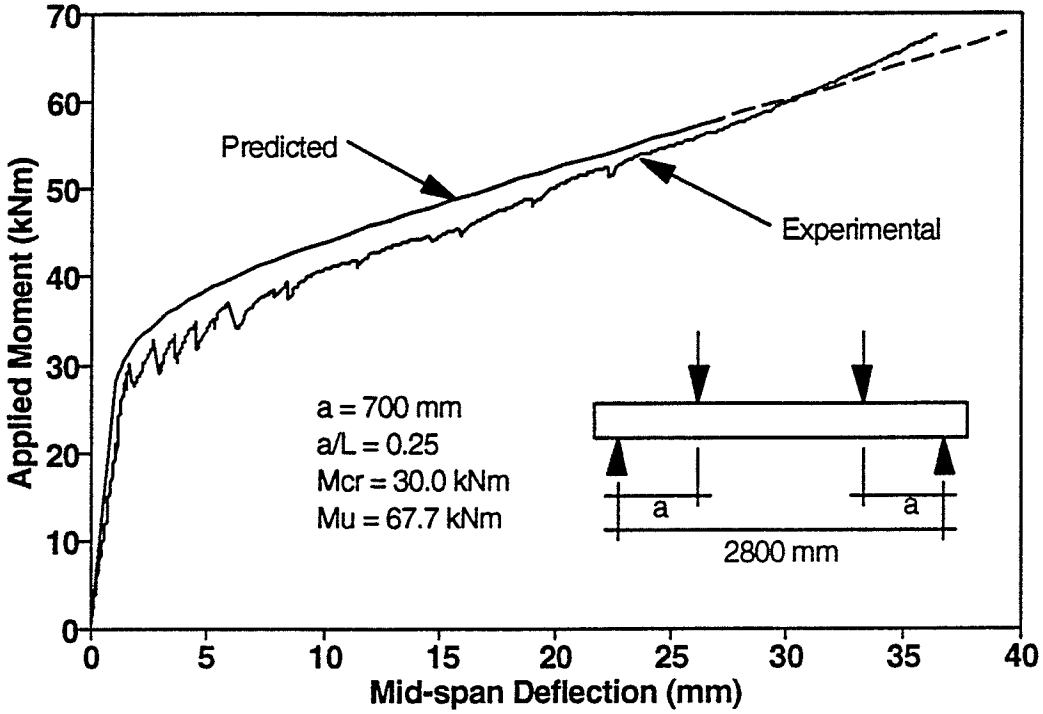

Figure 4.44 Moment-Deflection Relationship For Beam D5

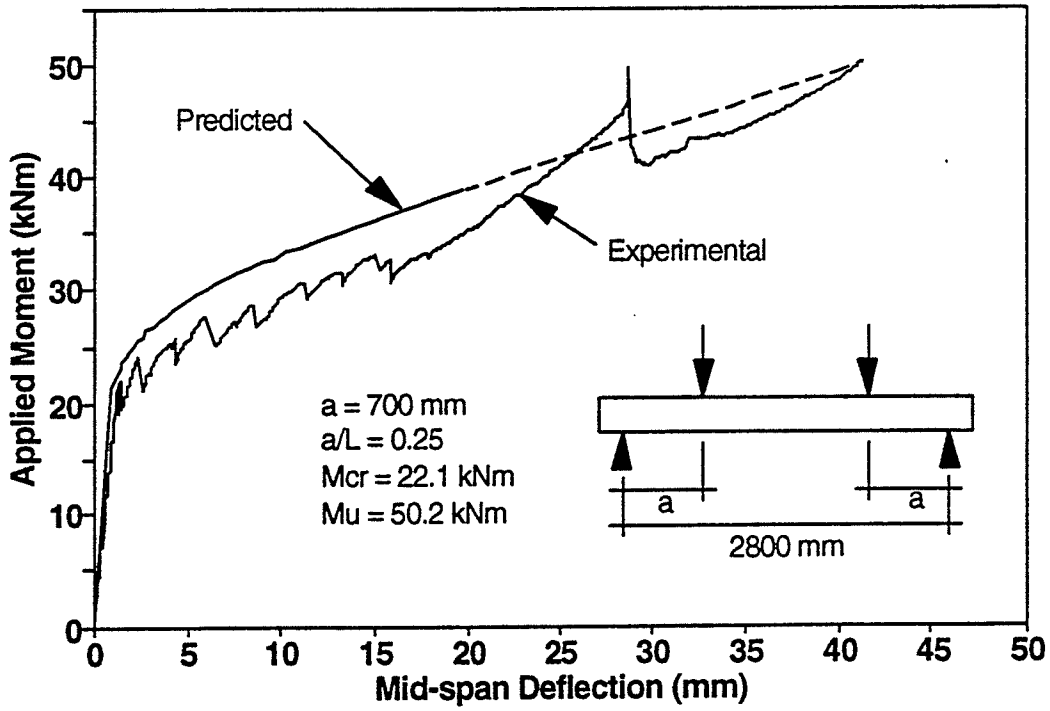

Figure 4.45 Moment-Deflection Relationship For Beam B6

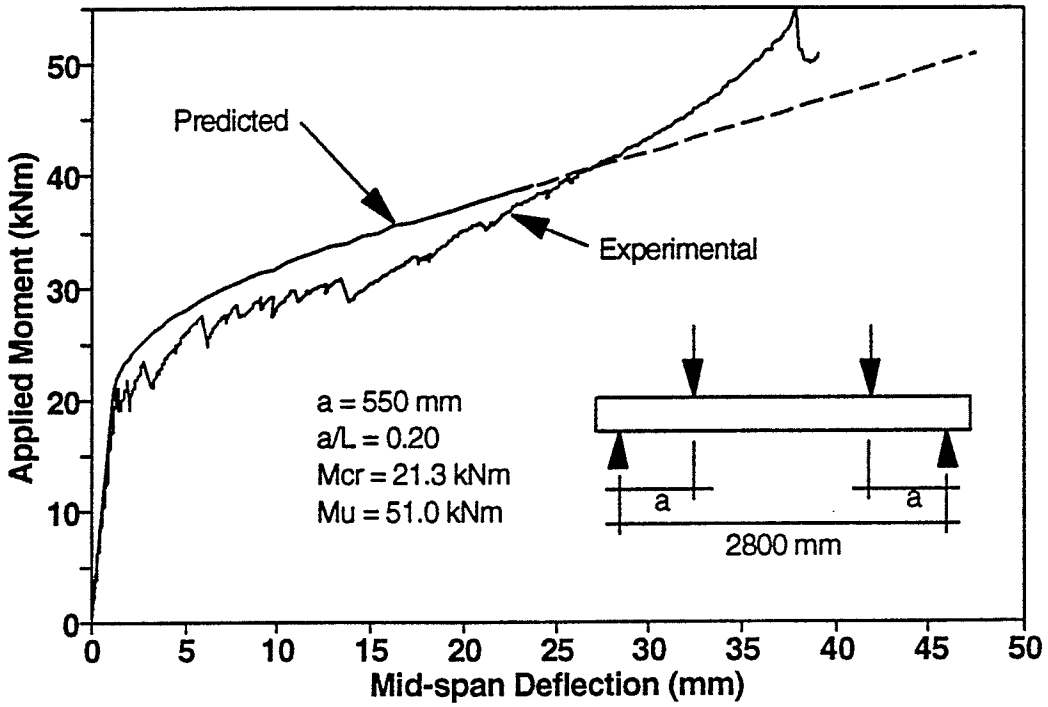

Figure 4.46 Moment-Deflection Relationship For Beam B7

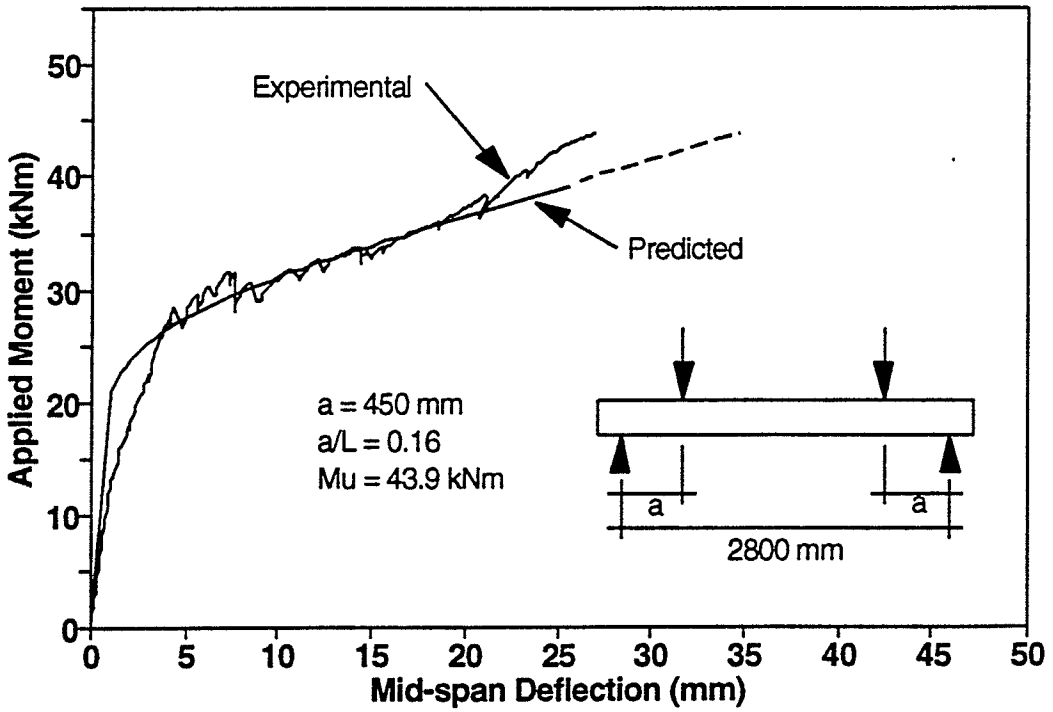

Figure 4.47 Moment-Deflection Relationship For Beam B8

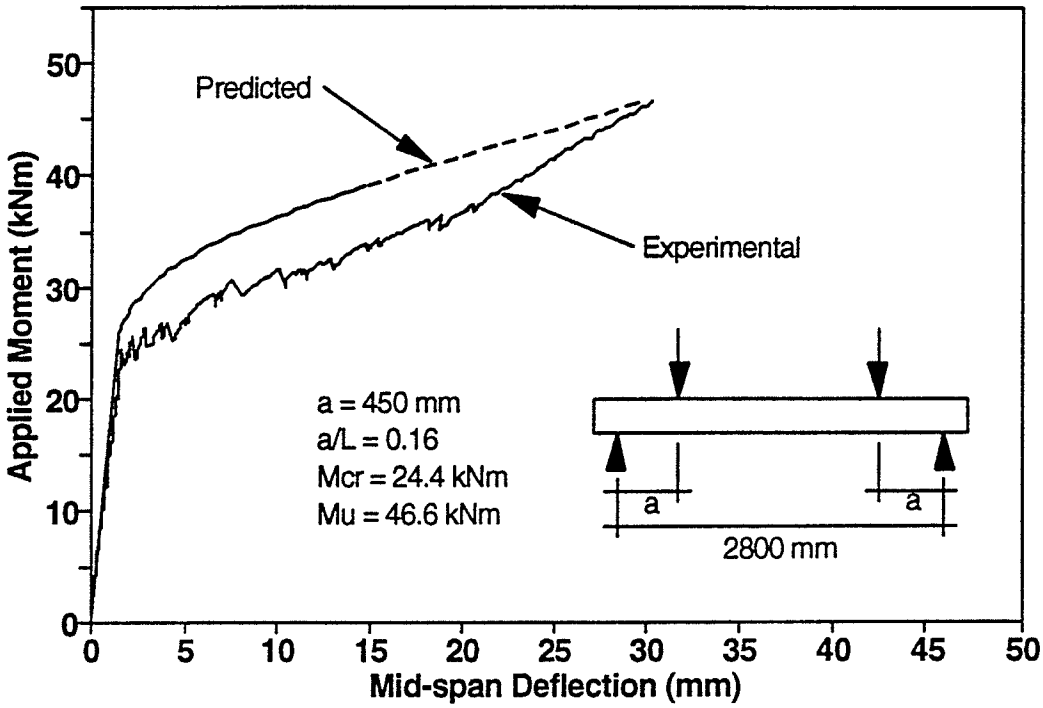

Figure 4.48 Moment-Deflection Relationship For Beam C9

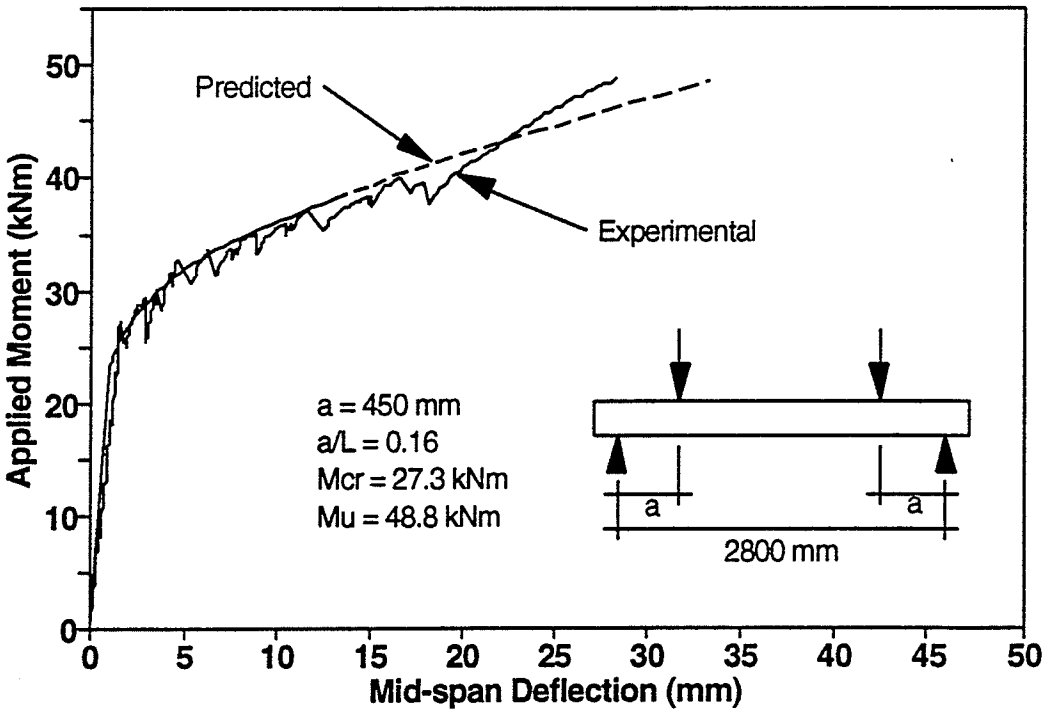

Figure 4.49 Moment-Deflection Relationship For Beam D10

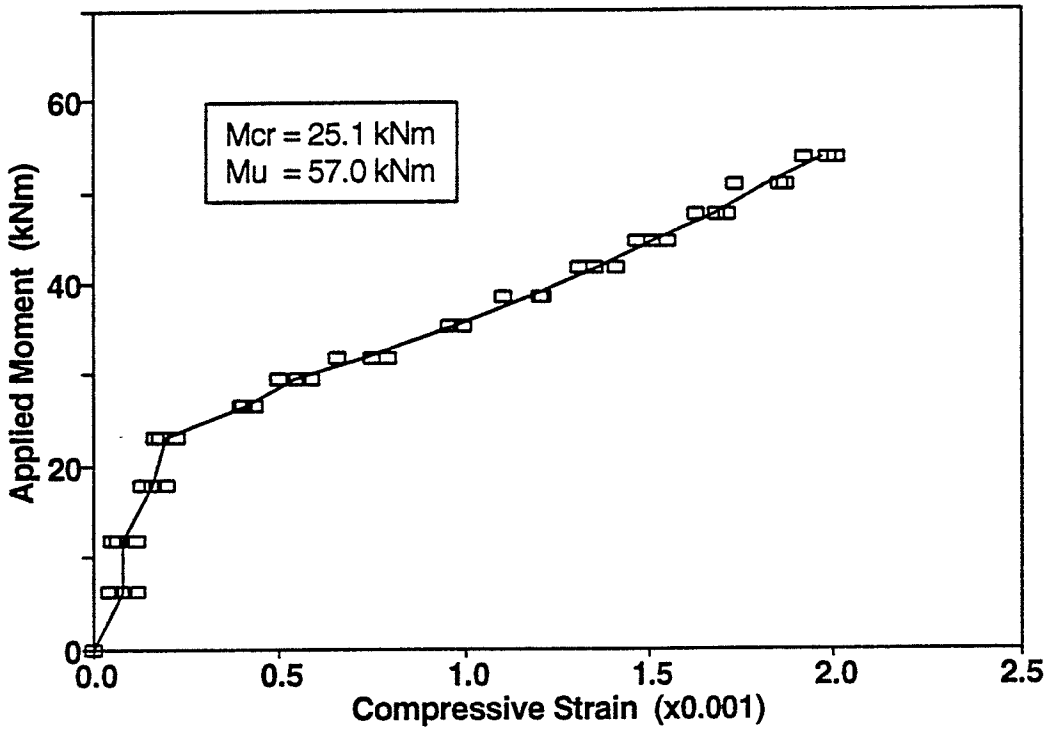

Figure 4.50 Strain in Extreme Compression Fibre at Midspan For Beam A1

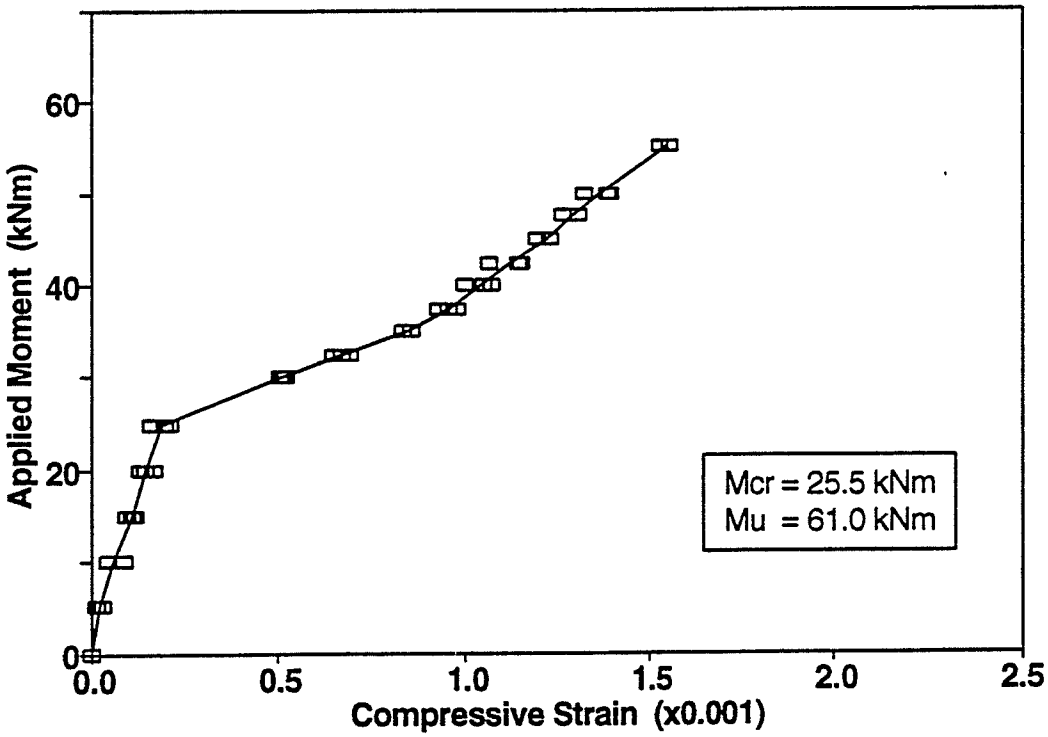

Figure 4.51 Strain in Extreme Compression Fibre at Midspan For Beam A2

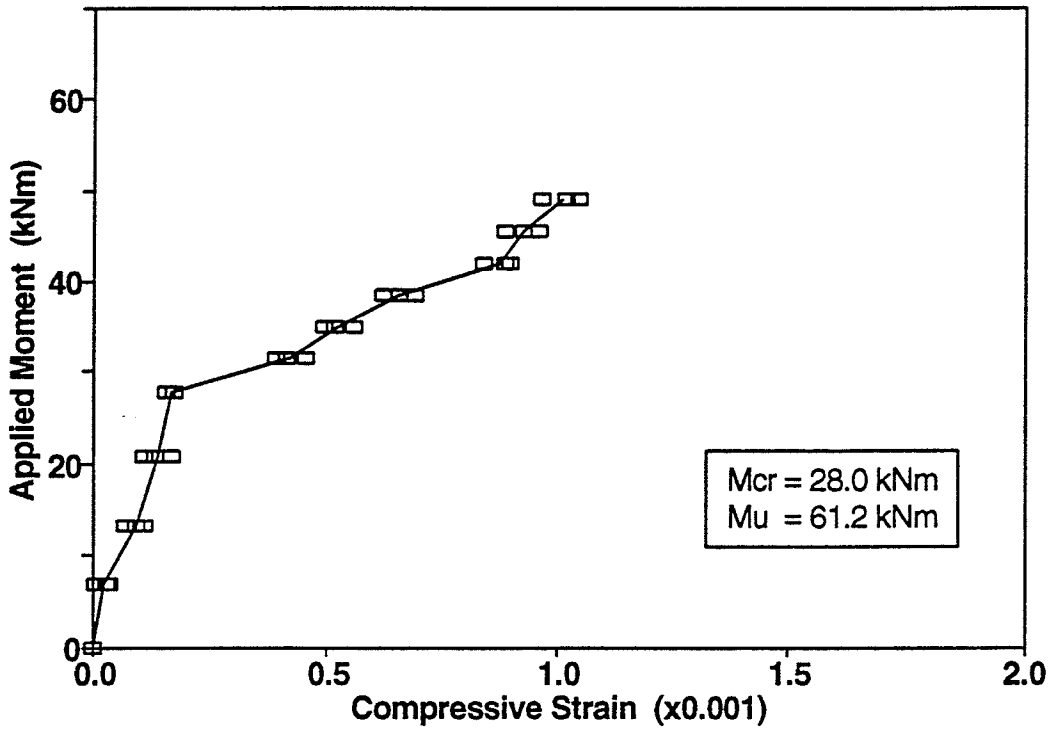

Figure 4.52 Strain in Extreme Compression Fibre at Midspan For Beam A3

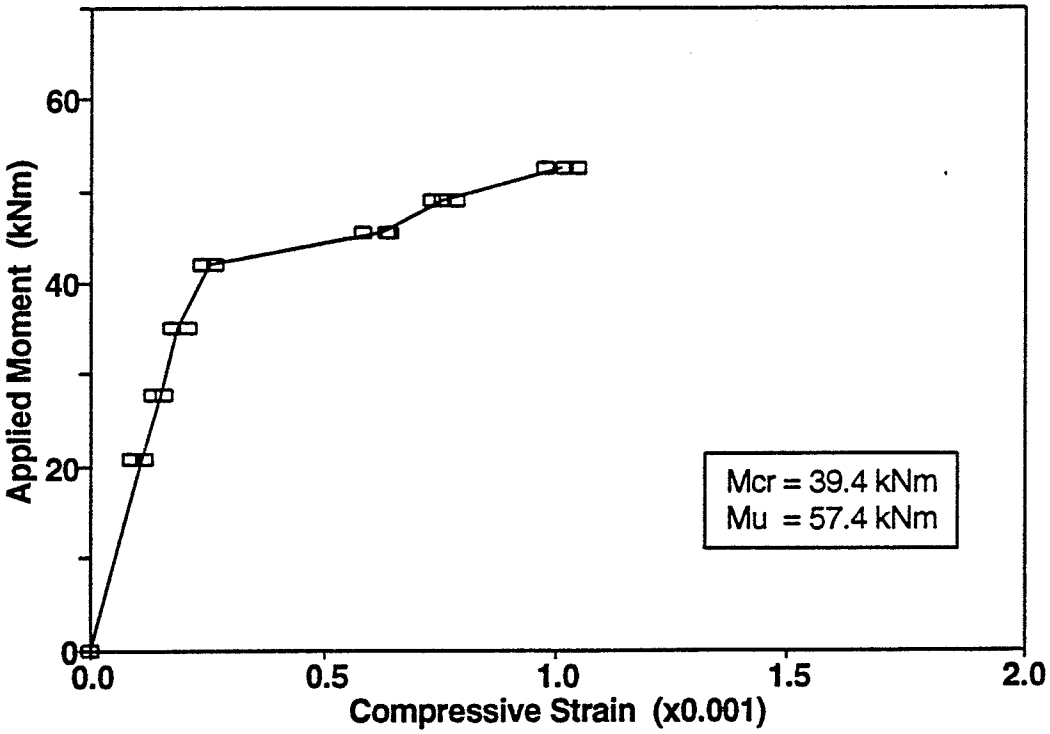

Figure 4.53 Strain in Extreme Compression Fibre at Midspan For Beam C4

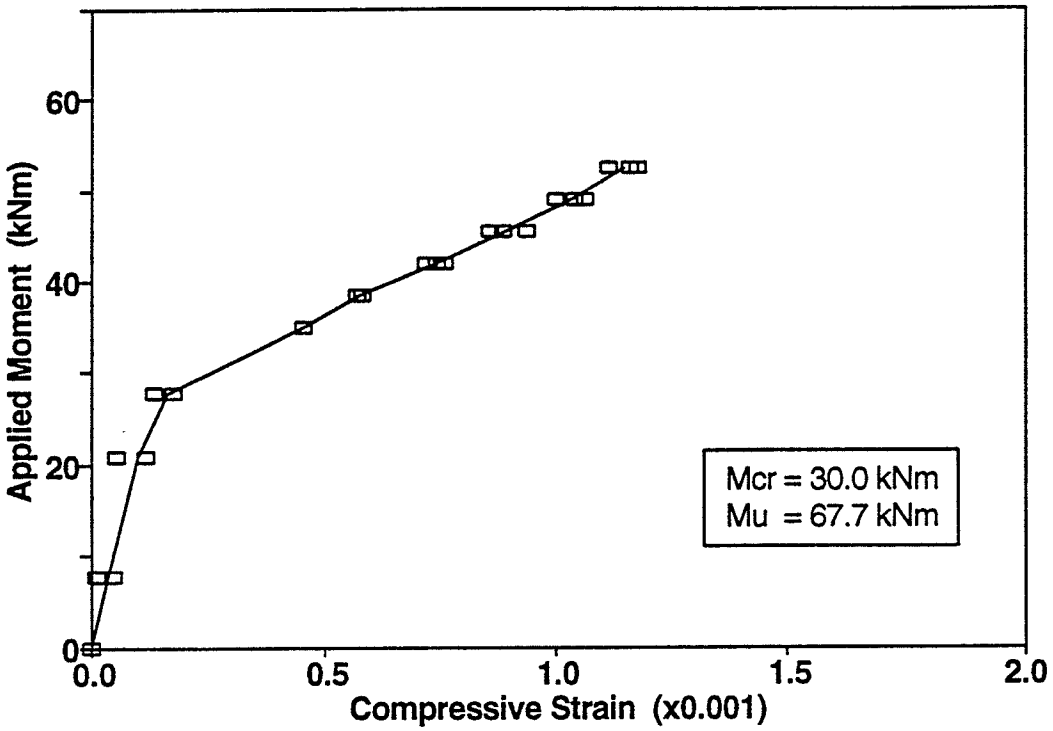

Figure 4.54 Strain in Extreme Compression Fibre at Midspan For Beam D5

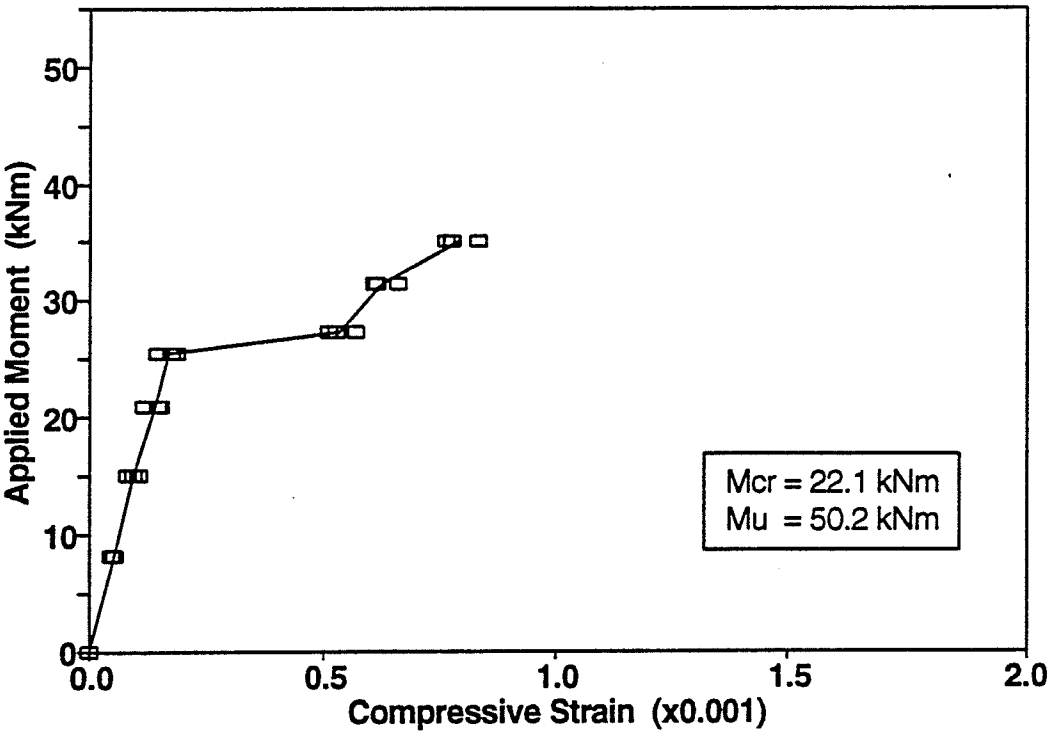

Figure 4.55 Strain in Extreme Compression Fibre at Midspan For Beam B6

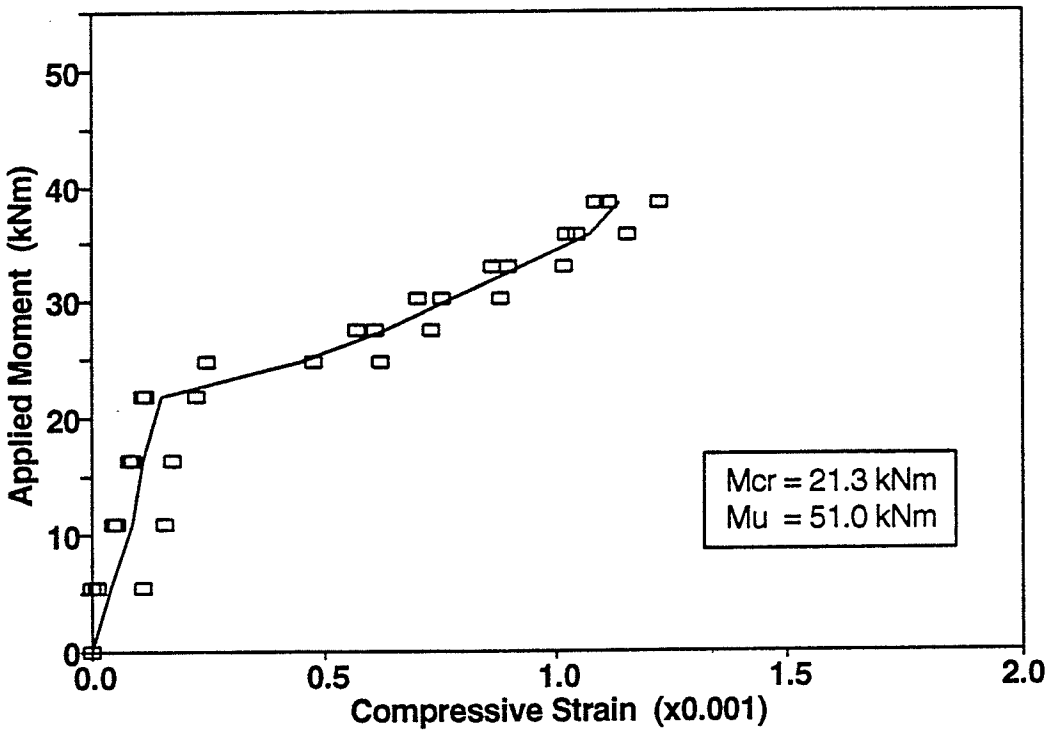

Figure 4.56 Strain in Extreme Compression Fibre at Midspan For Beam B7

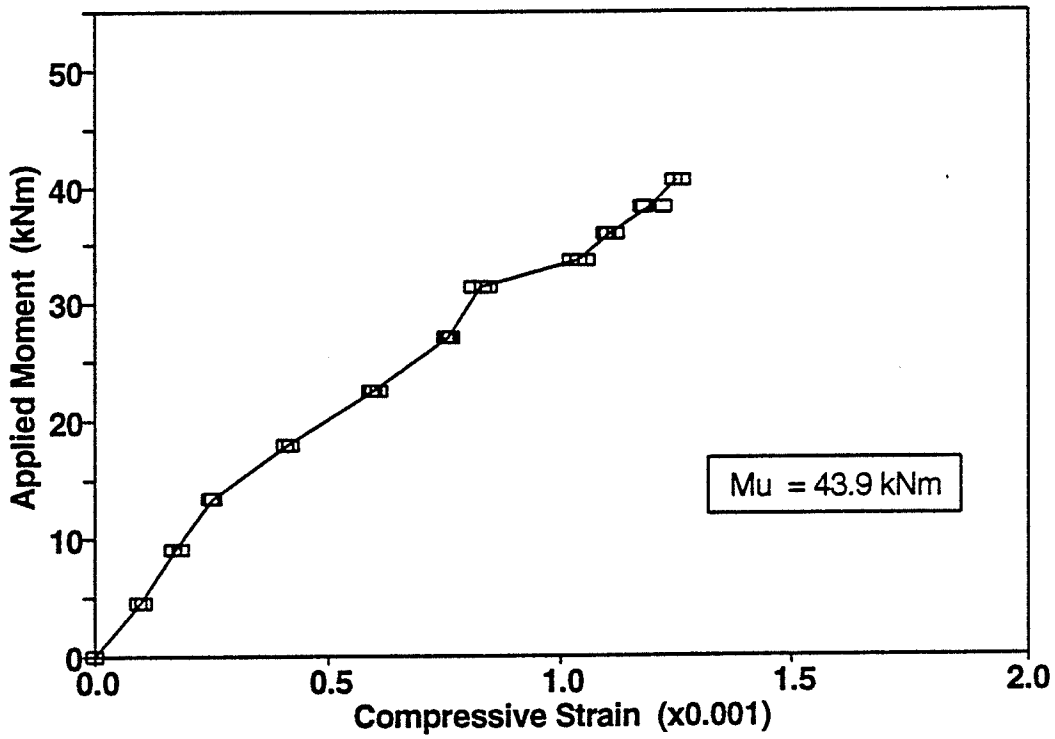

Figure 4.57 Strain in Extreme Compression Fibre at Midspan For Beam B8

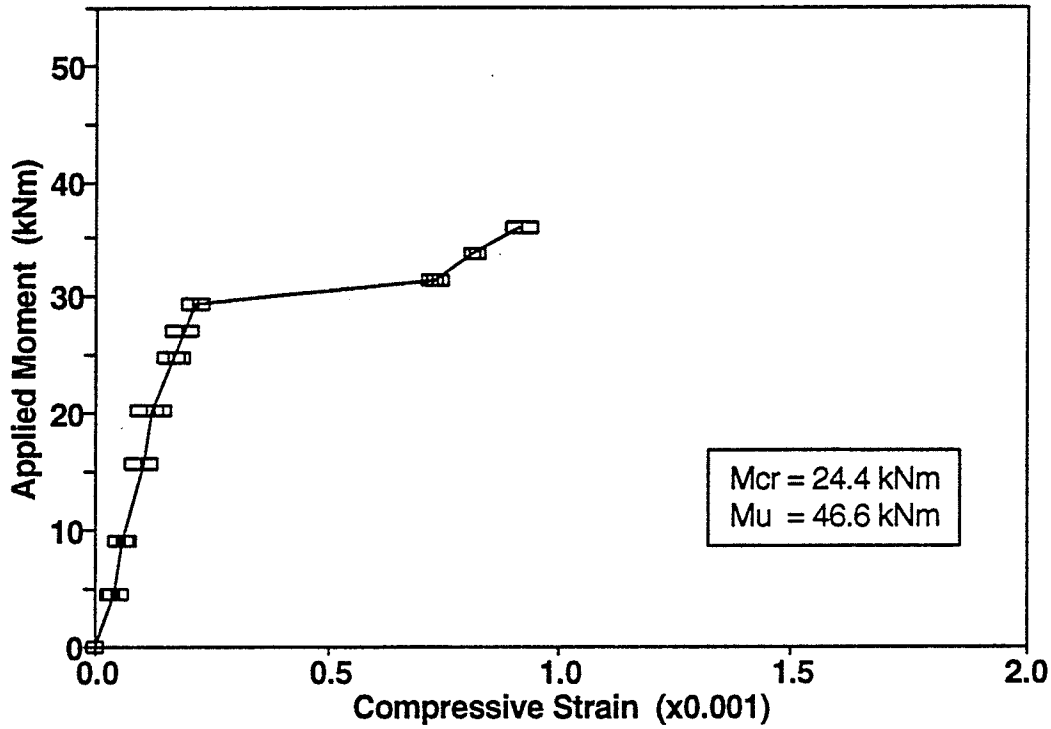

Figure 4.58 Strain in Extreme Compression Fibre at Midspan For Beam C9

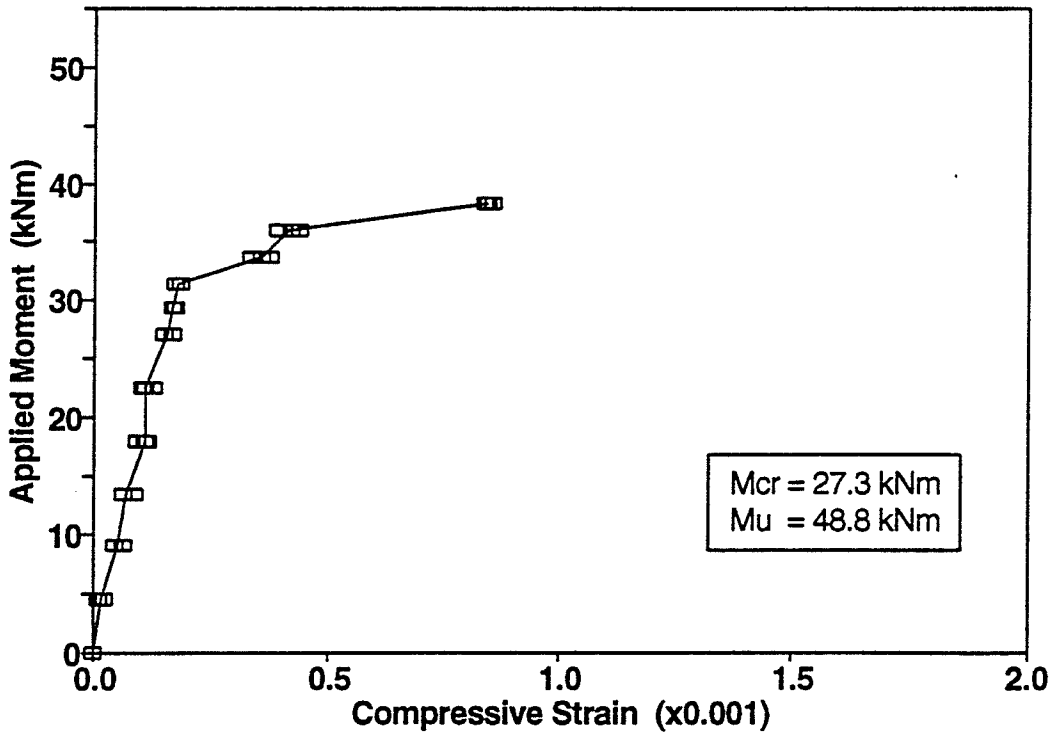

Figure 4.59 Strain in Extreme Compression Fibre at Midspan For Beam D10

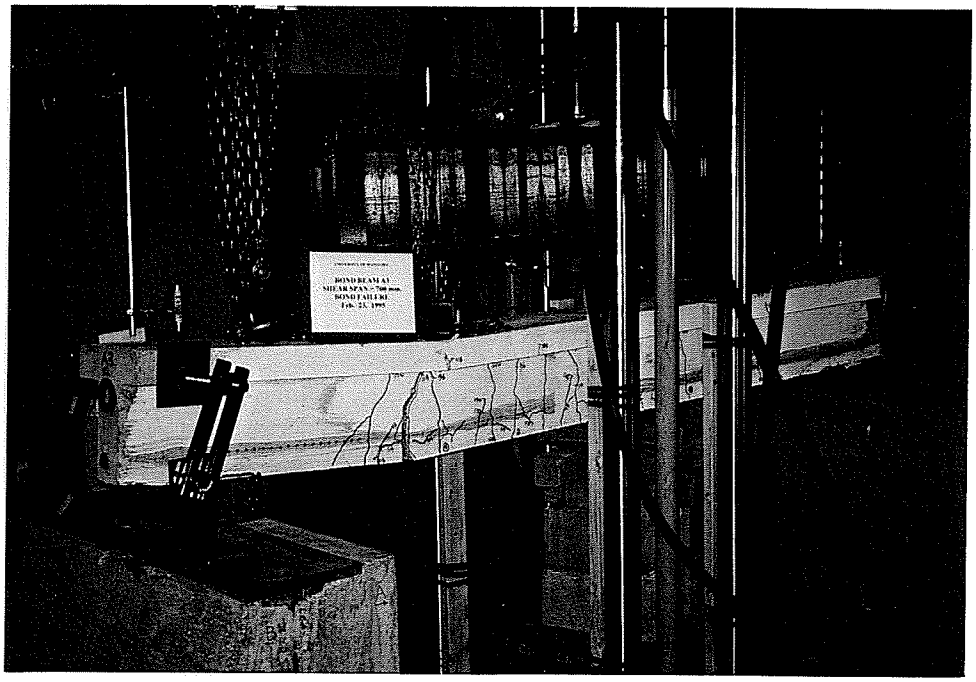

Figure 4.60 Failure of Beam A3

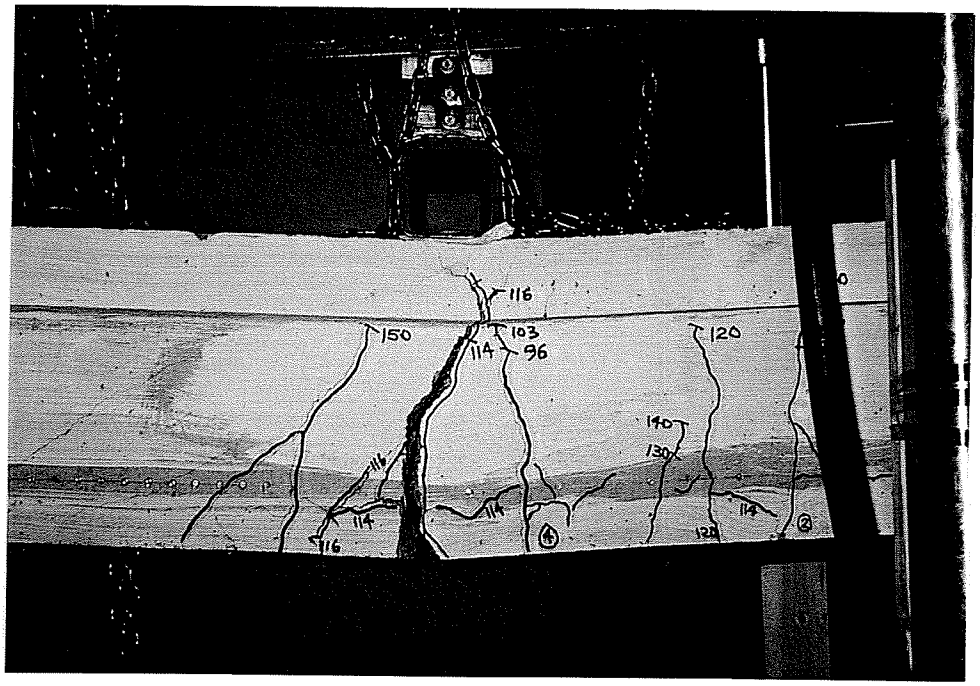

Figure 4.61 Failure of Beam A3 - Close-up

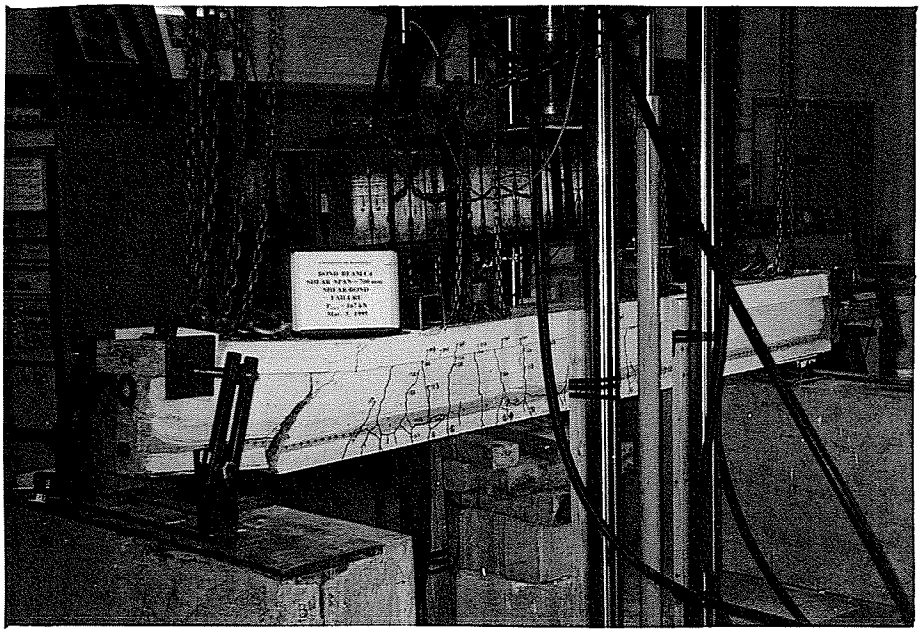

Figure 4.62 Failure of Beam C4

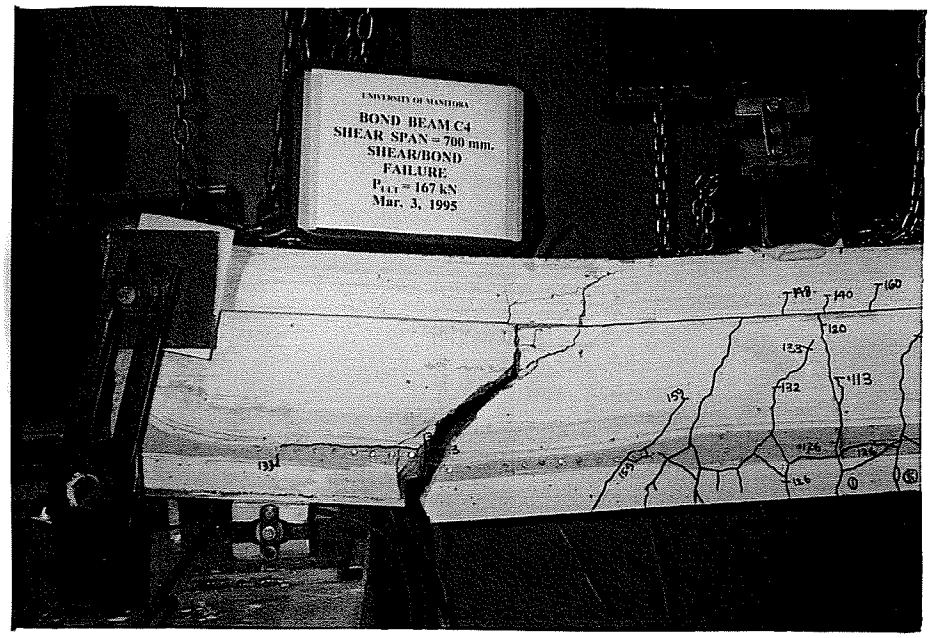

Figure 4.63 Failure of Beam C4 - Close-up

Figure 4.64 Failure of Beam D5

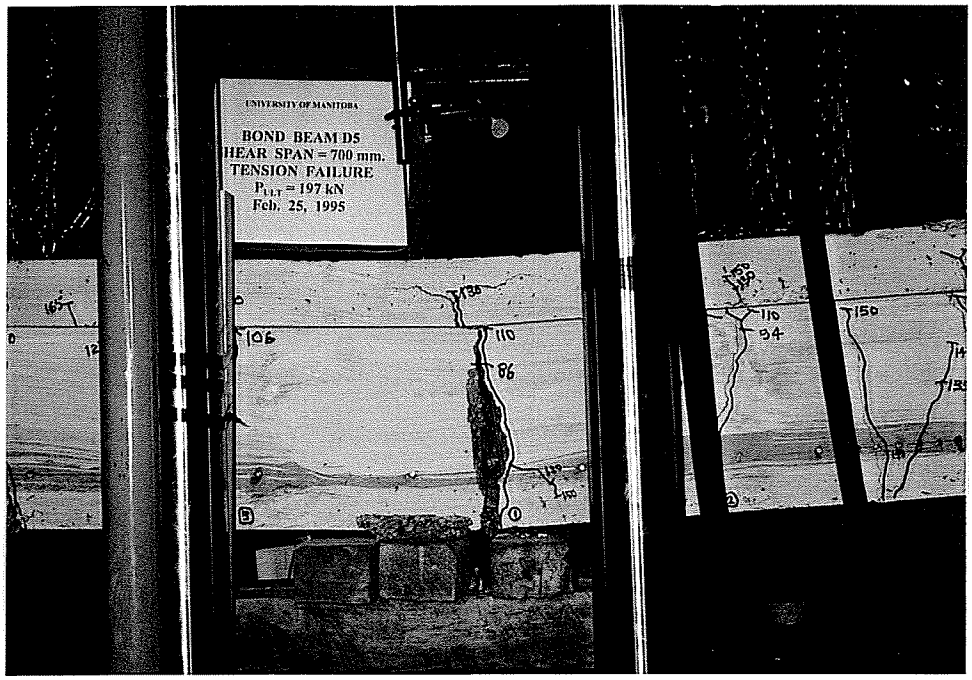

Figure 4.65 Failure of Beam D5 - Close-up

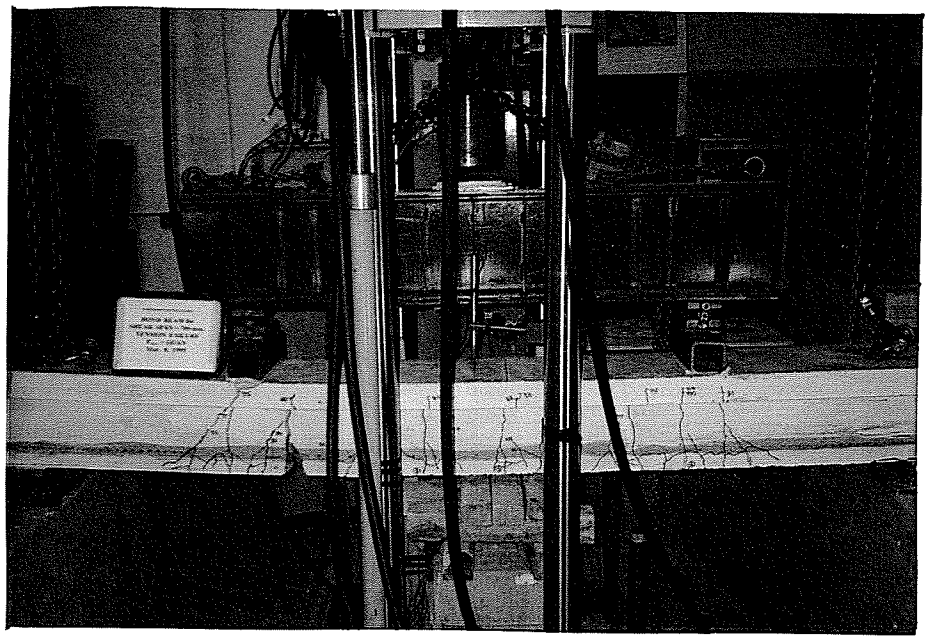

Figure 4.66 Failure of Beam B6

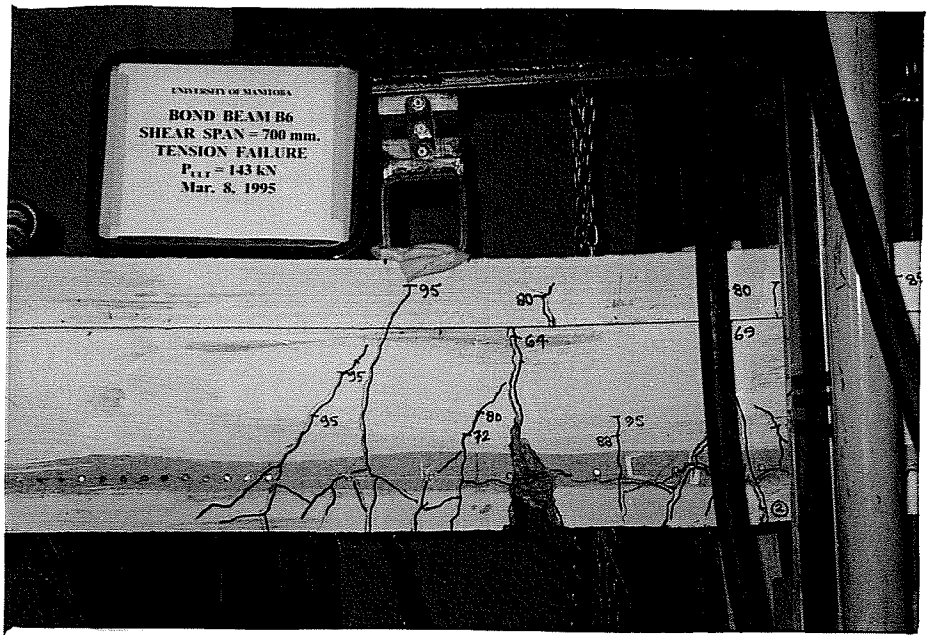

Figure 4.67 Failure of Beam B6 - Close-up

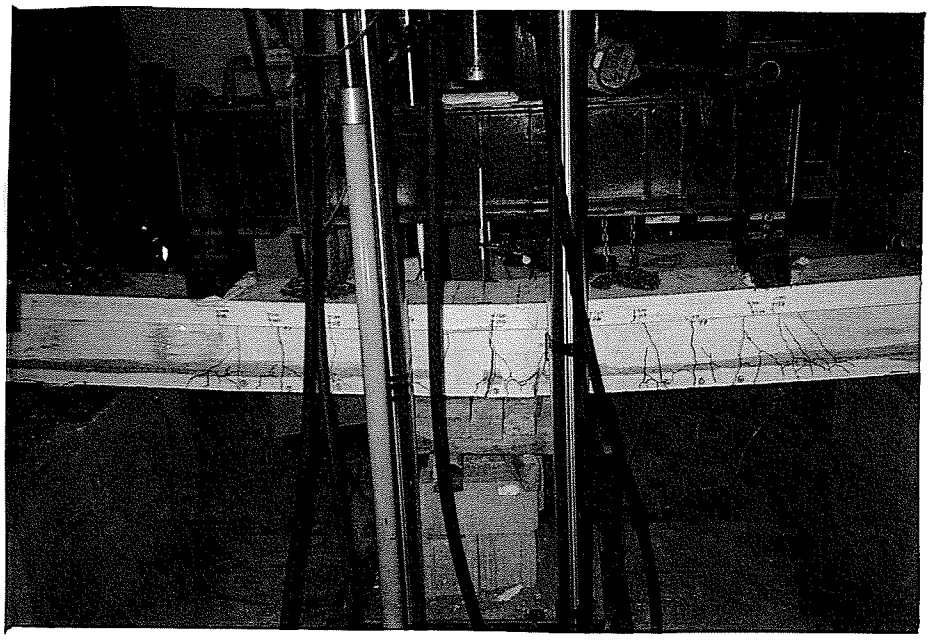

Figure 4.68 Failure of Beam B7

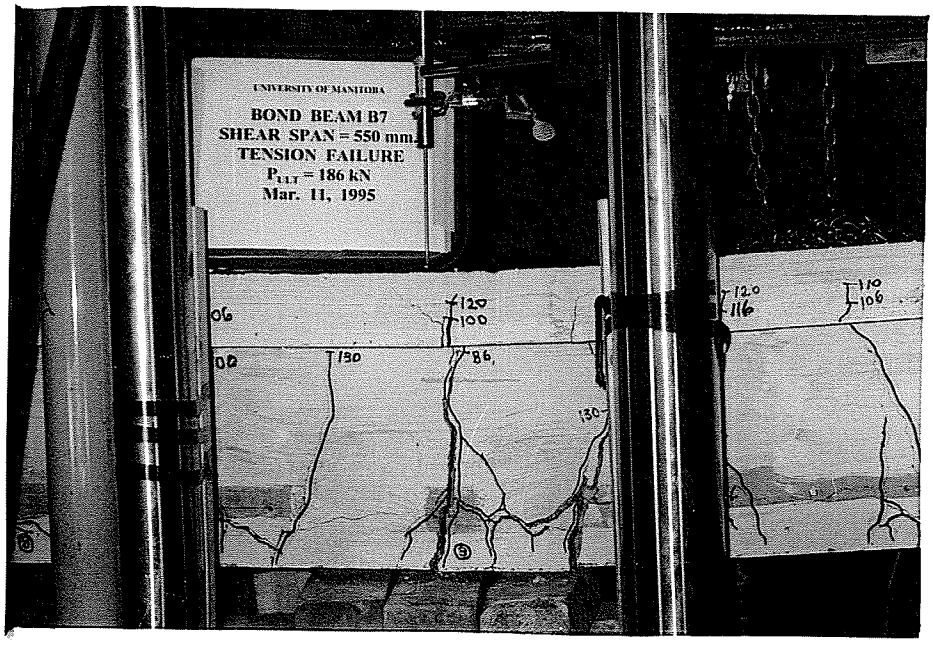

Figure 4.69 Failure of Beam B7 - Close-up

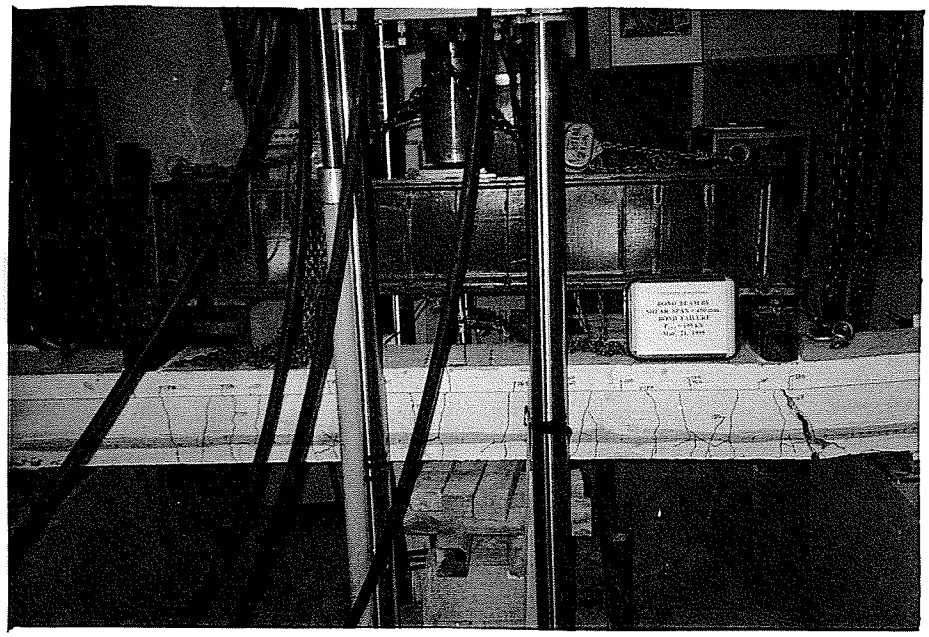

Figure 4.70 Failure of Beam B8

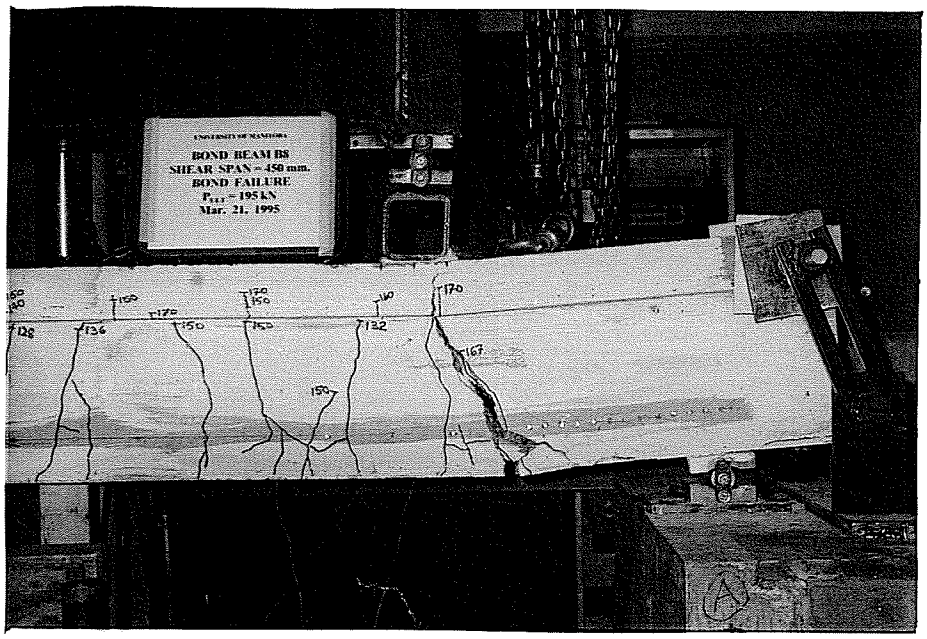

Figure 4.71 Failure of Beam B8 - Close-up

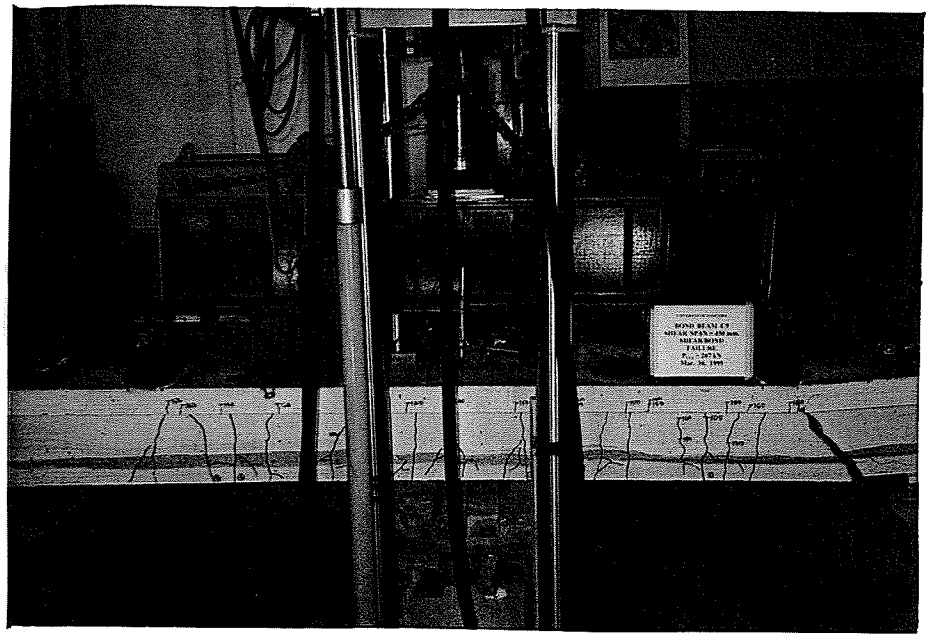

Figure 4.72 Failure of Beam C9

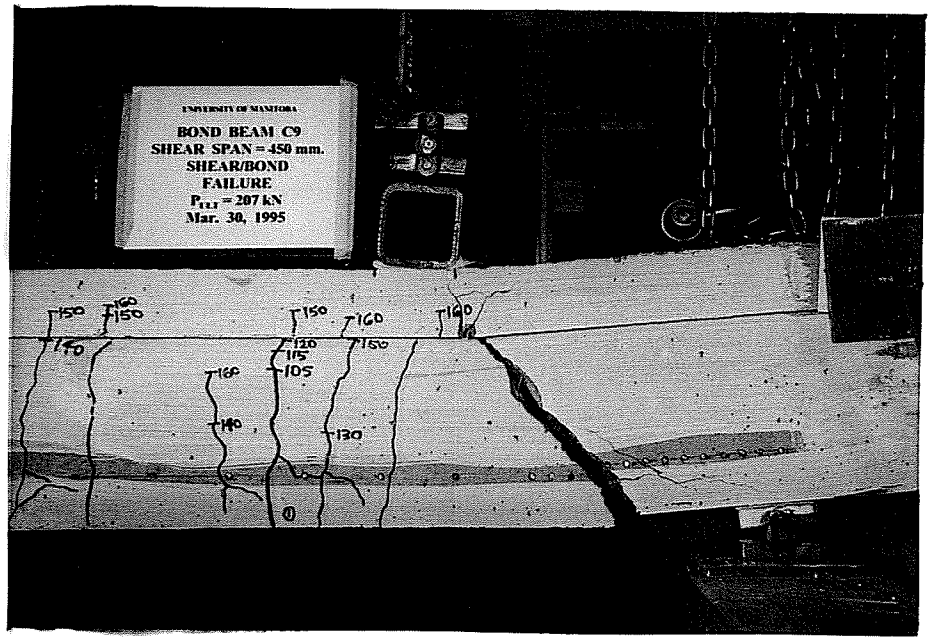

Figure 4.73 Failure of Beam C9 - Close-up

Figure 4.74 Failure of Beam D10

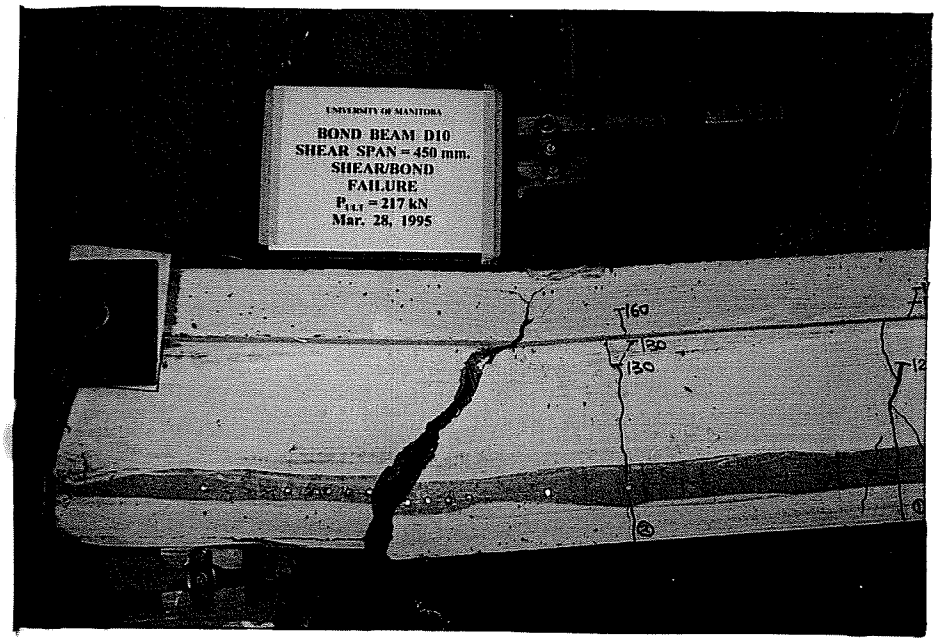

Figure 4.75 Failure of Beam D10 - Close-up

CHAPTER 5

ANALYSIS AND DISCUSSION

5.1. Introduction

Based on the experimental program, the transfer length, flexural bond length of CFCC and its corresponding bond strengths are determined. The various parameters included in this program were the CFCC diameter, prestress level, and concrete cover. This chapter of the report will briefly describe these findings and critically discuss the results.

5.2. Transfer Length

The measured transfer length values are given in Table 4.2. These values were obtained using the measured strain by the strain gauges attached to the CFCC strand and by demec point gauges attached to the concrete surface. Measurements of strain were recorded immediately before and after release of the prestressing force. Data was obtained for beams A3, C4, D5, B6, B7, B8, C9, and D10. The data obtained from beams A1 and A2 was deemed inconclusive due to the inappropriate selection of the strain gauge location within the transfer length zone. The transfer lengths obtained by demec gauges for beams C4, D5, B6, and C9 were also discarded due to their inconsistency. However, the experimental program provided a total of twelve reliable values of transfer lengths

which could be confidently used for the analysis.

Literature review indicates that the transfer length of a prestressing strand is greatly influenced by the Hoyer effect. The Hoyer effect is caused by swelling of the strand in the transfer zone after release as a result of Poisson's ratio. Since the swelling is resisted by the surrounding concrete, a confining force is produced normal to the strand which enhances the bond strength of the interface. The amount of confining force is therefore proportional to the stiffness of the surrounding concrete. It has been widely accepted that the stiffness of a concrete is a function of the square root of its compressive strength. It stands to reason that the bond enhancement caused by the Hoyer effect is proportional to the concrete stiffness. Therefore since the transfer length is inversely proportional to the bond strength, it can be assumed that the transfer length is inversely proportional to the square root of the concrete compressive strength.

It is reasonable to assume that an equation to describe the transfer length of a prestressing strand should be based on the effective prestressing force, the area of the strand, and the strength of the concrete. Therefore, it is proposed that the equation for transfer length be in the form of the following:

$$L_T = \frac{f_{pe} A_p}{C_T \sqrt{f'_{ci}}} \tag{5.1}$$

where

L_T = transfer length

A_p = cross-sectional area of prestressed reinforcement

f_{pe} = effective prestressing stress in the CFCC strand

f'_{ci} = concrete compressive strength at time of transfer

C_T = constant

The transfer length data from series A, B, C, and D beams was plotted against the respective beam properties. These properties were the effective prestressing stress in the CFCC strand times the cross-sectional area of CFCC divided by the square root of the concrete compressive strength at transfer. A linear regression line was passed through the data and forced through the origin which resulted in a very good linear relationship. This may be seen in Figure 5.1 . The figure shows that the measured data lie within the range plus or minus ten percent from the regression line. From the linear regression analysis a value of 80 for the coefficient C_T was obtained, the resulting R^2 value was 0.96, and the standard deviation of the error was 5.3 % . R^2 is a statistic which measures the validity of a model. It ranges up to 1, with 1 being optimal. The proposed formula is therefore as follows in SI units:

$$L_T = \frac{f_{pe} A_p}{80 \sqrt{f'_{ci}}} \qquad (5.2)$$

where L_T is in mm, A_p is in mm^2, and f_{pe} and f_{ci} are in MPa.

The proposed equation is compared to steel transfer length equations in Figures 5.2, 5.3, and 5.4 . The other steel equations were proposed by Olesniewicz (1975), Zia (1977), Balazs (1992), Mitchell (1993), and the ACI Code (1989). For the purpose of comparison in each of the three figures it was decided to vary one of either the prestressing stress, strand size, or the concrete strength while holding the other two

constant. The values of the constants were chosen as 12.5 mm for the strand diameter, 1116 MPa for the prestressing stress (1860 MPa x 60 %), and 40 MPa for the concrete compressive strength. It can be seen from the figures that the proposed equation for CFCC strand lies well below all of the other steel equations. The steel transfer lengths are on the order of 2.5 to 4 times the CFCC transfer lengths.

5.3. Flexural Bond Length

The measured development and flexural bond length values may be seen in Table 5.1 . These values were obtained by flexural testing of the beams which ended in bond failure. Data was obtained for beams A3, C4, B8, C9, and D10, however beams A1, A2, D5, B6, and B7 failed by strand rupture. As well, only beams A3 and B8 failed in a pure bond slip mode while beams C4, C9, and D10 failed in a combinations of shear and bond slip. Therefore, four values of flexural bond lengths were obtained for use in the analysis , two each from beams A3 and B8, while the results of the other tests were used as confirmation of the findings.

The flexural bond lengths were determined from the flexural testing of series A and series B beams. The specimens were identical except that series A used 15.2 mm diameter strands and series B used 12.5 mm strands. The beams were tested with different shear span lengths to achieve bond slip failure. Graphical illustrations of the testing of series A beams and series B beams are given in Figures 5.5 and 5.6 respectively, where the test results are compared to the ACI development length equation

for steel prestressing strands. In these figures the slope of the curves in the flexural bond zone is an indication of the flexural bond stress developed. The experimental results indicate that the slope increases with decrease of the shear span. The limiting value of the slope represents the flexural bond strength of the strand. For beam A3, which failed by bond slippage, the strand stress at ultimate is very close to that of beam A2, which failed by tendon rupture. From this it can be concluded that the development length for series A beams is very close to the shear span value of the A3 test. For beam B8, which also failed by bond slippage, the strand stress at ultimate is less than that of beam B7. From this it can be concluded that the development length for series B beams is between the shear span values of the B7 and B8 tests. The values for development length were determined by linear interpolation, then the values for flexural bond length were determined by subtracting the transfer lengths from the development lengths.

To obtain a comparison between the data points it was first assumed that the relationship between the flexural bond length and the beam properties would be similar to that for the transfer length. The data was plotted in terms of the flexural bond lengths versus the ultimate strand strength minus the effective prestressing stress, multiplied by the cross-sectional area of prestressing reinforcement, divided by the square root of the concrete compressive strength at the time of testing. A linear regression analysis resulted in the following equation:

$$L_{fb} = \frac{(f_{pu} - f_{pe})\, A_p}{40\ \sqrt{f_c'}} \qquad (5.3)$$

This relationship may be seen in Figure 5.7 . The coefficient of regression was

consequently 40 for SI units. The standard deviation of the error from the regression was 6.2 %.

The proposed equation is compared to steel flexural bond length equations in Figures 5.8, and 5.9 . The other equations were proposed by Mitchell (1993), Cousins (1990) and the ACI Code (1989). For the purpose of comparison in each of the two figures it was decided to vary one of either the strand size, or the concrete strength while holding the other constant, the same method as was used in the transfer length comparison. The values of the constants were chosen as 12.5 mm for the strand diameter, and 50 MPa for the concrete compressive strength. Also the steel prestressing stress was assumed as 1116 MPa, which is 60% of the strength of a normal steel prestressing strand, 1860 MPa. It can be seen from the figures that the proposed equation for CFCC strand lies well below all of the other steel equations. The steel flexural bond lengths are on the order of 2.5 to 4.5 times the CFCC flexural bond lengths.

5.4. Development Length

As previously stated the development length of a prestressing strand is the summation of the transfer length and the flexural bond length. Therefore, from the previous analysis, the entire development length of a CFCC prestressing strand can be calculated as:

$$L_d = \frac{f_{pe} A_p}{80 \sqrt{f'_{ci}}} + \frac{(f_{pu} - f_{pe}) A_p}{40 \sqrt{f'_c}} \qquad (5.4)$$

where the first part is the expression for the transfer length and the second part is the expression for the flexural bond length. The correlation between the experimental results, that is the development lengths determined from the two beams which failed by pure bond slip, and equation (5.4) is shown in Figure 5.10 .

The proposed equation is also compared to steel development length equations in Figures 5.11, and 5.12 . The steel equations were proposed by Mitchell (1993), Cousins (1990) and the ACI Code (1989). Again, for the purpose of comparison in each of the two figures it was decided to vary one of either the strand size, or the effective prestressing stress while holding the other variables constant, the same method as was used in the transfer length and flexural bond length comparisons. The values of the constants were chosen as 12.5 mm for the strand diameter, and 1116 MPa for the steel prestressing stress. Also other assumed values were 40 and 50 MPa for the concrete compressive strengths at transfer and at testing, respectively. It can be seen from the figures that the proposed equation for CFCC strand lies well below all of the other steel equations. The steel development lengths are on the order of 2.5 to 4 times the CFCC development lengths.

5.5. Bond Stresses

The force transfer between a prestressing strand and the surrounding concrete is accomplished by bond stress. This section of the report will discuss the bond stresses in the transfer and flexural bond zones.

5.5.1. Transfer Bond Stresses

It is known that the bond stresses in the transfer zone between the prestressing strand on the surrounding concrete vary somewhat along the transfer length. However, for the purpose of this analysis the bond stress along the CFCC strand in the transfer zone is expressed as an average value. The average bond stress was calculated for all beams based on the measured transfer lengths, the effective prestressing force, and the size of the CFCC strand. The formula used to calculate the average bond stress from testing is as follows:

$$U_T = \frac{f_{pe} A_p}{L_T P_o} \tag{5.5}$$

where

U_T = average bond stress

f_{pe} = effective prestressing force

A_p = cross-sectional area of prestressing strand

L_T = measured transfer length

P_o = perimeter of the prestressing strand

The transfer bond stresses were found to be in the range of 8 MPa to 12.5 MPa. The frequency distribution of the average bond stress may be seen in Figure 5.13 . The average value was 9.7 MPa with a standard deviation of error of 13.9 % .

Using the expression suggested by the ACI for steel transfer length and

equation 5.5, the average bond strength for steel was found to be approximately 3.0 MPa. Therefore, it can be concluded that the average bond stress in the transfer zone for CFCC is more than three times greater than that of steel strands.

Bond stresses are often expressed in terms of a bond stress index, U_T'. The definition of U_T' is the following:

$$U_T = U_T' \sqrt{f_{ci}'} \tag{5.6}$$

The purpose of defining the bond stress index is to account for variability in the concrete strength. For CFCC the average value of the bond stress index for the transfer zone was found to be 1.44 with the data having a standard deviation of error of 11.1 % . The frequency distribution of the transfer bond stress index is shown in Figure 5.14 . From the previously determined transfer bond strength, the bond strength index for steel was calculated as 0.48, assuming a concrete compressive strength of 40 MPa at transfer. Again these values indicate that the bond strength of CFCC is approximately three times that of steel prestressing strand.

To compare the bond strengths from the experimental program with the proposed transfer length equation, equations 5.2 and 5.5 were used to determine the bond strength predictions. The bond strengths based on the measured transfer lengths from testing are compared with the predictions in Figure 5.15 . The figure shows that all the experimental data lies within plus or minus ten percent of the predictions.

5.5.2. Flexural Bond Stresses

For the purpose of this analysis the bond stress along the CFCC strand in the flexural bond zone is expressed as an average value. The average bond stress was calculated for beams A3 and B8 based on the flexural bond lengths from testing, the effective prestressing force, the ultimate strength of the strand, and the size of the strand. The formula used to calculate the average bond stress is as follows:

$$U_{fb} = \frac{(f_{pu} - f_{pe})\, A_p}{L_{fb}\, P_o} \tag{5.7}$$

where

U_{fb} = average bond stress

f_{pu} = ultimate strength of the strand

f_{pe} = effective prestressing force

A_p = cross-sectional area of prestressing strand

L_{fb} = measured flexural bond length

P_o = perimeter of the prestressing strand

The average flexural bond stresses were found to be in the range of 4.7 MPa to 6.4 MPa. Using the expression suggested by the ACI for steel flexural bond length and equation 5.7, the flexural bond strength for steel was found to be approximately 1.0 MPa. Therefore, it can be concluded that the average bond stress in the flexural bond zone for CFCC is 4.5 to 6.5 times greater than that of steel strands.

The flexural bond stress index, U_{fb}', the same concept as the transfer bond stress index is defined as the following:

$$U_{fb} = U'_{fb} \sqrt{f'_c} \tag{5.8}$$

For CFCC the flexural bond stress index ranged from 0.62 to 0.83 . From the previously determined flexural bond strength, the flexural bond strength index for steel was calculated as 0.14 , assuming a concrete compressive strength of 50 MPa. Again these values indicate that the bond strength of CFCC is approximately 4.5 to 6 times that of steel prestressing strand.

To compare the flexural bond strengths from the experimental program with the proposed flexural bond length equation, equations 5.3 and 5.9 were used to determine flexural bond strength predictions. The bond strengths based on the measured flexural bond lengths from testing are compared with the predictions in Figure 5.16 . The figure shows that the experimental data lies within plus or minus ten percent of the predictions.

5.6. Parametric Study

From the previous analysis, equations have been proposed to determine the transfer length and flexural bond length, and these equations were used to calculate the corresponding bond strengths. The following section will examine the effect of various parameters on these equations and compare the findings with the experimental results.

5.6.1. Effect of Strand Diameter

Proposed equations 5.2 and 5.3 indicate that both the transfer length and flexural bond length are proportional to the cross-sectional area of the prestressing reinforcement. It is known that the cross-sectional area of a seven-wire strand is proportional to the square of the strand diameter. Therefore, the transfer length and flexural bond length are proportional to the square of the strand diameter. This relationship is compared with the experimental results in Figure 5.17 . The comparison seems to indicate that the relationship is true.

The equations proposed for the transfer length and flexural bond length when combined with the equations for bond stresses indicate that the bond strengths of CFCC are inversely proportional to the strand diameter. Comparisons are made in Figures 5.18 and 5.19 between the experimental results and the proposed equations. These show a definite inverse relationship between the bond strengths and the strand diameter.

5.6.2. Effect of Prestress Level

Proposed equation 5.2 shows that the transfer length is proportional to the effective prestressing stress in the prestressing reinforcement. This relationship is compared with the experimental results in Figure 5.20 . The comparison indicates that the relationship is true. This comparison cannot be made for the flexural bond length because the experimental data obtained does not have any variability in the prestress level.

Both the transfer bond strengths and transfer bond indexes when combined with the proposed transfer length equation, indicate that these bond properties should not be dependant on the prestress level. Comparisons are made in Figures 5.21 and 5.22 between the experimental results and the equations. These figures indicate that it is unlikely a relationship exists between the transfer bond stress properties and the effective prestress level. Again, this comparison cannot be made for the flexural bond strengths because the experimental data obtained does not have any variability in the prestress level.

5.6.3. Effect of Concrete Cover

To determine the effect of concrete cover on the bond properties of CFCC strands, the experimental data was plotted for comparison. Figure 5.23 shows that the concrete cover had no bearing on the measured transfer length data for both strand sizes. This agrees with the proposed transfer length equation which does not include concrete cover as a variable.

Figures 5.24 and 5.25 show that the concrete cover also had no effect on the transfer bond strength or transfer bond index for both strand sizes. This also agrees with the proposed equations which do not include concrete cover as a variable. These comparisons cannot be made for the flexural bond properties because the experimental results for flexural bond length or flexural bond strength do not have any variability in the concrete cover.

It should be noted that the range of concrete cover examined in the experimental

program was 50 to 75 mm or 3.3 to 6 strand diameters. Therefore, these findings are only applicable for this range of concrete cover. It has been previously suggested that the critical concrete cover to be used to avoid splitting is approximately 2.8 strand diameters. No splitting was observed in any of the test specimens after prestress transfer.

5.7. Ultimate Strength of CFCC

In the experimental program five beams failed by strand rupture, three with 15.2 mm diameter CFCC strands and two with 12.5 mm diameter CFCC strands. From these test results the stress in the CFCC strand at failure was calculated using the rectangular stress-block method as outlined in Collins and Mitchell (1987). The calculated ultimate tensile strengths are reported in Table 5.2 along with the strengths specified by the manufacturer. A high degree of variability exists between these strengths. The experimental results show a 20 % difference in strength from one strand size to the other as well as a maximum difference of 17 % within the 15.2 mm strand strengths. The average strength of the 15.2 mm strand was reasonably close to that reported by the manufacturer, however, for 12.5 mm strand the average strength was 16 % higher. It can be concluded from these results that for the purpose of designing members with CFCC strands, care must be taken to use the appropriate ultimate strength values with an adequate margin of safety.

Table 5.1 Experimental Bond Lengths (in mm)

Beam	Transfer Length	Flexural Bond Length	Development Length
A3	200 196	507 511	707
B8	125 124	397 398	522

Table 5.2 CFCC Tensile Strengths

CFCC Diameter (mm)	Experimental Results		Manufacturers Specifications	
	Ultimate Tensile Strength (MPa)	Average (MPa)	Average Tensile Strength (MPa)	Guaranteed Tensile Strength (MPa)
15.2	2027 2168 2394	2196	2140	1750
12.5	2632 2674	2653	2280	1870

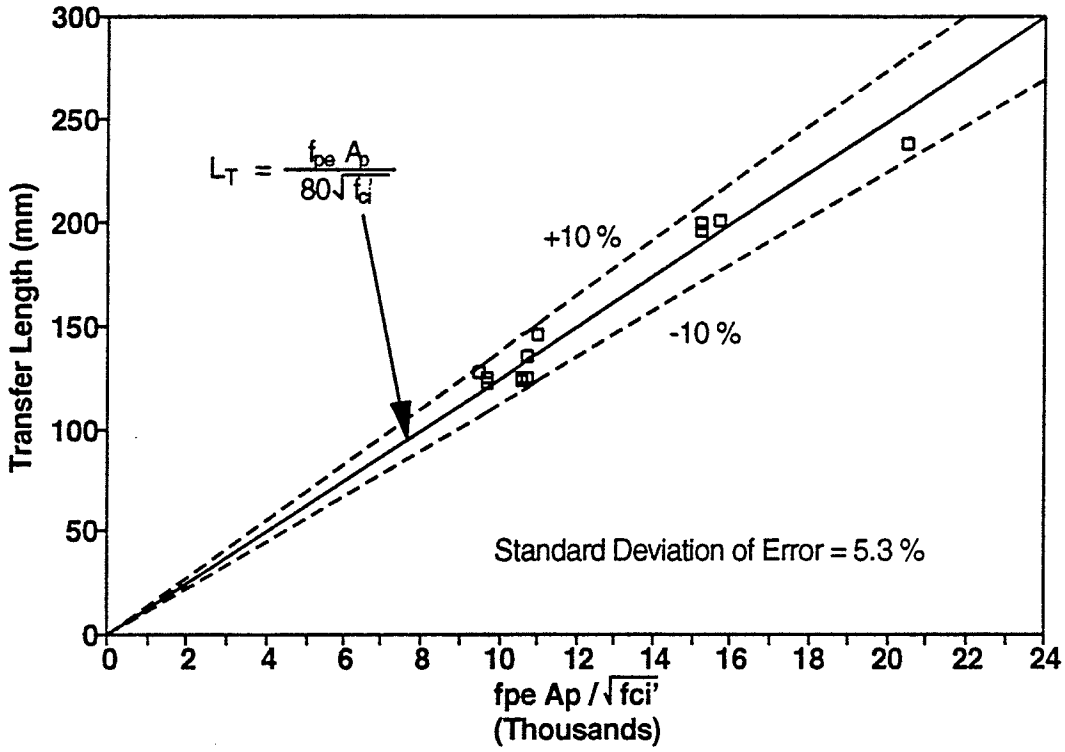

Figure 5.1 Measured Transfer Lengths For CFCC

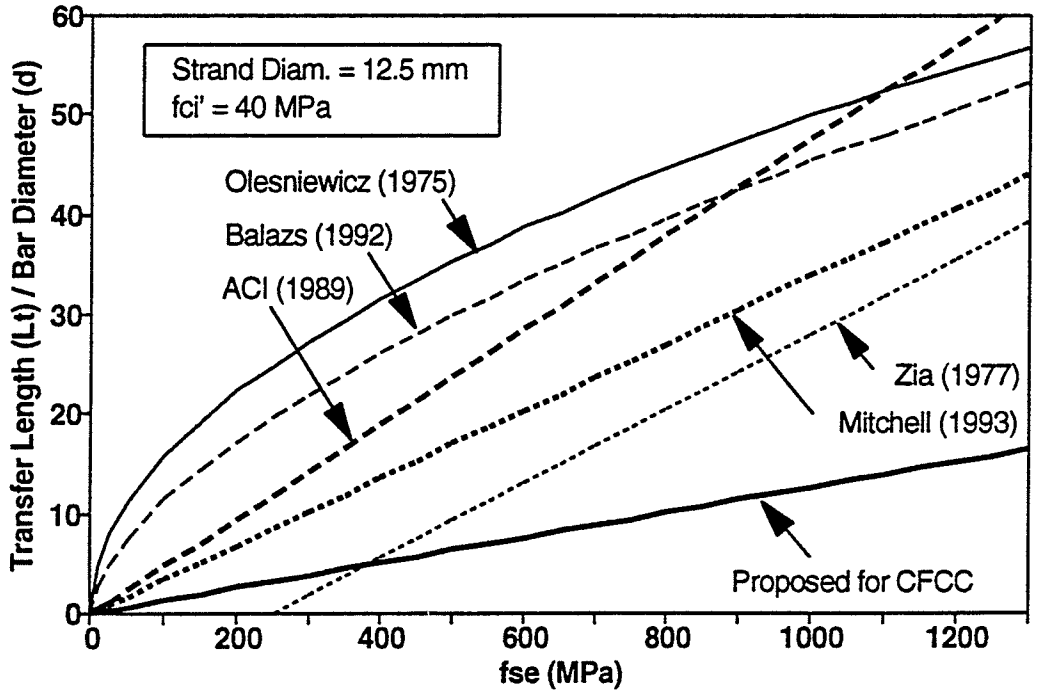

Figure 5.2 Transfer Length Comparison

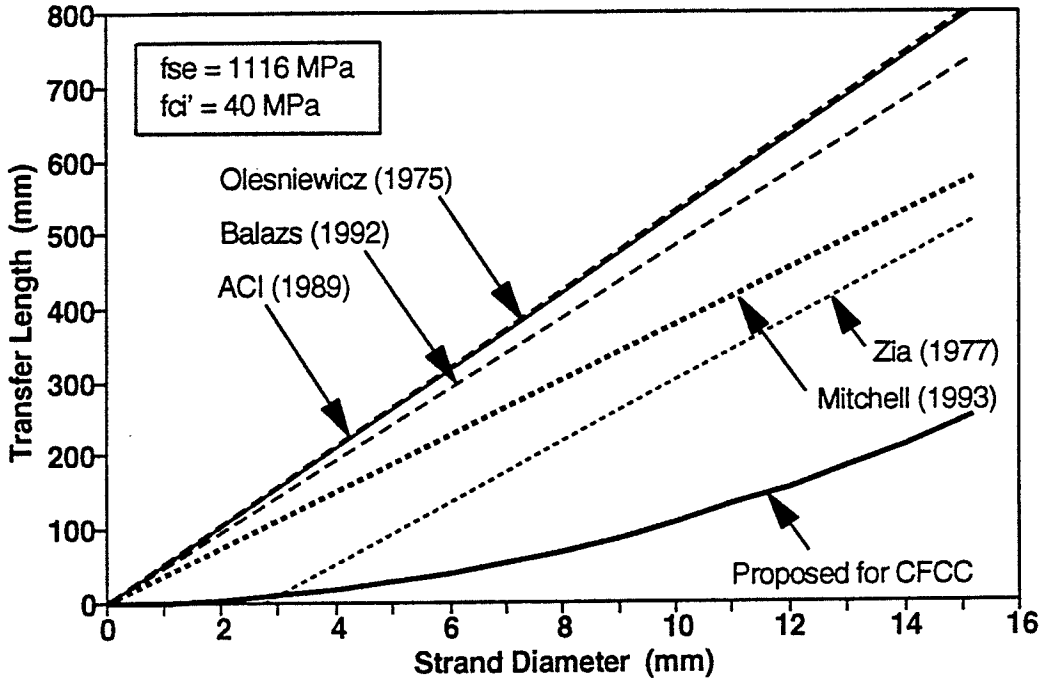

Figure 5.3 Transfer Length Comparison

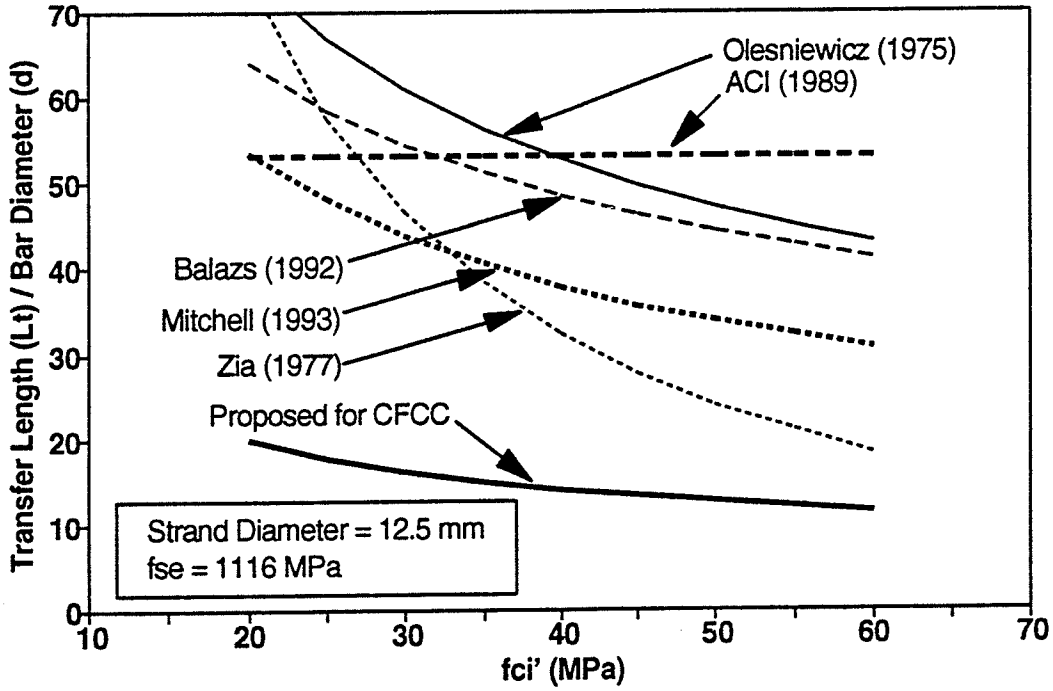

Figure 5.4 Transfer Length Comparison

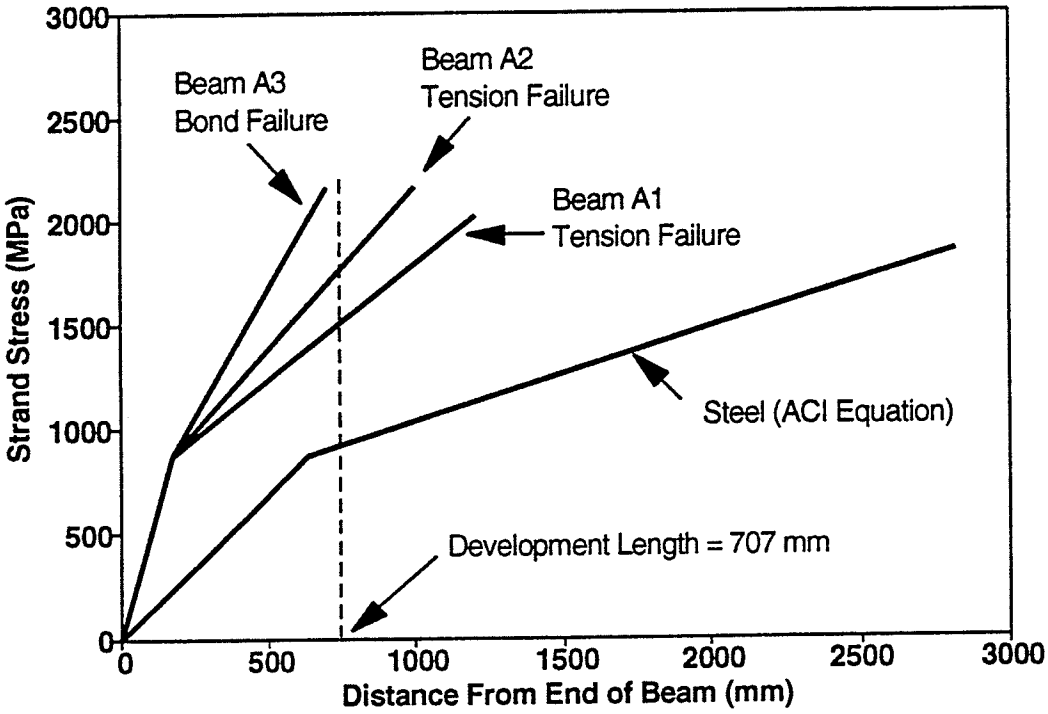

Figure 5.5 Failure of Series A Beams (15.2 mm strand)

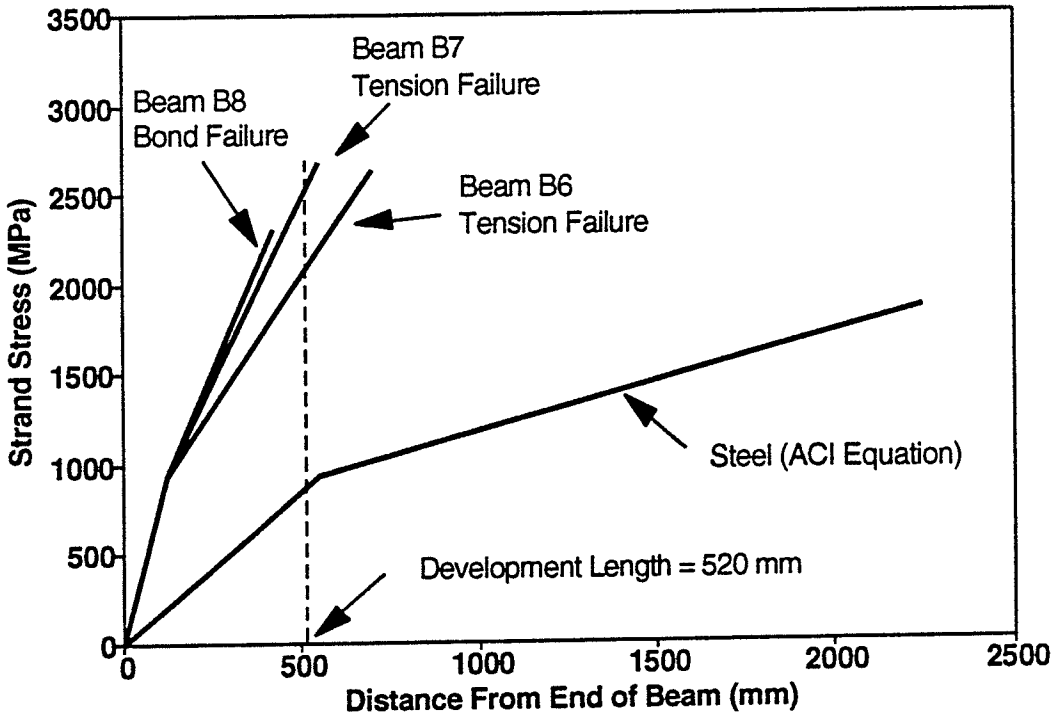

Figure 5.6 Failure of Series B Beams (12.5 mm strand)

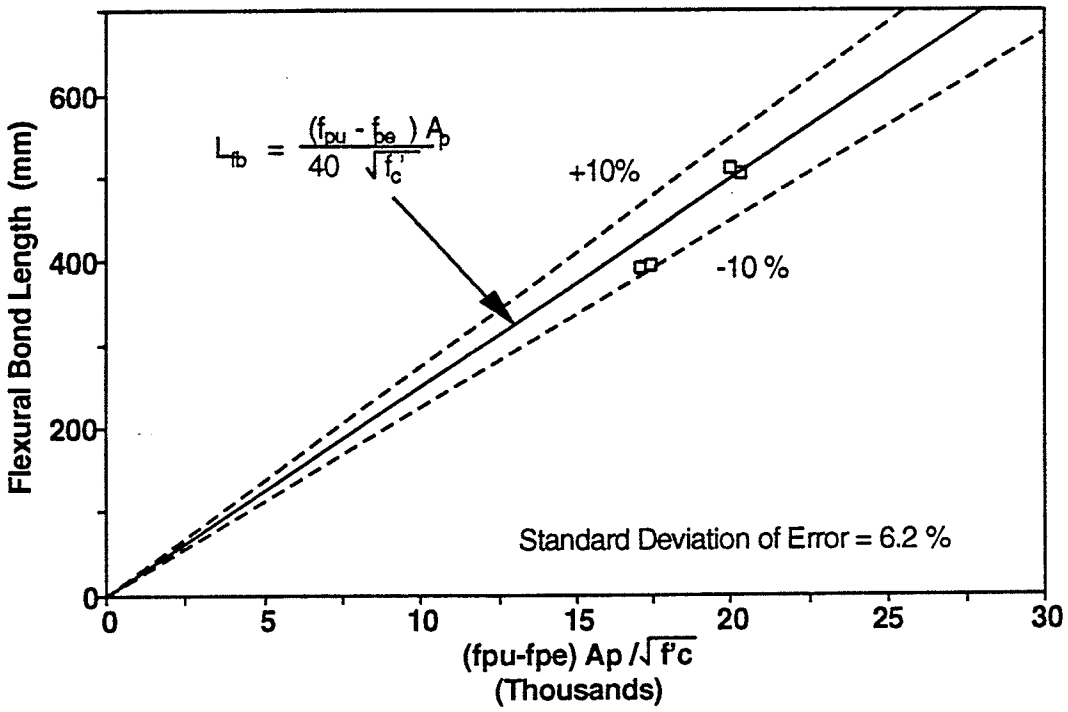

Figure 5.7 Measured Flexural Bond Lengths

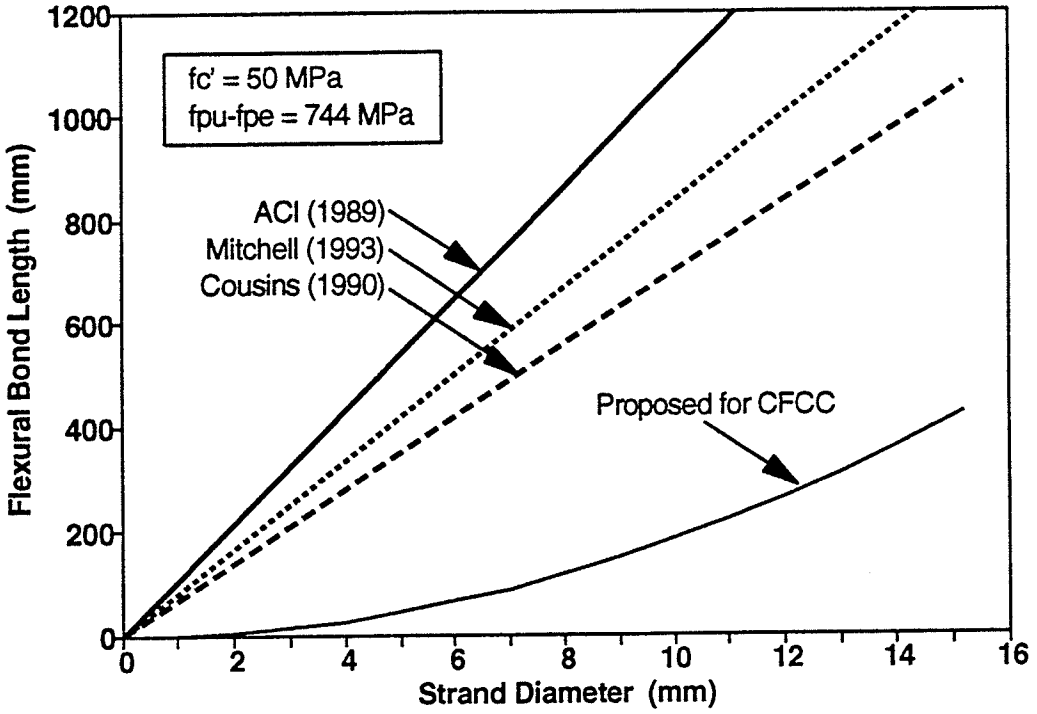

Figure 5.8 Flexural Bond Length Comparison Against Strand Diameter

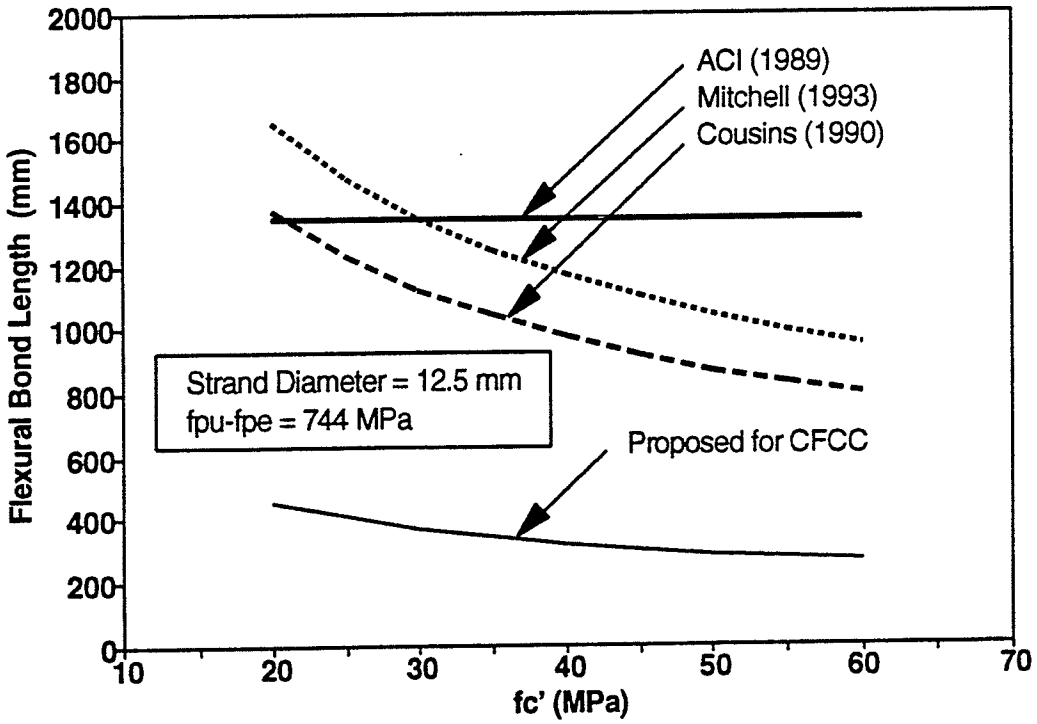

Figure 5.9 Flexural Bond Length Comparison Against Concrete Compressive Strength

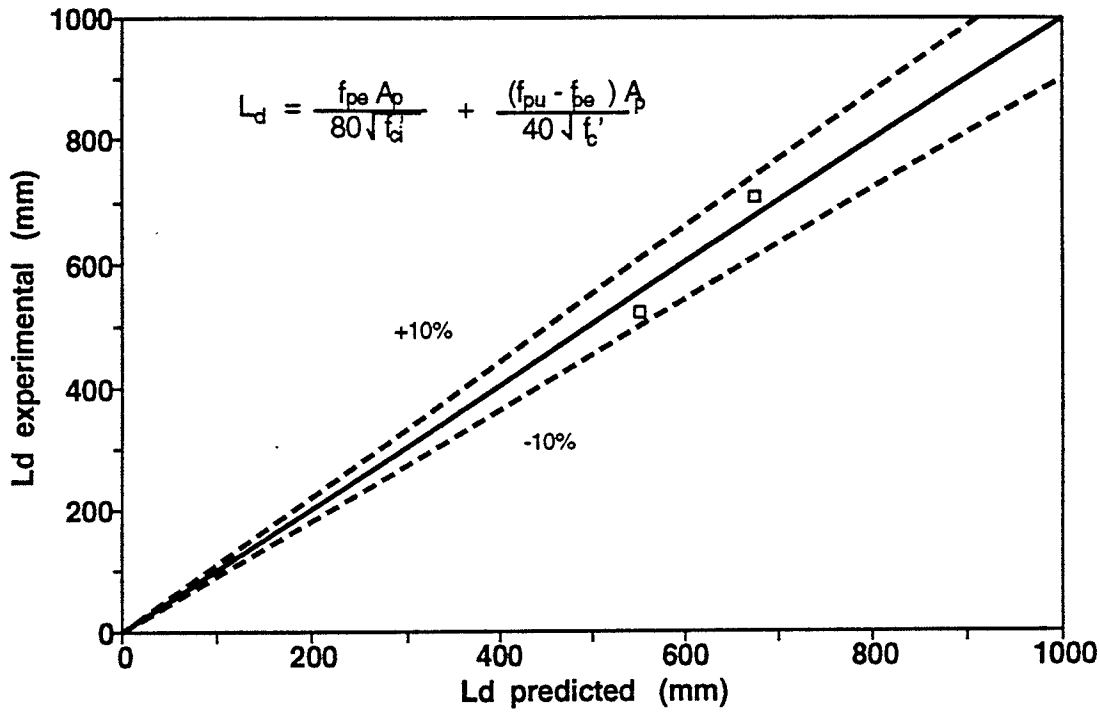

Figure 5.10 Development Length Correlation

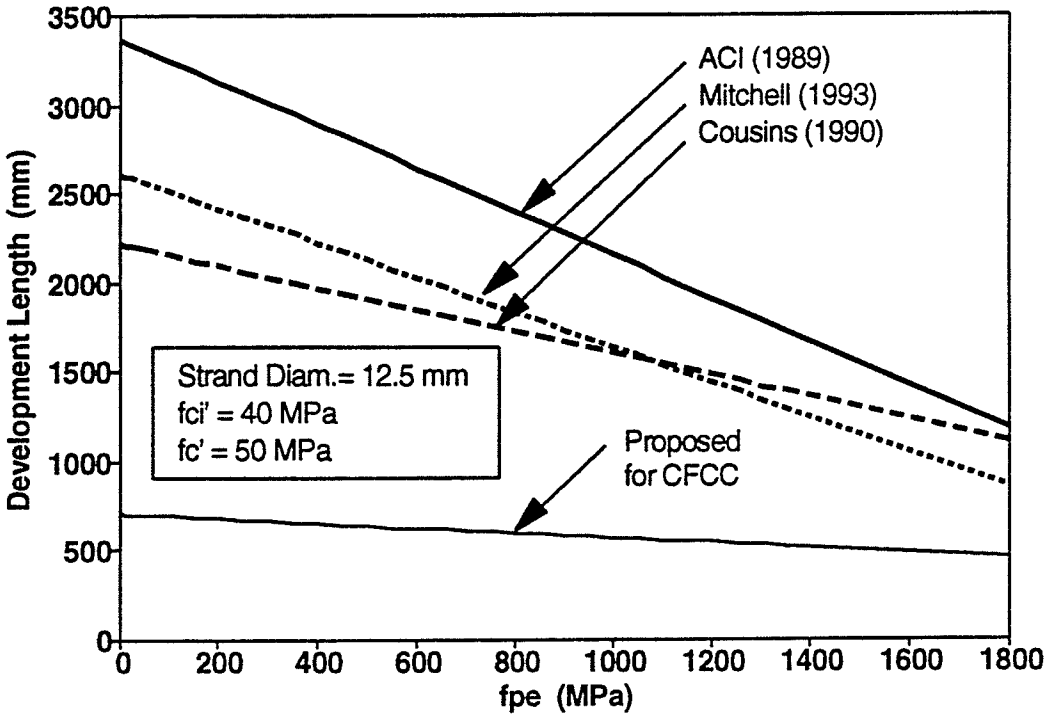

Figure 5.11 Development Length Comparison Against Effective Prestress Level

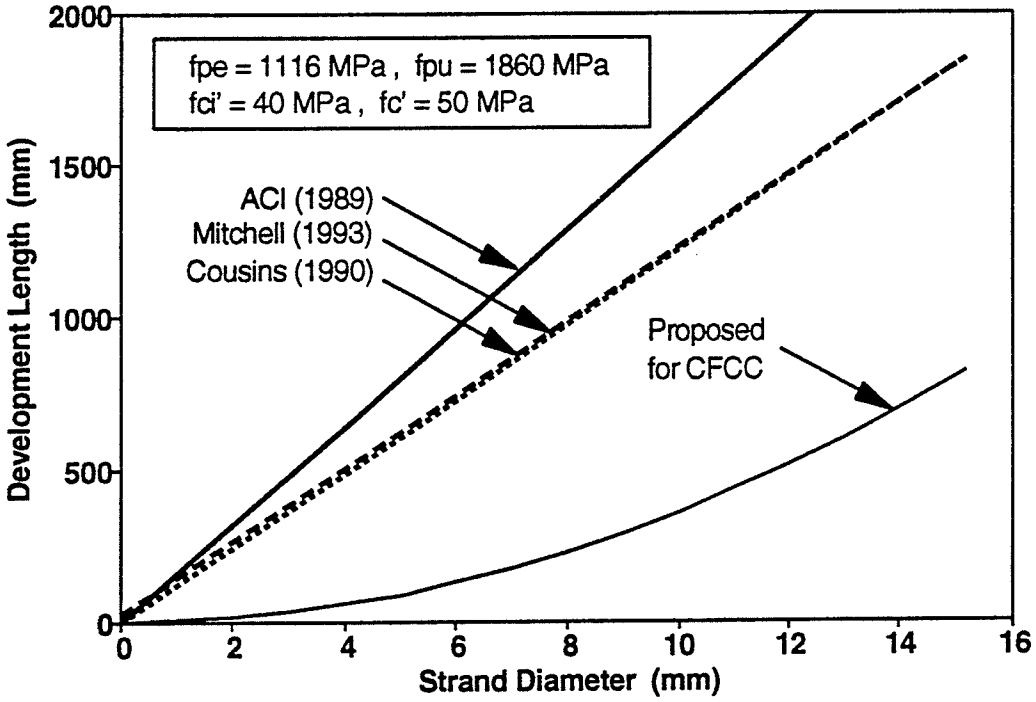

Figure 5.12 Development Length Comparison Against Strand Diameter

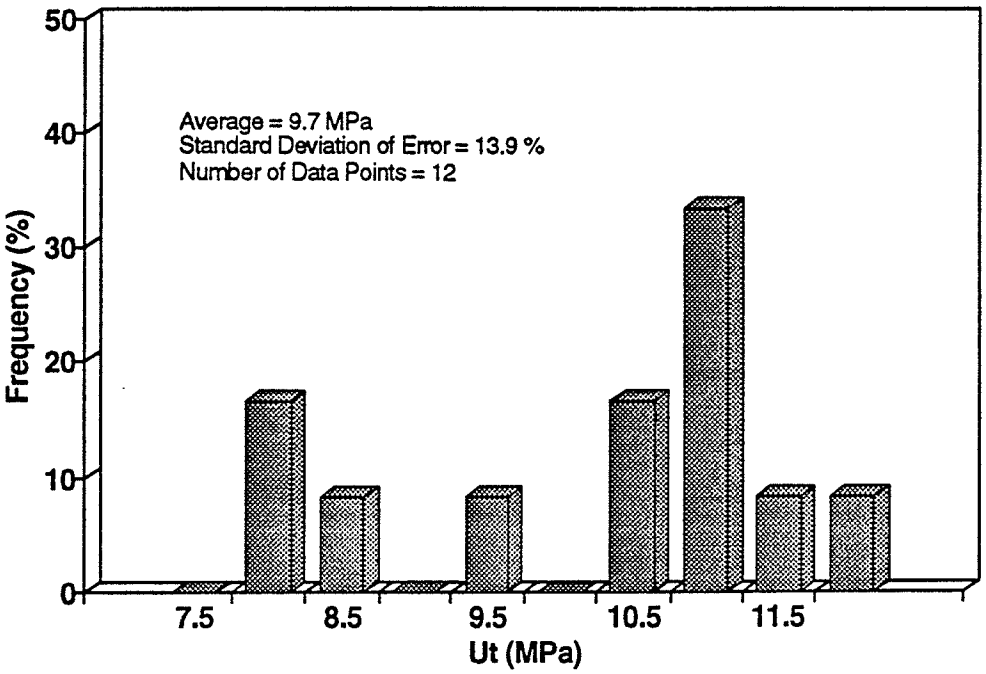

Figure 5.13 Transfer Length Average Bond Stresses

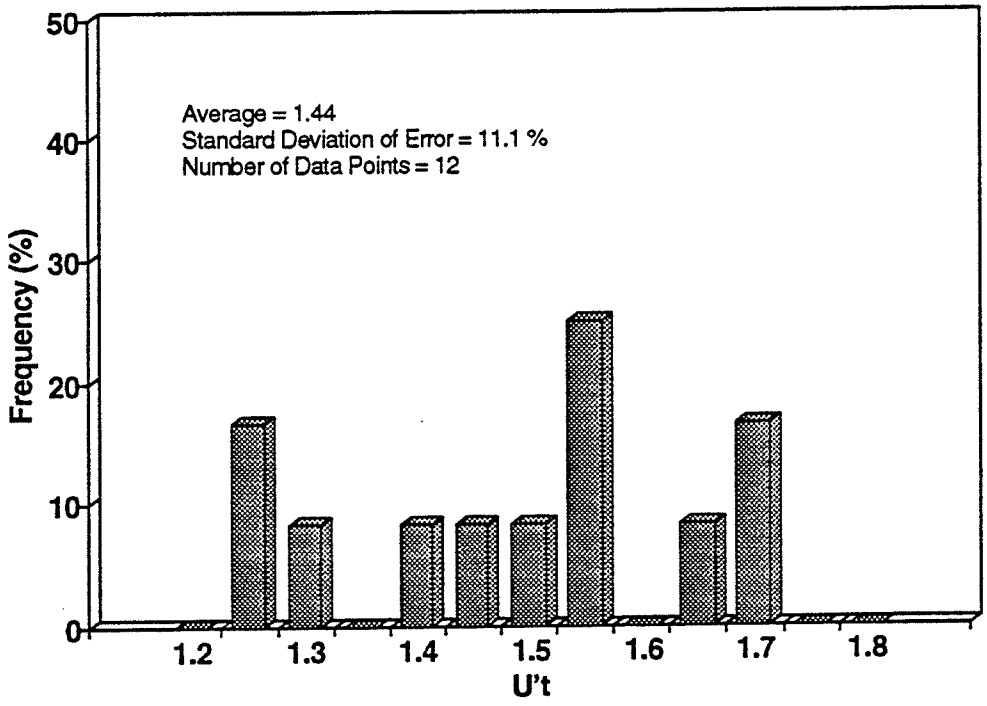

Figure 5.14 Transfer Length Bond Stress Index

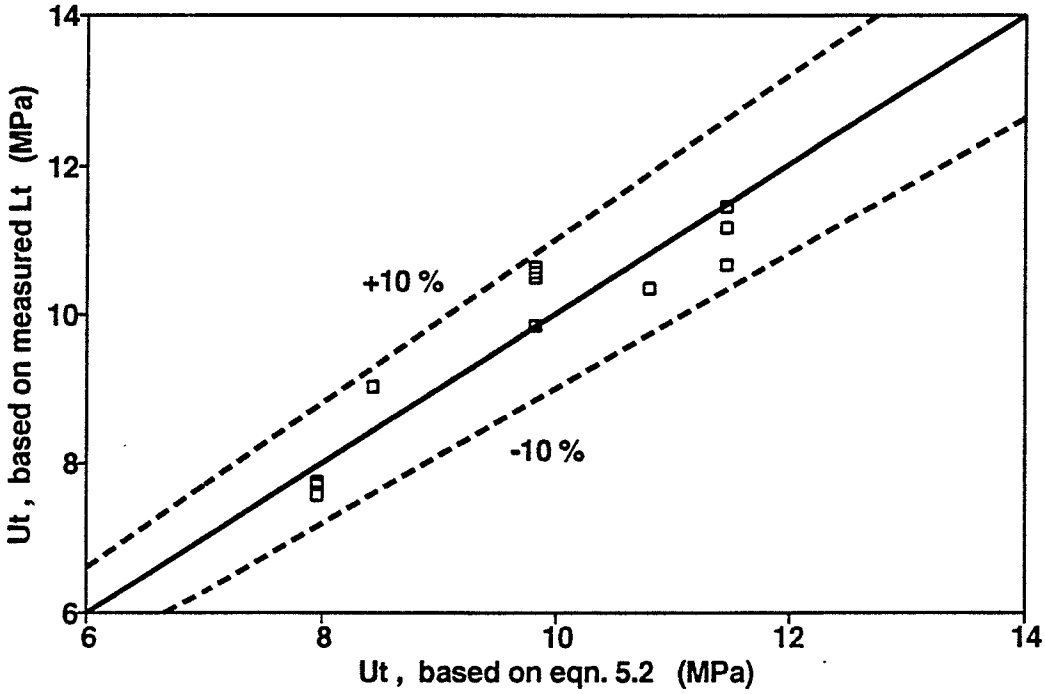

Figure 5.15 Transfer Bond Strength Correlation

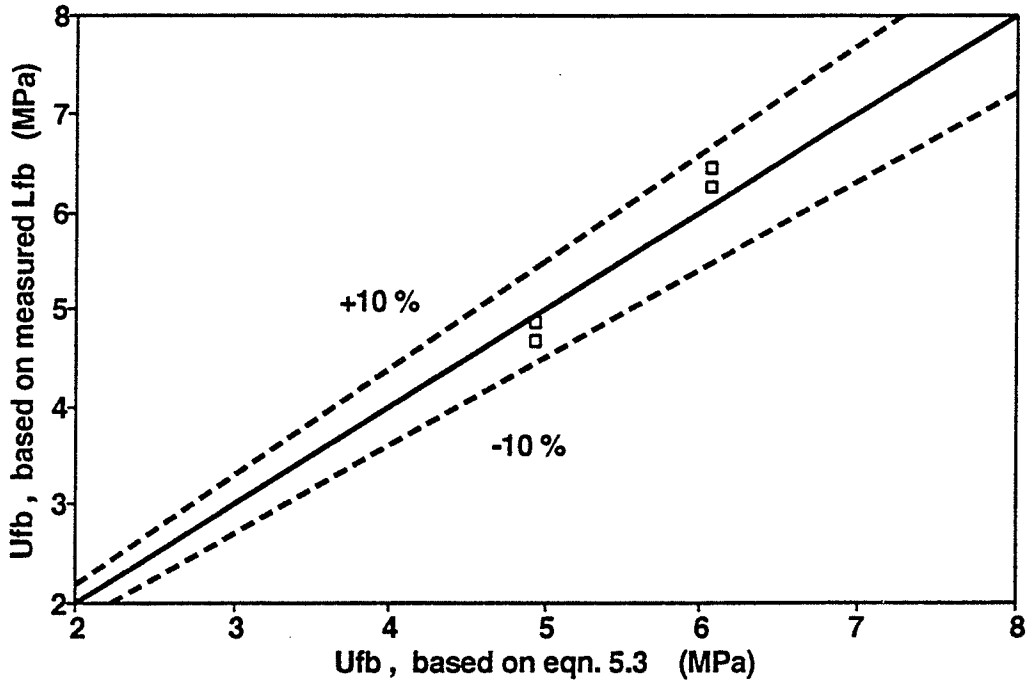

Figure 5.16 Flexural Bond Strength Correlation

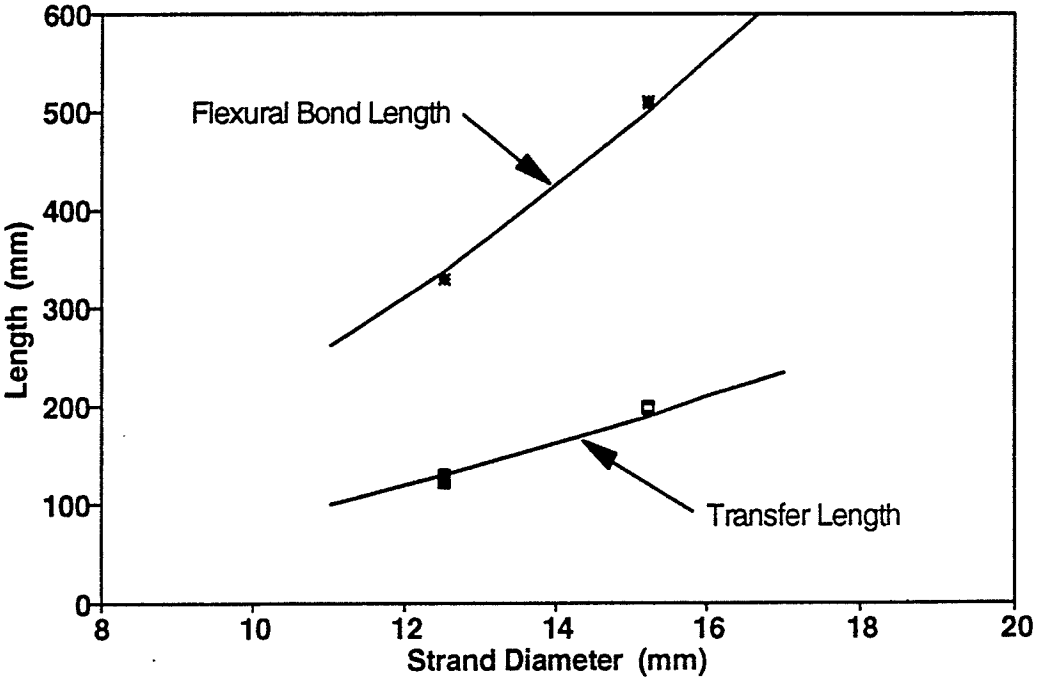

Figure 5.17 Effect of Strand Diameter on Transfer and Flexural Bond Lengths

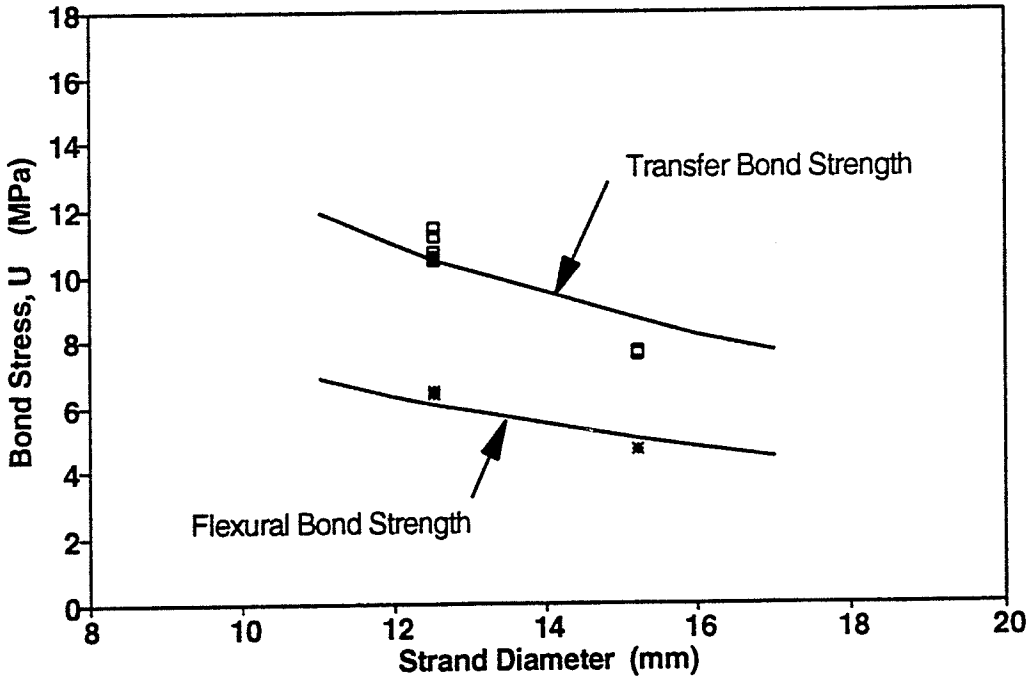

Figure 5.18 Effect of Strand Diameter on Transfer and Flexural Bond Strengths

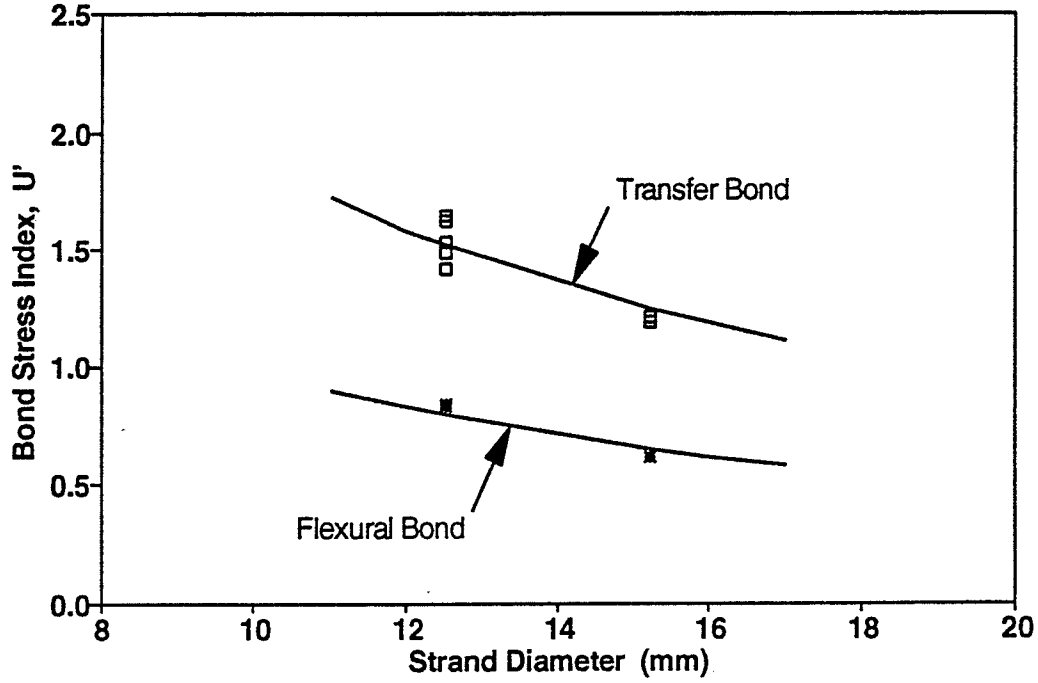

Figure 5.19 Effect of Strand Diameter on Transfer and Flexural Bond Indexes

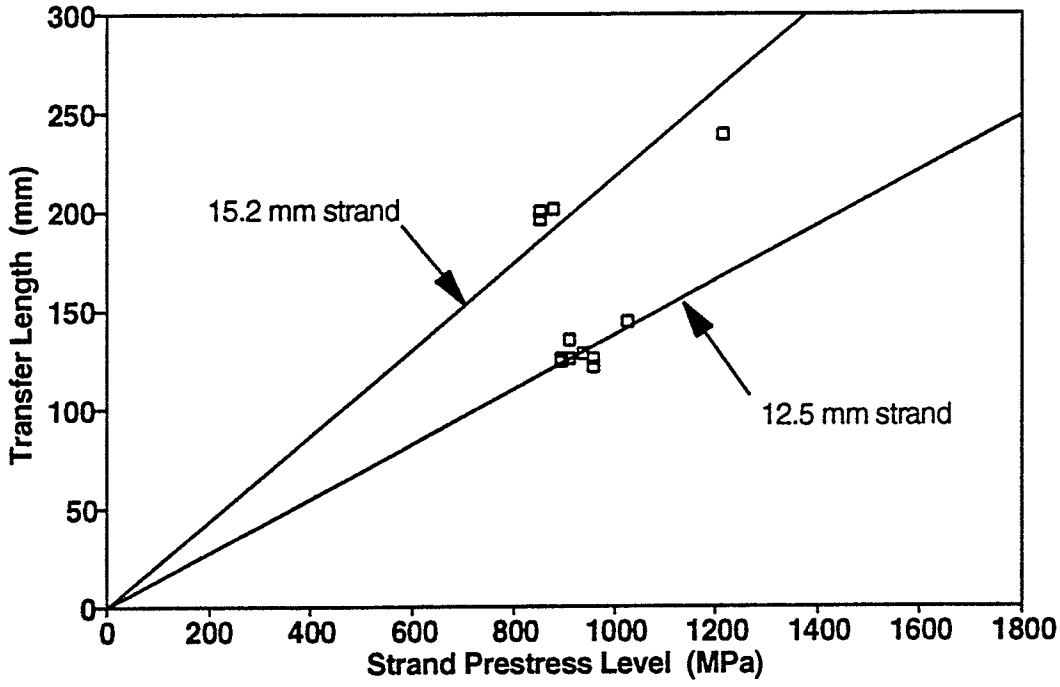

Figure 5.20 Effect of Strand Prestress Level on Transfer Length

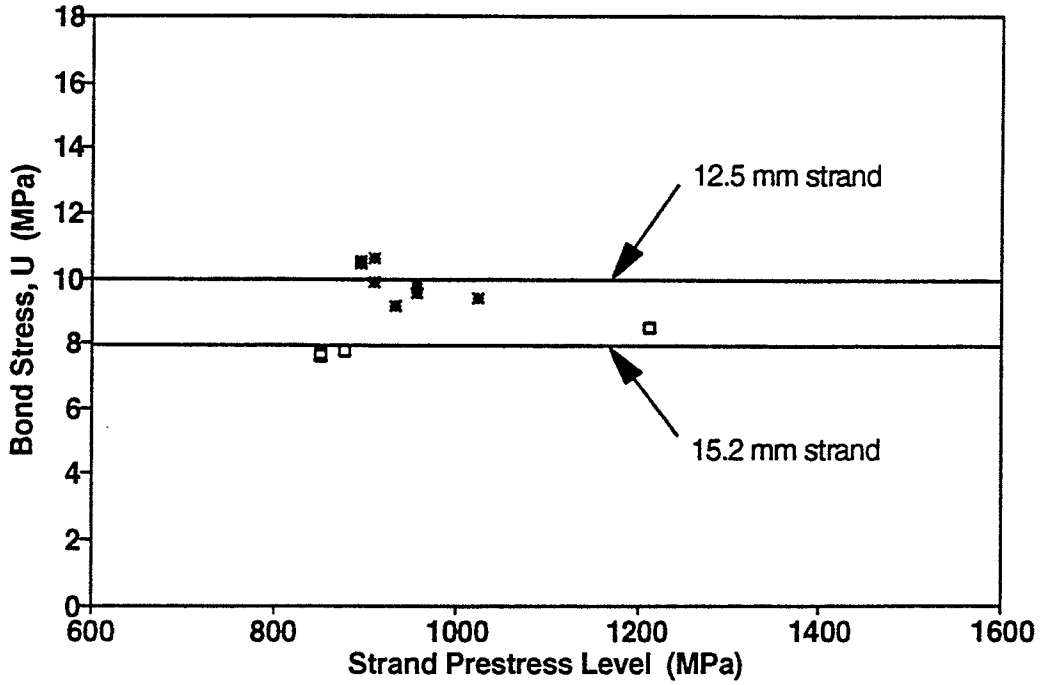

Figure 5.21 Effect of Strand Prestress Level on Transfer Bond Strength

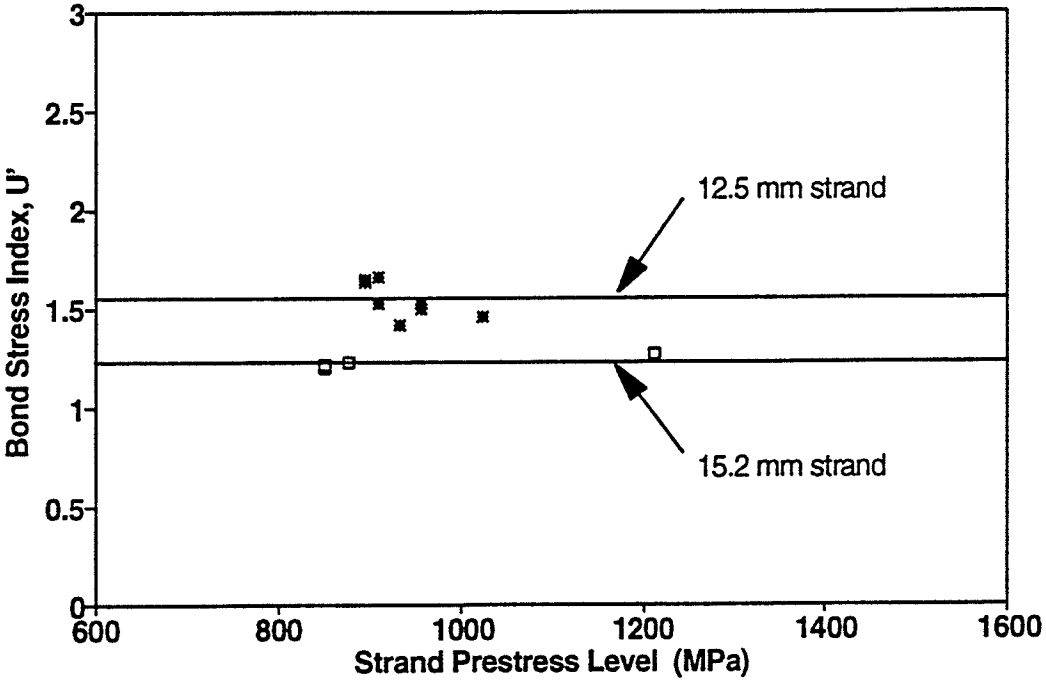

Figure 5.22 Effect of Strand Prestress Level on Transfer Bond Index

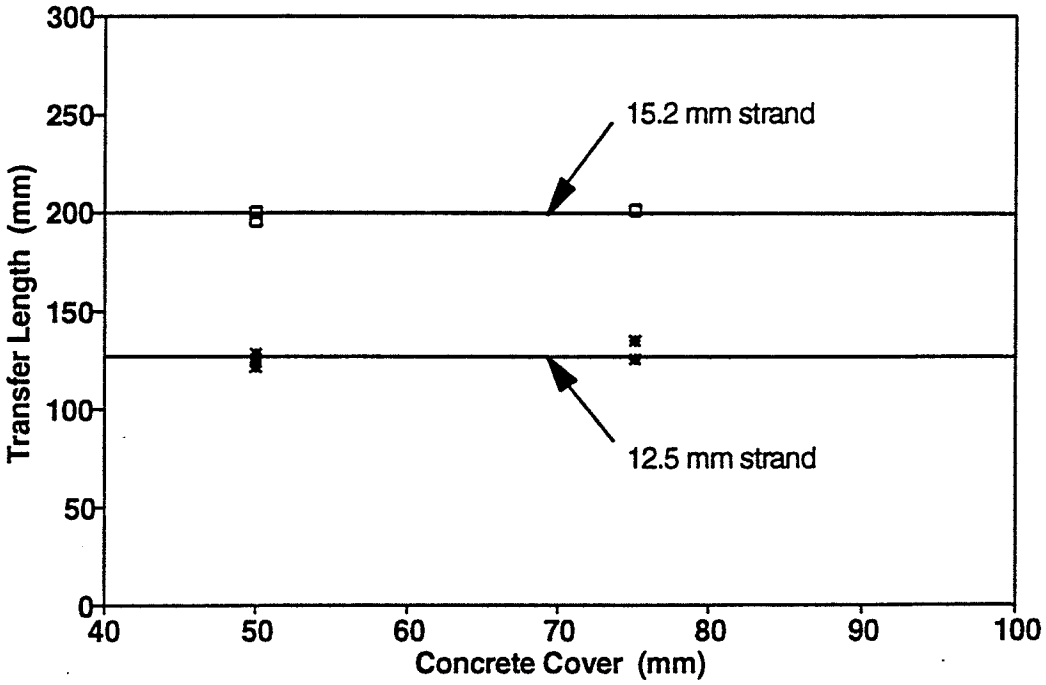

Figure 5.23 Effect of Concrete Cover on Transfer Length

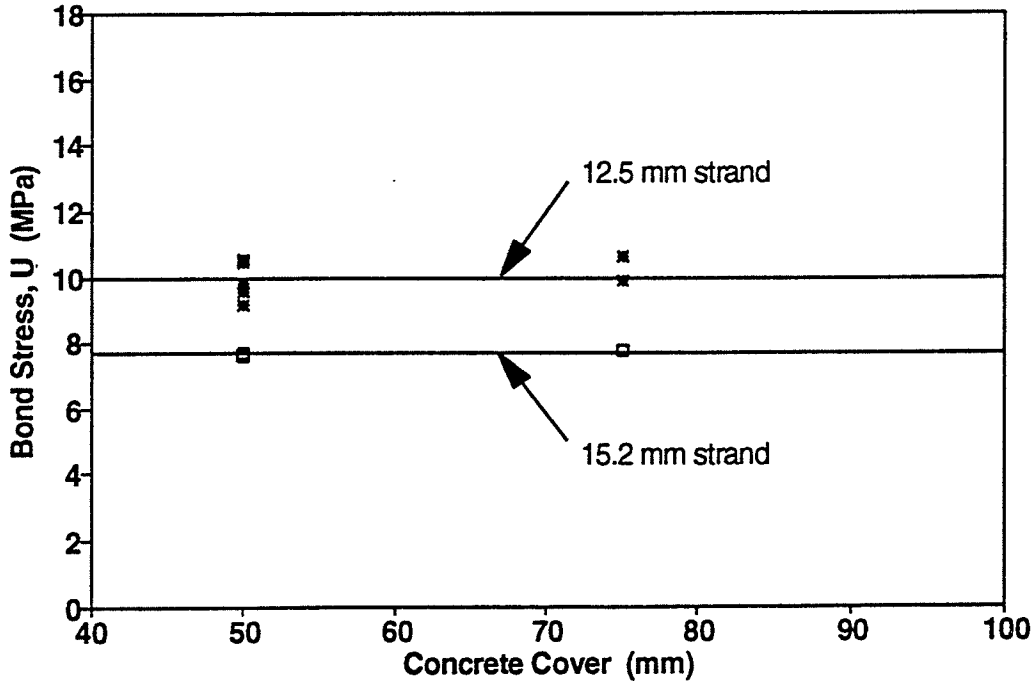

Figure 5.24 Effect of Concrete Cover on Transfer Bond Strength

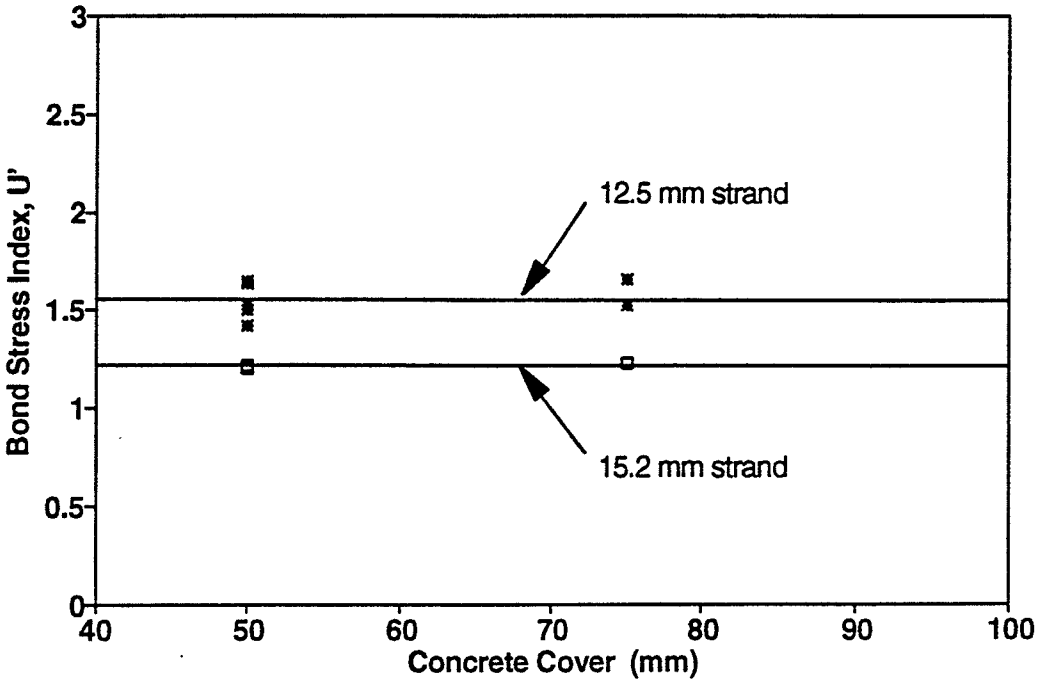

Figure 5.25 Effect of Concrete Cover on Transfer Bond Index

CHAPTER 6

SUMMARY AND CONCLUSIONS

6.1. Summary

The objective of this research program was to investigate the various bond characteristics of carbon fibre reinforced plastic prestressing strands in pretensioned concrete beams. The information is valuable for designers using CFCC for prestressing of concrete structures and for the development of future design considerations and codes for concrete beams pretensioned by FRP tendons. This thesis examines the bond test results and proposes equations which predict the bond properties of CFCC strands.

An experimental program was conducted at the University of Manitoba to examine the bond characteristics of CFCC strands. The bond characteristics are examined through measurements of the transfer and development lengths and their corresponding bond stresses for 15.2 mm diameter and 12.5 mm diameter seven-wire CFCC strands.

6.1.1. Experimental Program

Ten pretensioned prestressed concrete T-shaped beams were cast and tested in this experimental program. The beams were 3200 mm long with a 330 mm depth and 260 mm effective depth. The beams are tested quasi-statically as simply supported with a span of 2800 mm and 200 mm overhanging the supports. The prestressing tendons were debonded

over the 200 mm overhang at each end in order to minimize stress disturbances and confinement caused by the support reaction forces. The beams were prestressed to either 50 % , 60 % , or 70 % of the guaranteed strand strength, and had concrete cover of either 50 mm (2 in.) or 75 mm (3 in.).

6.1.2. Bond Lengths

Three days after casting of the concrete the prestressing force was released to the beams gradually by releasing the pressure in the jacks. At release the concrete strength was determined using standard concrete cylinder compressive tests. The strains in the tendons were monitored during release by electrical resistance strain gauges. Strain of the concrete was measured before and after release by demec point gauges.

Using the strain gauge data and the demec point gauge data, the transfer lengths were determined. The experimental program provided a total of twelve reliable values of the transfer length for the two CFCC sizes considered in this study using different concrete cover and prestressing level. Using the measured transfer length data, the following expression for the transfer length in terms of the effective prestressing level, the cross-sectional area of the CFCC strand, and the concrete compressive strength at the time of transfer is proposed as:

$$L_T = \frac{f_{pe}\, A_p}{80\, \sqrt{f'_{ci}}} \tag{6.1}$$

The transfer lengths obtained by the proposed equation for CFCC strand are well

below those of other equations for steel strands. The steel transfer lengths are in the order of 2.5 to 4 times the CFCC transfer lengths.

The flexural bond length was measured for beam series A and B by flexural testing to ultimate using variable shear span values. Using the same parameters used before for the transfer length, the flexural bond length is related to the increase of the strand stress from the prestress level to the ultimate tensile strength of CFCC as follows :

$$L_{fb} = \frac{(f_{pu} - f_{pe})\, A_p}{40\sqrt{f'_c}} \tag{6.2}$$

The proposed equation for CFCC strand lies well below other steel equations. The steel flexural bond lengths are on the order of 2.5 to 4.5 times the CFCC flexural bond lengths.

The development length of a prestressing strand is the summation of the transfer length and the flexural bond length. Therefore, based on the previous discussion, the proposed development length of a CFCC prestressing strand is:

$$L_d = \frac{f_{pe}\, A_p}{80\sqrt{f'_{ci}}} + \frac{(f_{pu} - f_{pe})\, A_p}{40\sqrt{f'_c}} \tag{6.3}$$

where the first part is the expression for the transfer length and the second part is the expression for the flexural bond length. Steel development lengths are on the order of 2.5 to 4 times the CFCC development lengths.

6.1.3. Flexural Behaviour

All beams exhibited a bilinear moment-deflection relationship. All beams displayed extensive flexural cracking extending up to the top flange prior to failure with some beams exhibiting some flexural-shear cracking. For beams A3, B6, and B7 a peak load value occurred on the moment-deflection curve after the beams were thoroughly cracked and before failure. This behaviour suggests that after extensive cracking the bond between the prestressing strand and the concrete was lost within the constant moment zone. However, the beam was able to carry load with the transfer zones anchoring the strand and the beam acting as an unbonded post-tensioned member.

6.1.4. Bond Stresses

The transfer bond stresses were found to be in the range of 8 MPa to 12.5 Mpa. An average value of 9.7 MPa with a standard deviation of error of 13.9 % could be adequately used for design purposes. The average bond strength for steel was calculated as 3.0 MPa which is approximately three times less than for CFCC.

The average flexural bond stresses were found to be in the range of 4.7 to 6.4 MPa with an average value of 5.5 MPa. The flexural bond strength for steel was calculated as approximately 1.0 MPa which is about five times less than for CFCC.

6.2. Conclusions

Based on the experimental program and analysis the following conclusions can be drawn:

1. Both the transfer length and flexural bond length are proportional to the cross-sectional area of the CFCC strand or the square of the strand diameter.

2. Both the transfer bond strength and flexural bond strength are inversely proportional to the strand diameter.

3. The transfer length is proportional to the prestress level while the transfer bond strength was not affected by the prestress level.

4. The amount of concrete cover had no bearing on the transfer length and transfer bond strength. However, the range of concrete cover examined in the experimental program was 3.3 to 6 strand diameters, therefore, these findings are only applicable for this range of concrete cover.

5. Flexural behaviour of the beams was bilinear up to failure. Some beams exhibited a spike in the moment-deflection relationship followed by a reduced stiffness up to failure. This phenomenon is attributed to debonding of the strand in the constant moment zone.

6.3. Design Recommendations

Based on the experimental program and analysis The following design recommendations are made:

1. The transfer length of CFCC pretensioned strands may be calculated based on the effective strand prestress, the cross-sectional area of the strand, the concrete compressive strength at the time of transfer, and a coefficient of 1/80 .

2. The flexural bond length of CFCC pretensioned strands may be calculated based on the residual strand strength (ultimate strand strength minus effective strand prestress), the cross-sectional area of the strand, the concrete compressive strength, and a coefficient of 1/40 .

3. The average bond strength for CFCC strands in the transfer zone is 9.7 MPa, however the bond strength is dependant on the strand size.

4. The average bond strength for CFCC strands in the flexural bond zone is 5.5 MPa, however the bond strength is dependant on the strand size.

6.4. Suggestions For Future Research

The experimental program investigated the effect of three parameters on the bond properties of CFCC strands with a limited number of tests for each. Clearly more tests are needed to make more definitive conclusions about the variables examined, and to include other variables. Suggestions for future research are:

1. Additional specimens pretensioned by CFCC strands of different diameters other than 12.5 mm and 15.2 mm should be tested to determine their bond properties.

2. A detailed investigation into the effects of smaller concrete covers to determine what is the critical concrete cover to avoid splitting and its relationship to the bond properties of CFCC strands.

3. An investigation into the effects of confinement to determine the relationship between transverse reinforcement and the bond properties of CFCC strands.

4. Research is also needed to investigate the effects of temperature on the bond properties of CFCC strands.

5. An investigation into the effect of the method of prestress transfer, either sudden or gentle release, on the bond properties of CFCC strands.

REFERENCES

1. **Abdelrahman, A., Rizkalla, S.**, "Serviceability of Concrete Beams Prestressed by Carbon Fibre Reinforced Plastic Rods", Submitted for publication, Second International Symposium for Non-metallic (FRP) Reinforcement for Concrete Structures, Ghent, Belgium, 1995

2. **ACI Committee 208**, "Test Procedure to Determine Relative Bond Value of Reinforcing Bars", *ACI Journal*, V.30, No.1, July 1958

3. **ACI Committee 208**, "Proposed Test Procedure to Determine Relative Bond Value of Reinforcing Bars", *ACI Journal*, Vol.28, No.13, July 1957, pp.89-104

4. **ACI Committee 318**, "Building Code Requirements for Reinforced Concrete and Commentary (ACI 318-89/ACI 318R-89)", American Concrete Institute, Detroit, 1989, 353 pp.

5. **Arockiasamy, M., Shahawy, M., Sandepudi, K., Zhuang, M.**, "Studies on Bond Behaviour of Concrete Double-Tee Beams Prestressed With Aramid FRP Tendons", Session on Bond of FRP Rebars and Tendons, ACI 1994 Spring Convention, San Francisco, USA, March 1994

6. **Balazs, G.**, "Transfer Length of Prestressing Strand as a Function of Draw-In and Initial Prestress", *PCI Journal*, Vol.38 No.2, March-April 1993, pp.86-93

7. **Balazs, G.**, "Transfer Control of Prestressing Strands", *PCI Journal*, Vol.37 No.6, November-December 1992, pp.60-71

8. **Benmokrane, B.,Tighiouart, B.,Chaallal, O.**, "Investigation on Bond Performance of FRP Beams", Session on Bond of FRP Rebars and Tendons, ACI 1994 Spring Convention, San Francisco, USA, March 1994

9. **Bennet, E.W, Snounou, I.G**, "Bond-Slip Characteristics of Plain Reinforcing Bars Under Varying Stress", Bond In Concrete, Editor Bartos,P., 1982

10. **Canadian Standards Association**, "Design of Concrete Structures for Buildings", CSA CAN3-A23.3-M84, Rexdale, Ontario, 1984

11. **Collins, M.P., Mitchell, D.**, Prestressed Concrete Basics, Canadian Prestressed Concrete Institute, Ottawa, Ontario, 1987

12. **Comité Euro-International du Béton-Fédération Internationale de la Précontrainte**, "CEB-FIP Model Code for Concrete Structures", CEB-FIP International Recommendations, 3rd Edition, 1978

13. "Comparing Concretes on the Basis of the Bond Developed With Reinforcing Steel", ASTM C234-91a, American Society for Testing and Materials

14. **Cousins, T.E, Badeaux, M.H, Moustafa, C.**, "Proposed Test for Determining Bond Characteristics of Prestressing Strand", *PCI Journal*, January-February 1992

15. **Cousins, T.E, Johnston, D.W, Zia, P.**,"Development Length of Epoxy-Coated Prestressing Strand",*ACI Materials Journal*, V.87, No.4, July-August 1990

16. **Cousins, T.E, Johnston, D.W, Zia, P.**,"Transfer and Development Length of Epoxy-Coated and Uncoated Prestressing Strand", *PCI Journal*, V.35, No.4, July-August 1990

17. **Daniali, S.**, "Development Length for Fibre-Reinforced Plastic Bars", Advanced Composite Materials in Bridges and Structures, Editors Neale,K.W. and Labossiere,P., 1992

18. **Diederichs, U., Schneider, U.**, "Changes In Bond Behaviour Due To Elevated Temperature", Bond In Concrete, Editor Bartos,P., 1982

19. **Dolan, C.**, "Developments in Non-Metallic Prestressing Tendons", *PCI Journal*, Vol.35, No.5, September-October 1990, pp.80-88

20. **Dolan, C.**, "FRP Development in the United States", Fiber-Reinforced-Plastic (FRP) Reinforcement for Concrete Structures: Properties and Applications, Elsevier Science Publishers B.V., Netherlands, 1993

21. **Ehsani, M., Saadatmanesh, H., Tao, S.**, "Investigation of Bond Behaviour of GFRP Rebars to Concrete", Session on Bond of FRP Rebars and Tendons, ACI 1994 Spring Convention, San Francisco, USA, March 1994

22. "Epoxy-Coated Reinforcing Bars", ASTM A775/A775M-91b, American Society for Testing and Materials

23. "Epoxy-Coated Seven-Wire Prestressing Steel Strand", ASTM A882/A882M-91, American Society for Testing and Materials

24. **Erki, M., Rizkalla, S.**, "FRP Reinforcement for Concrete Structures", *Concrete International*, June 1993, pp.48-53

25. **Fukuyama, H., Sonobe, Y., Fujisawa, M., Kanakubo, T., Yonemaru, K.**, "Bond Splitting Strength of Concrete Members Reinforced With FRP Bars", Session on Bond of FRP Rebars and Tendons, ACI 1994 Spring Convention, San Francisco, USA, March 1994

26. **Hanson, N., Kaar, P.**, "Flexural Bond Tests of Pretensioned Prestressed Beams", *Journal of the American Concrete Institute*, Vol.30, No.7, January 1959, pp.783-803

27. **Issa, M., Sen, R., Amer, A.**, "Comparative Study of Transfer Length in Fibreglass and Steel Pretensioned Concrete Members", *PCI Journal*, Vol.38, No.6, November-December 1993, pp.52-63

28. **Iyer, S., Khubchandani, A.**, "Evaluation of Graphite Composite Cables For Prestressing Concrete", First International Conference on Advanced Composite Materials in Bridges and Structures, CSCE, Sherbrooke, Quebec, Canada, 1992

29. **Jiang, D.H, Andonian, A.T, Shah, S.P**, "A New Type of Bond Test Specimen", Bond In Concrete, Editor Bartos,P., 1982

30. **Kanakubo, T., Yonemaru, K., Fukuyama, H., Sonobe, Y.**, "Bond Performance of Concrete Members Reinforced With FRP Bars", Fiber-Reinforced-Plastic (FRP) Reinforcement for Concrete Structures: Properties and Applications, Elsevier Science Publishers B.V., Netherlands, 1993

31. **Kawamoto, Y., Suzuki, M.**, "Application of CFRP Strand to Pretensioned Prestressed Concrete Bridge", Modern Prestressing Techniques and Their Applications, Proceedings Vol.2, FIP Symposium '93, Kyoto, Japan, October 1993, pp.827-834

32. **Khin, M., Matsumoto, S., Harada, T., Takewaka, K.**, "Experimental Study on Bond and Anchorage of FRP Rods", Session on Bond of FRP Rebars and Tendons, ACI 1994 Spring Convention, San Francisco, USA, March 1994

33. **Malvar, L.**, "Bond Stress-Slip Characteristics of FRP Bars", Session on Bond of FRP Rebars and Tendons, ACI 1994 Spring Convention, San Francisco, USA, March 1994

34. **Martin, H.**, "Bond Performance of Ribbed Bars (pull-out-tests): Influence of Concrete Composition and Consistency", Bond In Concrete, Editor Bartos,P., 1982

35. **Martin, L., Scott, N.**, "Development of Prestressing Strand in Pretensioned Members", *ACI Journal*, Vol.73, No.8, August 1976, pp.453-456

36. **Mathey, R.G, Watstein, D.**,"Investigation of Bond in Beam and Pull-Out Specimens With High-Yield-Strength Deformed Bars", *ACI Journal*, 32, March 1961

37. **Mitchell, D., Cook, W., Khan, A., Tham, T.**, "Influence of High Strength Concrete on Transfer and Development Length of Pretensioning Strand", *PCI Journal*, Vol.38, No.3, May-June 1993, pp.52-66

38. **Nanni, A., Liu, J., Ash, K., Nenninger, J.**, "Bond Behaviour of Braided, Hybrid, FRP Rods for Concrete Reinforcement", Session on Bond of FRP Rebars and Tendons, ACI 1994 Spring Convention, San Francisco, USA, March 1994

39. **Nanni, A., Tanigaki, M.**, "Pretensioned Prestressed Concrete Members With Bonded Fibre Reinforced Plastic Tendons: Development and Flexural Bond Lengths (Static)", *ACI Structural Journal*, V.89, No.4, July-August 1992

40. **Nanni, A., Utsunomiya, T., Yonekura, H., Tanigaki, M.**, "Transmission of Prestressing Force to Concrete by Bonded Fibre Reinforced Plastic Tendons", *ACI Structural Journal*, V.89, No.3, May-June 1992

41. "Nonmetallic Coatings For Concrete Reinforcing Bars", FHWA-RD-74-18, Federal Highway Administration, National Bureau of Standards, August 1975

42. **Over, S., Au, T.**, "Prestress Transfer Bond of Pretensioned Strands in Concrete", *Journal of the American Concrete Institute*, Vol.62, No.11, pp.1451-1459

43. **Pallemans, I., Taerwe, L.**, "Tests Concerning the Transfer Length and Splitting in the Anchorage Zone of Concrete Members Pretensioned With AFRP Bars - Parts 1 and 2", Reports BREU 2-93 and 5-93, March and September 1993

44. **Shima, H., Suga, T., Honma, M.**, "Local Bond Stress-Slip Relationship of Continuous Fibre Reinforcing Materials Obtained by Pull Bond Tests With Long Embedment", *Transactions of the Japan Concrete Institute*, Vol.15, 1993, pp.297-304

45. State-of-the-art Report on Continuous Fibre Reinforcing Material, Research Committee on Continuous Fibre Reinforcing Material, JSCE, Tokyo, Japan, October 1993

46. **Stoffers, H.**, "Influencing Factors on the Transmission of Prestress Force to Concrete", Modern Prestressing Techniques and Their Applications, Proceedings Vol.2, FIP Symposium '93, Kyoto, Japan, October 1993, pp.719-726

47. **Tabatabai, H., Dickson, T.**, "The History of the Prestressing Strand Development Length Equation", *PCI Journal*, Vol.38, No.6, November-December 1993, pp.64-75

48. **Taerwe, L., Lambotte, H., Miesseler, H.**, "Loading Tests on Concrete Beams Prestressed With Glass Fiber Tendons", *PCI Journal*, Vol.37 No.4, July-August 1992, pp.84-97

49. **Taerwe, L., Pallemans, I.**, "Transmission Length of Aramid Fibre Composite Prestressing Bars Embedded in Concrete Prisms", Magnel Laboratory for Concrete Research, University of Ghent, Belgium, 1993

50. **Thompson, C., Ehsani, M., Saadatmanesh, H.**, "Transfer and Flexural Bond Behaviour of Carbon and Aramid Prestressing Tendons", Session on Bond of FRP Rebars and Tendons, ACI 1994 Spring Convention, San Francisco, USA, March 1994

51. **Tokyo Rope Manufacturing Company Limited**, "Technical Data on CFCC", Japan, October 1993, 100 pp.

52. **Tsuji, Y., Kanda, M., Tamura, T.**, "Applications of FRP Materials to Prestressed Concrete Bridges and Other Structures in Japan", *PCI Journal*, Vol.30 No.4, July-August 1993,pp.50-58

53. **Zia, P., Mostafa, T.**, "Development Length of Prestressing Strands", *PCI Journal*, Vol.22, No.5, September-October 1977, pp.54-65